UAB

**Universitat Autònoma
de Barcelona**

*Especiación directa en biomateriales mediante
técnicas no-destructivas. Técnica XAS de Sincrotrón y
técnicas Hiperespectrales, para la caracterización de
muestras alimentarias, trazabilidad e indicadores
medioambientales.*

Maribel Restituyo Silis

Tesis doctoral

Programa de doctorado en Química

Directores: Manuel Valiente Malmagro y Montserrat López-Mesas

Departamento de Química

Facultad de Ciencias

Año 2015

ANEXOS

ANEXO I

Trace-element composition and stable-isotopic ratio for geographical origin assignment of Iberian, French, Italian, and Portuguese dry-cured ham. (ENTREGADO)

Trace-element composition and stable-isotopic ratio for geographical origin assignment of Iberian, French, Italian, and Portuguese dry-cured ham

Maribel Restituyo Silis[1], Ekaterina Epova[2], Olivier F.X. Donard[2], Sylvain Berail[2] and Manuel Valiente[1]*

(1) *Universitat Autònoma de Barcelona. Dept of Chemistry. Center GTS. Campus de la UAB, 08193 Bellaterra (Barcelona), Spain*

(2) *Institut des Sciences Analytiques et de Physicochimie pour l'Environnement et les Matériaux, Université de Pauet des Pays de l'Adour, CNRS UMR 5254, Technopole Hélioparc 2 avenue Pierre Angot, PAU, Aquitaine, 64053, PAU*

*e-mail of corresponding author: manuel.valiente@uab.cat

Abstract

There is an increasing interest by consumers for high quality food products with a clear geographical origin. Suitable analytical techniques are needed to accomplish appropriate quality control. Conventional chemical methods of analysis are not able to determine the regional provenance of cured ham. At present work, traceability of selected cured hams including Iberian, French, Italian and Portuguese hams, have been performed. At first, we have used traditional inorganic analysis and discrimation using Principal Component Analysis. This first approach allowed us to classify the different hams by identifying the main differences using the trace metal content. In a second step, we have also used for the first time, stable isotope ratio determination of heavy element, Sr (a trace element). Indeed, stable isotope ratios of these non traditional elements in natural cycles present slight variations according to the geogenic background and is a good tracer for the origine. Results are given for Iberian ham from various Spanish and Italian cured ham regions . The results indicate that both trace metals content and the use stable isotope ratios of Sr contribute to provide clear identification of ham samples from different geographical origin. The trace-elements composition using Principal Component Analysis (PCA) allowed to evidence a good classification of our samples. Further, the use of stable isotope ratios provides additional information for the ham samples classification by establishing clear distinction between different lots which can be traced back to the geogenic origin and combines with the trace metal content information.. We present some of the first traceability results for ham samples based on isotopic ratio measurements and will discuss their protential value for traceability of the ham geo-origin.

Key words: Dry-cured ham; Geographic origin , Multielement trace analysis; stable isotope ratios; Food traceability; Strontium isotopes, Multicollector ICP-MS

INTRODUCTION

Food traceability, including origin of the product may be assessed by specific chemical identification of particular trace elements. These approaches where used to evaluated the potential of discrimination of origine of hams coming from different countries.

Conventional authentification of foods relies on the availability of site-specific chemical parameters. However, the results of these analyses can reveal chemical differences between ham samples from a specific region and but also could include information with regards to the cured hams process applied to hams from different regions. The use of selected stable isotope analysis (here Sr which is linked to the geogenic origine) enables to further promote the differentiation of chemically identical substances using their specific isotopic fingerprints. It appears to overcome the limitations of conventional methods [1]. Nevertheless, the conventional methodsusing trace metal determination and PCA are powerful tool for elemental analysis and rely on the possibility of providing limits of detection (LODs) for more than 20 elements at low concentrations [2].

In order to characterize the trace elements content we used the conventional technique inductively coupled plasma mass spectrometry ICP-MS. It is a powerful tool for the quantitative determination of a range of metals and non-metals (inorganic elements) in a wide variety of samples at trace (ppb–ppm) and ultra-trace (ppq–ppb) concentration levels, ICP-MS has clear advantages in its multi-element characteristics, speed of analysis, detection limits, and isotopic capabilities [3]. However, conventional ICP-MS systems cannot provide the lowest LODs, because of the polyatomic interferences that can increase the background signal and result in the overlapping of the signals of the most abundant isotopes. The use of a dynamic reaction cell (DRC) can remove unwanted interferences by creating specific chemical reactions with a supplementary gas, which improves dramatically the selectivity and the sensitivityfor trace elements determination. When precise isotopic ratios are needed the use of multicollector ICP/MS appears to be a very powerfull tools to strengthen origin discrimination [4].

The aim of this work is to provide an example to classify Iberian and Italian hams by geographical origin using trace-elements and stable-isotope analysis.

MATERIAL AND METHODS

To characterize origin we have determined trace elements content using traditional analytical methods as ICPM/MS for trace metals determination and applying principalcomponent analysis, PCA, for data analysis.

On he other hand, according to the abundance of the elements, the isotopic ratio, IR, was determined using Multicollector ICP/MS, after appropriate sample treatment, including digestion, purification and concentration.

A total of 16 hams samples were obtained from ham processing factories in Spain, Portugal, Italy and France.

This study included four ham sample sets. The first lot presents 10 samples from Spain, the second one , one sample from Portugal, the third is reprersented by three samples from France and fourth one, two samples from Italy. The authenticity of all samples had been certified by valid custom documents, specifying the place and slaughter date.

Experiments we carried out in by 2 distincts approaches::

Trace elements analysis: samples were lyophilized and prepared as homogeneous power. 0.5 grams of target sample was mineralized using 4 ml of nitric acid and 1 ml of hydrogen peroxide during heating 4 hours, then, the corresponding solution was prepared to analyze major and trace metals, acidity was adjusted to the desired value with nitric acid.*Isotopic analysis*: Isotope intensities were measured by using mass-spectrometer MC-ICP-MS Nu-Instruments, Great Britain) with instrumental mass bias and interferences corrections Accuracy and precision were monitored with a Standard Reference Material (SRM 987; www.nist.gov/srm). The mean $\pm\}$ s.d. value of $^{87}Sr/^{86}Sr$ in SRM 987 ($n = 40$) run throughout the analyses was $0,71034 \pm 0, 00003$, which compares favourably with the accepted value of $0,71034 \pm 0,00026$.The complete process was carried out using a procedure reported elsewhere [5]. The instrumental parameters were adjusted according to [+ Martin J. 2015] [6, 7]. All determinations were performed by triplicate analysis, reported data correspond to the average value

Due to the large number of variables involved, multivariate data analysis is required to extract the relevant information. Principal component analysis (PCA) identifies, in the hyperspace of the variables studied, the directions on which most of the information is retained, thus reducing the dimensionality of the system. By projecting the objects of the data set in the space of the first few components, it is possible to demonstrate differences between the various objects, also identifying the main contributing variables [8].This chemometric methods have been applied to evaluate the regional origin of ham samples based on their trace-element profile. See Fig.1
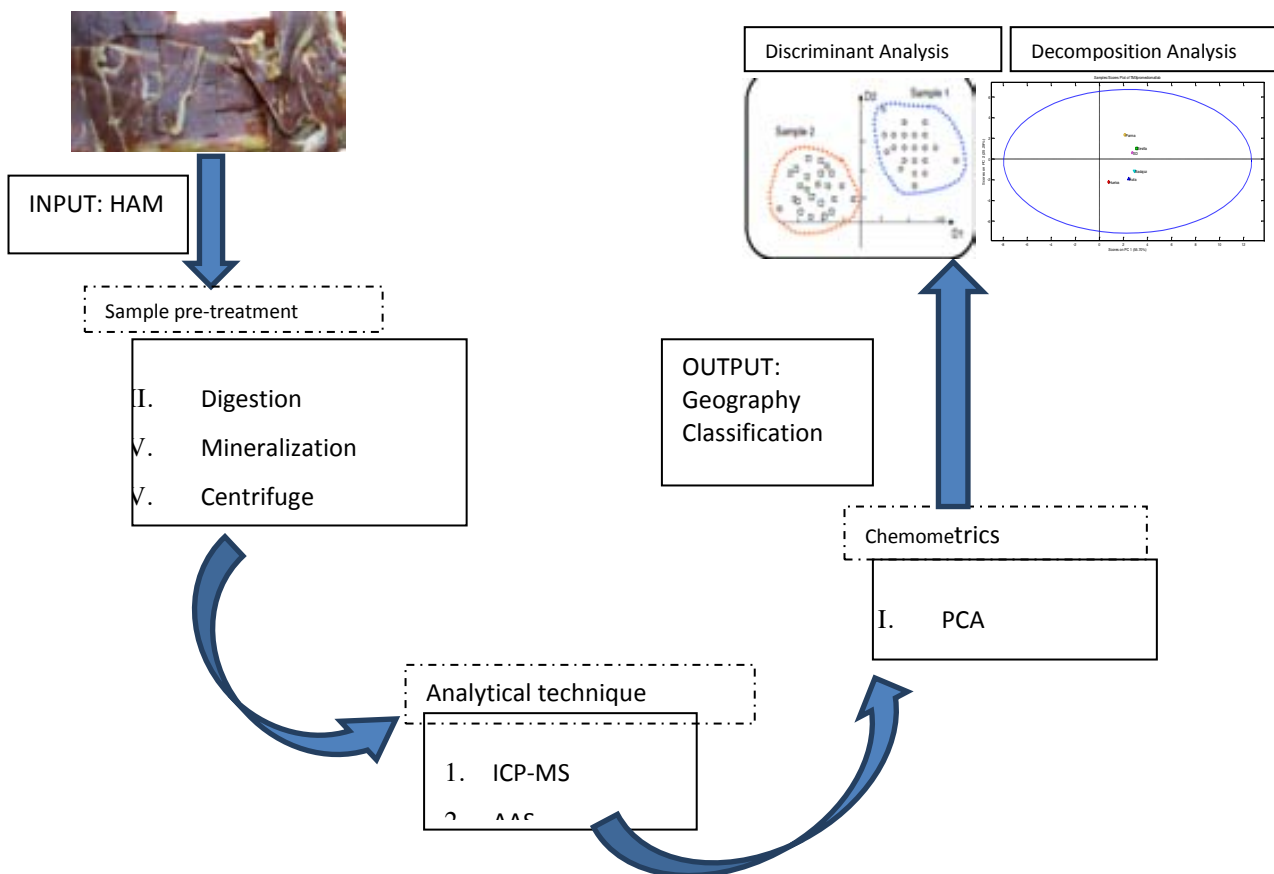
Figure1. Strategies ofanalytical process used in the present sudy

RESULTS AND DISCUSSION

*Trace metal content in ham samples*

Trace elements are considered as a promising group of meat components to indicate the geographic origin considering their presence in the local environment. It is characterized by the trace element profile of the soil as well as the site-specific profile of drinking water, feed, litter and air. Generally, a migration through the food chain is known and quantified in several trace elements.

The composition of elements in the soil is typical for particular regions due to main difference in the geology [4]. For example, Rb is a trace element signaling natural differences between soil contents [9] showed that the Rb concentration in plants and drinking water was highest on granite and gneiss weathering soil. Herbivores were found to store 37 and 33 % more Rb in the liver than carnivores and omnivores, respectively.

Results for dry-cured ham trace metal contents are given in Table 1, The principal components analysis (PCA) was used to correlate the variation between the ham samples with the different origin (Figure 2), the results demonstrated for the PC1 that samples from France are very similar constitutionally in all of the elements that we had analyzed, the Portugal sample is independent for the rest of the other samples.

E /S	Spain set										Portugal	France			Italy	
	1	2	3	4	5	6	7	8	9	10	11	12	13	14	15	16
Ppm																
B	1633	5,2	2,8	2,4	3,0	14	1,7	≤	3	≤	2	≤	≤	≤	0,9	0,5
Mn	0,5	0,8	0,3	0,6	0,3	0.4	0,2	0.3	0,4	0,2	0,2	0,9	0,4	0,6	0,3	0,3
Fe	51	67	46	52	32	34	23	47	31	19	23	33	25	23	29	28
Cu	3	5	4	4	3	2	2	3	3	2	2	3	2	2	2	2
Zn	44	60	44	48	34	26	16	48	21	16	16	36	36	30	21	27
Rb	12	14	11	18	14	10	10	8	13	7	9	14	22	14	17	18
Sr	3	2	0,7	0,9	0,8	≤	0,6	≤	1	0,5	1	4	4	3	4	1
ppb																
Li	48,7	22	23	21	18	23	11	12	17	14	13	98	148	48	27	14
V	7,5	6	8	≤	≤	8	4	6	8	6	6	5	≤	5	7,5	5,6
Cr	73	66	87	85	52	82	58	72	67	94	60	59	58	63	75	87
Co	18	7	4	8	5	5	4	5	5	10	4	≤	≤	≤	10	5
Ni	62	118	49	48	20	160	48	39	55	376	30	11	11	8	1996	631
Cd	54	43	15	7	28	20	8	9	7	22	15	≤	≤	≤D	62	39
Cs	41	145	104	521	203	31	332	16	241	23	106	94	115	89	419	82
Ti	≤	1,4	≤	2	≤	≤	1,6	≤	≤	1,3	1	3,4	3	4	1,2	2
Pb	72	79	132	85	22	43	18	23	69	39	13	7	≤	5	61	72

Table1. Trace metals content in ham samples. The ≤ value indicates below the detection limits.
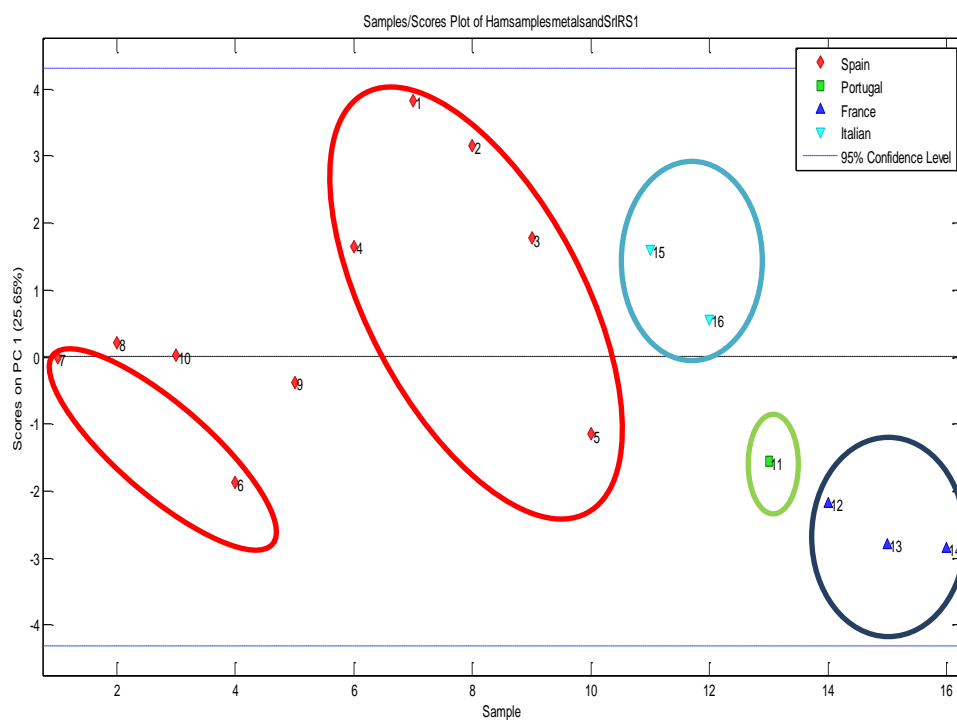
Figure 2. PCA results, the complete analysis had performed with 6 PCs, thus the first PCs (25.6%) had given the distribution samples set.

Strontium Isotopes

Isotopic ratios of the element of Sr in ham provide a means by which regions with similar or identical geological characteristics can be identified. Table 2 shows the corresponding values for the 16 ham samples .

Sample		$^{87/86}$ Sr Ratio	SD
Spain	1	0,709259	0,00012
	2	0,709274	0,00012
	3	0,709473	0,00012
	4	0,709467	0,00012
	5	0,709270	0,00012
	6	0,708981	0,00012
	7	0,709281	0,00012
	8	0,709002	0,00012
	9	0,709505	0,00012
	10	0,709032	0,00012
Portugal	11	0,709558	0,00012
France	12	0,708545	0,00012
	13	0,708538	0,00012
	14	0,708578	0,00012
Italy	15	0,709227	0,00012
	16	0,709245	0,00012

Table 2. $^{87/86}$ Sr measured in dry-cured ham samples from different countries of origin.

Figure 3 presents Sr isotopic ratio values, indicating clearly four different ham groups of different geological characteristics. This observation can be attributed to differences and similarities of animal food sources for the
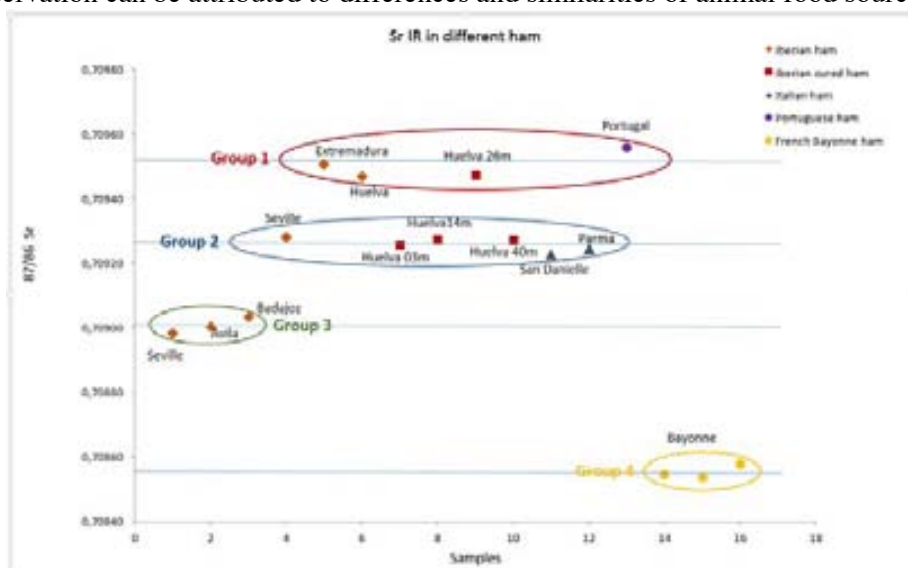
different selected hams.
Figure 3. Group distribution identified with the IR $^{87/86}$ Sr ham samples content.

Conclusions

From results obtained in the present study, the following conclussions can rise:

- ✓ Trace element contents in ham samples show a clear discrimination between hams of different regions.
- ✓ Isotope ratio analysis offer a most promising hypothesis driven approach to establish the geographical origin of dry-cured ham.

In addition, the study presents an overview of the observed value ranges of trace elements. Combining the measured data with a Sr isotopic analysis, it is possible to provide the authenticity control and not only to estimate the isotopic signature of dry-cured ham,

References

[1] Drivelos S., Georgiou CA., Multi-element and multi-isotoperatio analysis to determine the geographical origin of foods in the European Union . Trends in Analytical Chemistry, Vol. 40, 2012

[2] Rossmann A., Haberhauer G., Hölzl S., Horn P., Pichlmayer F., Voerkelius S. The potential of multielement stable isotope analysis for regional origin assignment of butter. Eur Food Res Technol (2000) 211 :32–40

[3] Franke B.m., Koslitz E.S.,Micaux E.F., Piantini U., Maury E.U., Pfammatter E., Wunderli S., Gremaud G., BossetO.,Hadorn R., Kreuzer M. Tracing the geographic origin of poultry meat and dried beef with oxygen and strontium isotope ratios. Eur Food Res Technol (2008) 226:761–769.

[4] Franke B.M., Gremaud G.R., Hadorn R., Kreuzer M. Geographic origin of meat—elements of an analytical approach to its authentication. Eur Food Res Technol (2005) 221:493–503.

[5] Voerkelius S.,Gesine D. Susanne R.,Christophe R.,Gerhard I., Malcolm B., Christophe B. Peter D., Hoelzl S., Hoogewerff J.,Ponzevera E.,Van ocxstaele M.,ckermann H. Strontium isotopic signatures of natural mineral waters, the reference to a simple geological map and its potential for authentication of food. Food Chemistry 118 (2010) 933–940.

[6] Rossmann, A., Haberhauer, G., Hoelzl, S., Horn, P., Pichlmayer, F., & Voerkelius, S. (2000). The potential of multielement stable isotope analysis for regional origin assignment of butter. European Food Research and Technology, 211(1), 32–40.

[7] Rummel, S., Hoelzl, S., Horn, P., Rossmann, A., & Schlicht, C. (2008). The combination of stable isotope abundance ratios of H, C, N and S with 87Sr/86Sr for geographical origin assignment of orange juices. Food Chemistry, doi:10.1016/ j.foodchem.2008.05.115.

[8] S. Wold, K. Esbensen, P. Geladi, Chemometr. Intell. Lab. Syst. 2 (1987) 37–52.

[9] Faure G (1991) Principles of isotope geology. Wiley, New York

ANEXO II

Spectral study of dry-cured ham using a hyperspectral imaging system in the near infrared (NIR).
(EN PREPARACIÓN)

Spectral study of dry-cured ham using a hyperspectral imaging system in the near infrared (NIR)

Maribel Restituyo Silis [b], Jordi Coello Bonilla [b], *Silvia Serranti [a], Giuseppe Bonifazi [a], Manuel Valiente [b]

a) Department of Chemical Engineering Materials & Environment. Sapienza—Universita di Roma, Via Eudossiana 18, 00184 Rome, Italy.

b) Departament de Química, Química Analítica, Universitat Autònoma de Barcelona, 08193 Bellaterra, Barcelona, Spain

Abstract

The goal of this study was to explore the potential of near-infrared (NIR) hyperspectral imaging in combination with multivariate analysis for the classification of dry-cured ham samples according to the geographic origin. In this study, seven different dry-cured ham from Spain and four from Italy were collected and used for image acquisition and quality measurements. Hyperspectral images were acquired using a push broom NIR hyperspectral imaging system in the spectral range of 901–1713 nm. Spectral data were analyzed using principal component analysis (PCA). Partial least-squares discriminant analysis (PLS-DA) was used to correlate the NIR spectra with the origin of the ham. The results revealed the potentiality of NIR hyperspectral imaging as an objective and non-destructive method for the authentication and classification of dry-cured ham.

Keywords: Hyperspectral images, near-infrared, dry-cured ham, principal component analysis.

Introduction

The development of screening methods for fast classification of meat quality is demanded by the industry. Near infrared spectroscopy (NIR) has proven to be a rapid and effective tool for meat quality assessment [1, 2]. It is an easy to use, non-destructive, accurate and robust technique which allows several parameters to be simultaneously determined.

The recent applications of hyperspectral imaging systems, as an analytical tool in quality assurance of various food products, are capturing a growing interest and attention. The simultaneous spatial and spectral information provided by this system, along with its non-invasive and chemical-free nature nominated this technology to be a deliberated tool for continuous monitoring of food production processes and for consistent optimization of production systems.

The basic principles of hyperspectral imaging, also called 'imaging spectroscopy', involve the production, recording and interpretation of images acquired at several contiguous spectral wavelengths. Hyperspectral imaging has been emerged by integrating both spectroscopy and imaging techniques in one system to provide detailed information of the tested products which otherwise cannot be achieved with either conventional imaging or spectroscopy alone.[3,4,5] One hyperspectral image is a group of images displaying the tested object at different wavelengths where each pixel in the image represents a spectrum for this specific point of the object.

As a result, each hyperspectral image contains a large amount of information in a three-dimensional (3D) form called "hypercube" which can be analyzed to characterize the object more reliably than the single traditional machine vision [6, 7] or spectroscopy techniques [8-11].

Therefore, hyperspectral imaging can be a very useful research tool for determining important spectral bands, which later can be implemented in a multispectral imaging system. These bands can be obtained through different analysis methods such as the spectral difference or principal component analysis [12, 13]. There are various contributions on the usefulness of near infrared spectroscopy (NIRS) to predict meat quality attributes, such as drip loss, pH, water holding capacity and tenderness in fresh as well as in processed meat. Few researches have been carried out to evaluate the quality of the ham. Luque de Castro et al. investigated the feasibility of VIS/NIR spectroscopy for the classification of dry-cured hams as a function of their texture and color [14]. Sheridan et al. [15] measured the color stability of pre-packaged sliced hams. Sensory characteristics of dry-cured ham have been evaluated by Ortiz et al. [16] using visible and near infrared spectroscopy.

The main aim of this study was to investigate the potential of hyperspectral imaging system in the NIR spectral region of 880–1720 nm to assess the of quality characteristics of dry-cured ham from two different European countries. The work was conducted by (1) developing a suitable hyperspectral imaging based detection/analytical architecture in the NIR spectral

region; (2) identifying the part of the ham suitable for obtaining the samples for the studies, and (3) using chemometric techniques for classifying dry-cured ham regarding geographical origin.

2. Material and methods

2.1 Sample preparation

For Spanish and Italian dry-cured ham, sea salt is the only ingredient used in the curing process. The technological process includes: Salting and washing, Resting period, Drying and maturation, Bodega phase, where both Spanish and Italian dry-cured ham were obtained.

Seven Spanish dry-cured hams were selected, all of them fed with acorn, with the following characteristics:

Sample A1: Ham from 100% Black Iberian Pigs taken from the "Caña" part, between the shinbone and the fibula.
Sample A2: Ham from 100% Black Iberian Pigs taken from the "Babilla" part, found between femur and coxal bones.
Sample A3: Ham from 100% Black Iberian Pigs taken from the "Maza" part, the main part of the ham.
Sample B1: Ham from cross-bred pigs (75% Iberian) cured for 3 years.
Sample B2: Ham from cross-bred pigs (75% Iberian) cured for 26 months.
Sample B3: Ham from 100% Black Iberian Pigs cured for 2 years.
Sample B4: Ham from 100% Black Iberian Pigs cured for 22 months.

In the case of Italian dry-cured ham, two EU protected designations were selected:

Sample C1: Prosciutto di San Daniele, Italian dry-cured ham for 18 months.
Sample C2: Prosciutto di San Daniele, Italian dry-cured ham for 22 months.
Sample C3: Prosciutto di Parma, Italian dry-cured ham for 22 months.
Sample C4: Prosciutto di Parma, Italian dry-cured ham for 30 months.

For each sample, we have made five slices of approximately 3×3 cm and 0, 5 cm in thickness, using a ceramic knife. Immediately after slicing, each slice was analyzed.

2.2 Spectral image collection

2.2.1 Hyperspectral imaging system

A laboratory NIR hyperspectral imaging system (HIS) in the range 880-1720 nm was used; it is shown in Figure 1. The HIS acquisitions of dry-cured ham samples have been carried out at the Laboratory for Particles and Particulate Solids Characterization (Latina, Italy) of the Department of Chemical Engineering, Materials and Environment (Sapienza University of Rome). A specifically designed hyperspectral imaging based platform (DV srl, Italy) was utilized to perform all the analyses. The HSI based detection architecture was realized to allow not only static, but also dynamic analysis, that is the possibility to carry out tests on particle flow streams transported on a conveyor belt in order to perform, at laboratory scale, particles on-line detection in a sorting and/or quality control perspective.

The platform, in terms of hardware components, is based on a controlled conveyor belt (width = 26 cm and length=160 cm) with adjustable speed (variable between 0 and 50 mm/s). The utilized acquisition system is an NIR Spectral Camera™ (Specim, Finland), embedding an ImSpector N17E™ imaging spectrograph working in spectral range from 880 to 1720 nm, with a spectral sampling/pixel of 2.6 nm, coupled with a Te-cooled InGaAs photodiode array sensor (320×240 pixels) with the pixel resolution of 12 bits. A diffused light cylinder source, providing the required energy for the sensing unit, was set-up. The cylinder, aluminum internally coated, embeds five halogen lamps producing a continuous spectrum signal optimized for spectra acquisition in the NIR wavelength range. The device works as a push-broom type line scan camera, allowing the acquisition of spectral information for each pixel in the line. The transmission diffraction grating and optics provide high-light throughput and high quality and distortion-less image for the device. The result of acquisition is a digital image where each column represents the discrete spectrum values of the corresponding element of the sensitive linear array. The device is controlled by a PC unit equipped with the Spectral Scanner TM v.2.3 acquisition/pre-processing software, specifically developed to handle the different unit and the sensing device constituting the platform and to perform the acquisition and the collection of spectra. The software was designed as a flexible architecture to be easily integrated with new software modules embedding new characterization and/or classification tools [17].

2.2.2. Hyperspectral image acquisition

Spectral SScanner software (Version 4.5) CV SRL, Inc., Italy) was used to obtain hyperspectral images of dry-cured ham, in the 880–1720 nm wavelength range, with a spectral resolution of 7 nm, for a total of 121 wavelengths. The spectrometer was coupled to a 15 mm lens. The images were acquired scanning the investigated sample line by line. The image width was 320

pixels, while the number of frames was variable from 200 to 350, depending on the length of the sample.

Calibration was performed recording two images in black and white references. The black image (B) was acquired to remove the effect of dark current of the camera sensor, turning off the light source and covering the camera lens with its cap. The white reference image (W) was acquired for a standard white ceramic tile under the same conditions of the raw image. Image correction was thus performed adopting equation (1):

$$I = \frac{I_0 - B}{W - B} \times 100 \qquad (1)$$

Where I is the corrected hyperspectral image in relative reflectance (%) unit, I_0 is the original reflectance of the hyperspectral image, B is the black reference image (~0% reflectance) and W is the white reference image (~99.9% reflectance).All the corrected images were then used to perform the HIS based analysis.

3. Spectral data analysis

3.1 Image treatment

The treatment of the image started by transforming NIR image to a false RGB color image with the aid of ENVI 5.0 software (ITT visual information solutions, Boulder, CO, USA). Red channel was assigned to the band at 1447 nm; green channel to 1181 nm; and blue channel to 971 nm. A simplified representation of the RGB image was made differentiating areas of low and high reflectance, green and red, respectively. The images are shown in figure 2. For each slice, 5 regions of 17x17 pixels were selected, and the NIR spectra of all the pixels were averaged for each region. Both types of ham, Spanish and Italian, were treated in the same way.

3.2 Spectral preprocessing

NIR spectra were analyzed using The Unscrambler X software (v. 10.3; CAMO, Oslo, Norway).

The spectra of each region, originally recorded in reflectance, R, were transformed to apparent absorbance A using equation 2.

$$A = log_{10}\left(\frac{1}{R}\right) \qquad (2)$$

For further processing, spectral data were limited to the wavelength range of 901-1370 nm (with only 68 channels), since high wavelengths there was a saturation of the detector for some measurements and the noise level of the camera was rather high.

Figure 3a shows NIR spectra in absorbance (log1/R) between 901-1713 nm. The wavelengths selected for each channel of the false RGB image are marked in the figure. In order to minimize the effect of light scattering, the data needed to be pre-treated; we used Standard Normal Variate (SNV) [18]. Figure 3b shows the spectra of figure 3a after SNV pretreatment (901-1370 nm).

3.3 Exploratory data analysis using principal component analysis

The complexity of NIR spectra requires the use of chemometrics procedures to extract and visualize the useful analytical information. Principal Component Analysis (PCA) is often the first step for data analysis in order to detect patterns in the measured data. It is a well-known bilinear modeling method which gives an interpretable overview of the main information in a multidimensional data table by extracting and displaying the existing systematic variation [19]. The information carried by the original variables is projected onto a smaller number of uncorrelated variables called principal components (PCs). The first principal component (PC1) accounts for the maximum of the total variance, the second (PC2) is orthogonal to the first one and covers as much of the remaining variation as possible, and so on, until the total variance is accounted for. The decomposition of the spectroscopic data table is performed according to the following equation:

$$X = TP^T + E \qquad\qquad\qquad (3)$$

where X is the matrix of NIR spectra after performing all necessary corrections to data, T is the scores matrix that presents as many rows as the original data matrix, P^T corresponds to the loadings matrix transpose that has as many columns as the original data matrix and E is an error matrix with the same dimensions as the original data matrix. The number of columns in the scores matrix equals the number of rows in the loadings matrix transposed and corresponds to the PCs that are calculated to describe the information contained in the data. By plotting the scores, we are able to detect and interpret sample patterns, groupings, similarities, differences and to discover outliers.

6

NIR spectra in the range 901–1370 nm were pre-treated using SNV. After mean centering the data, singular value decomposition algorithm and full cross validation were used to build the model.

3.4 Partial least squares discriminant analysis

Principal component analysis is a powerful method for data exploration, however, PCA is an unsupervised technique and it cannot be used for building predictive models to classify samples in one or another category. In that case, a supervised pattern recognition approach should be adopted. Discriminant Analysis (DA) is a supervised classification technique where the number of groups and the samples that belong to each group are previously defined Discrimination of the groups is achieved by calculating the Mahalanobis distance of a sample from the centers of the groups considered [20]. The greater the spectral differences between two given groups, the greater the Mahalanobis distance between them. This distance is used to classify unknown samples; the unknown sample is classified as belonging to the group with a closest distance to the center. However, DA requires a higher number of samples than variables and, using data from a spectroscopic technique the number of variables is the number of wavelength of the spectra, so it is necessary compressing the information contained in the spectra into a few variables.

Partial least squares (PLS) regression is a well-known method that is used to find the fundamental relations between independent variables (X) and dependent variables (Y), which are simultaneously modeled by taking into account not only X variance, but the covariance between X and Y [21]. Hence, the PLS algorithm attempts to find factors (also called Latent Variables) that maximize the amount of variation explained in X that is relevant for predicting Y. Partial least squares discriminant analysis (PLS-DA) is a variant of PLS that is used to improve the separation between classes using a categorical response variable Y [22]. In this way, PLS-DA could be used to make one model covering many classes. In this case, the X matrix is composed of the NIR spectra after SNV treatment and the Y vector is a set of dummy variables that codes class membership of the objects. Dummy variables were assigned to the calibration samples set as follows: 1 to Spanish ham and 2 to Italian ham. Then, X and Y are decomposed in a product of two matrices of scores and loadings; the loadings of the X block are calculated from the scores of the Y block, while the loadings of the Y block are calculated from the scores of the X block. A sample from the prediction set is considered to be correctly categorized if it fulfills two criteria: it must have a NIR spectrum that is not significantly different from the

spectra that form the calibration set and a predicted value of the dummy variable within the range defined by a cutoff value. The optimum number of factors to build the model was determined by the minimum value of predicted residual error sum of squares (PRESS) criterion [23]. Full cross-validation (CV), was used to validate PCA and PLS calibration models. Statistics evaluated for the calibration model included root mean square error of calibration (RMSEC), root mean square error of cross validation (RMSECV) and determination coefficient r-square.

4. Experimental results and discussion

4.1 Spectral data

The spectra of near infrared radiation from the samples are presented in Figure 2. On this region there is an important contribution of the absorption of fat, protein and moisture that cannot be individualized. At 931 nm there is absorption of fat and, between 946 and 1062 nm absorption of the three compounds. At 970 nm appears the second overtone of O-H stretch, and 1190 nm is a combination band of O-H stretch and O-H bend from moisture, although all these bands may shift as result of variations in hydrogen bonding in the food matrix. Around 1200 nm there is the 2nd overtone of CH_2 from the long chain of fatty acids [24]. The dispersion of NIR spectra from Italian samples is higher than that of the Spanish ones.

4.2 Principal component analysis.

PCA was performed with different objectives. In a previous step, to study differences between several parts of the ham, samples A1-A3 of Spanish ham were taken from the same piece, with the purpose of checking if "Babilla" part was different to the others because the more activity of their muscles [25]. Before the analysis, the images were pre-treated as indicated in section 3.1 and 3.2. Figure 4 shows the plot of the scores of PC1 (that explain 94.8% of the variance) for samples of the different parts of a ham, and it is seen that samples taken from "Caña" or "Maza" have very similar spectra, as they have similar scores values, but the samples taken from "Babilla" are really different, presenting negative scores values; therefore all other samples in the study were taken from this part.

In order to obtain a global view of the samples, a PCA was performed on all NIR spectra of samples B1 to C4 after SNV preprocessing. Data were previously mean centered and singular

8

value decomposition algorithm for the calculation and cross correlation for model validation were used.

PCA compresses the data by projecting the samples into a low dimensional subspace, whose axes (the principal components, PCs) point in the directions of maximal variance. As the main sources of data variability are concentrated in a few variables (often 2 or 3) it means that, from the observation of the distribution of the samples onto the PC space it is possible to analyze their common features and/or their grouping. On the other hand, inspection of the loadings allows interpreting the observed differences and similarities among the samples in terms of the original spectral data. The two-vector PCA score plot gives a picture of the overall variation of the data (Figure 5). The first principal component accounts for 86% of the variation of the NIR measurements, and the second PC for 11%, both for calibration and cross-validation variance. The separation in PC1 of the spectra from Spanish and Italian samples is very clear. Spanish data, plotted as blue boxes, are more compact than Italian ones and all of them present negative values of the scores. The Italian data, plotted as orange dots, have positive scores values and show more spread in PC2.

As with all non-supervised methods for classification, PCA provides a picture that explains and shows patterns of the samples studied, but the assignation of new samples to a class may be a difficult task, and not intended in this work, as the method does not calculate a rule to generate boundaries or regions for the groups of samples obtained. Hence, a supervised method was tried in order to improve the results.

4.3 Partial least squares discriminant analysis

From each slice, four spectra were used to build the calibration set, and one was assigned to the prediction set.

Variations in dummy Y vector and X matrix were described by 2 factors (Fs) with an explained variance of 86% and 90%, respectively. This relatively small number of Fs suggests low chemical correlation in spectra from different classes, but similarities in spectra within classes; i.e., the low number of Fs provides an indication of the good capability of the model to describe the proposed classes. The regression statistics showed an RMSEC of 0.114, an RMSECV of 0.116 and r^2 from the CV of 0.947. Figure 6 shows the scores plot of the PLS-DA model. The cutoff value was determined by regarding the predicted vs reference regression line (Figure 7) and error on predictions and was set to ± 0.30 for the Spanish or Italian ham

class. This means that all predicted samples that have been estimated within the limits established by the Hotelling T^2 value and Q residuals value in a confidence level of 95% and with a Y value from 0.70 to 1.30, will be classified as belonging to the Spanish class, while those with a Y value from 1.70 to 2.30, will be classified as belonging to the Italian class; the overall results after both steps are shown in Table 1. All the samples were correctly classified.

5. Conclusions

The results of this study suggest that a hyperspectral imaging system in the near infrared region, coupled with multivariate statistical analysis methods, can be used for authenticating and classifying dry-cured ham as a function of their geographical origin. The technique is rapid and non-destructive, and may be performed directly on a whole slice of ham.

These results were obtained using a laboratory made device. Refinement of this may allow for non-destructive and rapid quality measurements at the processing plant.

However, much more samples with different qualities should be studied to ascertain properly the classification power of this method.

References

[1] G. Monin. The role of major genes and DNA technology in selection for meat quality in pigs. Meat Sci. 49 (1998) 231.

[2] M. Prevolnik, M. Candek-Potokar, D. Skorjanc, Czech J. Predicting intramuscular fat content in pork and beef by near infrared spectroscopy. Anim. Sci. 49 (2004) 500.

[3] ElMasry, G., Wang, N., Vigneault, C., Qiao, J., & ElSayed, A. (2008). Early detection of apple bruises on different background colors.

[4] Mizrach, A., Lu, R., & Rubino, M. (2009). Gloss evaluation of curved-surface fruits and vegetables. Food and Bioprocess Technology, 2(3), 300–307.

[5] Cruz Ortiz , M., Sarabia, L., Grarcia-Rey, R., Luque de Castro, M. D. Sensitivity and specificity of PLS-class modelling for five sensory characteristics of dry-cured ham using visible and near infrared spectroscopy. Analytica Chimica Acta, 558(2006) 125-131.

[6] S. Kumar, G.S. Mittal, Food Bioprocess Technol. 3 (2010) 741–751.

[7] F. Pallottino, P. Menesatti, C. Costa, G. Paglia, F.R. De Salvador, D. Lolletti, Food Bioprocess Technol. 3 (2010) 155–159.

[8] F. Liu, Y. He, L. Wang, Anal. Chim. Acta 615 (2008) 10–17.

[9] D. Wu, Y. He, P. Nie, F. Cao, Y. Bao, Anal. Chim. Acta 659 (2010) 229–237.

[10] R. Quevedo, J.M. Aguilera, Food Bioprocess Technol. 3 (2010) 561–567.

[11] W. Klaypradit, S. Kerdpiboon, R.K. Singh, Food Bioprocess Technol. 4 (2011) 475–480.

[12] Lu, R., 2003. Detection of bruises on apples using near-infrared hyperspectral imaging. Trans. ASAE 46, 523–530.

[13] Liu, Y., Ying, Y., 2005. Use of FT-NIR spectrometry in non-invasive measurements of internal quality of 'Fuji' apples. Postharvest Biol. Technol. 37, 65–71.

[14] Garcia-Rey, R. M., Garcia-Olmo, J., De Pedro, E., Quiles-Zafra, R., Luque de Castro, M. D. 2005. Prediction of texture and color of drycured ham by visible and nir spectroscopy using a fiber optic probe. Meat Science, 70, 357–363.

[15] Sheridan, C., O'Farrell, M., Lewis, E., Flanagan, C., Kerry, J. F., & Jackman, N. 2006. An examination of ham colour fading using optical fibre methods. Proceedings of SPIE: The International society for Optical Engineering, 6381.

[16] Ortiz, C, Sarabia,L, Garc´ia-Rey, R & Luque de Castro, M. D.(2006). Sensitivity and specificity of PLS-class modelling for five sensory characteristics of dry-cured ham using visible and near infrared spectroscopy. Analytica Chimica Acta 558, 125– 131.

[17] Silvia Serranti a,n, DanielaCesare a, FedericoMarini b, GiuseppeBonifazi Classification of oat and groat kernels using NIR hyperspectral imaging. Talanta 103 (2013) 276–284

[18] Barnes R.J., Dhanoa M.S. and Lister S.J., Standard Normal Variate Transformation and De-trending of Near-Infrared Diffuse Reflectance Spectra. Applied Spectroscopy 43 (1989) 772-777.

[19] S. Wold, K. Esbensen, P. Geladi, Chemometr. Intell. Lab. Syst. 2 (1987) 37–52.

[20] J. R. Lucio-Gutierrez, J. Coello and S. Maspoch. Application of near infrared spectral fingerprinting and pattern recognition techniques for fast identification of Eleutherococcus senticosus. Food Research International 44 (2011) 557-565.

[21] S. Wold, M. Sjöstrm, L. Eriksson. PLS-regression: a basic tool of chemometrics. Chemometrics and Intelligent Laboratory Systems 58 (2001) 109-130.

[22] M. Barker, W. Rayens. Partial least squares for discrimination. J. Chemometrics 17 (2003) 166-173.

[23] R.G. Brereton, Applied Chemometrics for Scientists, John Wiley & Sons, Ltd, 603 Great Britain, 2007, pp.145-191.

[24] Osborne, B. G., & Fearn, T. "Near infrared spectroscopy in food analysis". Longman Scientific and Technical. Harlow, Essex, UK (1986).

[25] Guerrero, L., Gou, P., Alonso, P., y Arnau, J., Study of the physico-chemical and sensorial characteristics of dry-cured hams in three pig genetic types. Journal of the Science of Fod and Agriculture, 1996, 70, 526-530.

Table1. Classification of the NIR spectra of the prediction set using a PLS-DA model with 2 factors.

Sample	Reference	Predicted Y	St. Dev.	Sample	Reference	Predicted Y	St. Dev.
B1	1	1,12	0,12	C1	2	1,95	0,09
B1	1	1,23	0,08	C1	2	2,01	0,10
B1	1	1,05	0,06	C1	2	1,97	0,06
B1	1	1,10	0,13	C1	2	1,98	0,07
B1	1	1,00	0,14	C1	2	1,98	0,05
B2	1	0,96	0,10	C2	2	1,96	0,06
B2	1	1,18	0,09	C2	2	2,03	0,04
B2	1	0,88	0,17	C2	2	1,96	0,05
B2	1	0,84	0,10	C2	2	1,93	0,09
B2	1	0,84	0,11	C2	2	1,95	0,07
B3	1	0,90	0,08	C3	2	1,93	0,09
B3	1	1,08	0,26	C3	2	1,93	0,08
B3	1	0,94	0,21	C3	2	2,07	0,10
B3	1	1,14	0,11	C3	2	1,94	0,11
B3	1	0,82	0,12	C3	2	2,13	0,13
B4	1	1,13	0,09	C4	2	1,98	0,23
B4	1	1,14	0,08	C4	2	2,00	0,05
B4	1	1,27	0,11	C4	2	2,04	0,05
B4	1	1,19	0,05	C4	2	1,95	0,07
B4	1	0,92	0,10	C4	2	2,00	0,10

FIGURE CAPTIONS

Figure 1. Main components of the NIR hyperspectral imaging system.

Figure 2. Images obtained from dry-cured samples of Spanish and Italian ham. RGB images were obtained using reflectance at 971, 1181 and 1447 nm as blue, green and red channels, respectively. Bicolor images indicate areas of high (in green) and low (in red) reflectance.

Figure. 3. A) NIR spectra corresponding to both 100 Spanish ham spectra(blue) and 100 Italian ham spectra (orange). The wavelengths used for the false RGB image are indicated. B) The same spectra after SNV pre-treatment in the range 901 – 1370 nm.

Figure 4. PCA analysis of the samples from different parts of a ham.

Figure 5. Scores plot of PCA model obtained from NIR spectra. In brackets, for each PC, explained variance. Spanish data are the blue boxes, and Italian data the orange dots.

Figure 6. Scores plot for NIR spectra of the calibration set in PLS-DA. Model with 2 factors. Blue box: Spanish origin. Orange dot: Italian origin. In brackets, for each factor, X variance and Y variance explained by the factor.

Figure 7. Predicted by cross validation vs reference values of the NIR spectra of the calibration set in PLS-DA. Model with 2 factors. Slope: 0.948. Offset: 0.077. RMSECV: 0.116. r^2: 0,947. Blue box: Spanish origin. Orange dot: Italian origin.

Figure 8. Classification of the NIR spectra of the prediction set using a PLS-DA model with 2 factors. The blue box around the predicted value spans the deviation and it is an estimate of the prediction uncertainty.

Hyperspectral camera

Computer display

Energizing unit (i.e. lighting)

Translation stage (i.e conveyor belt)

Hyperspectral camera and support unit (detail)

Figure 1.

Figure 2.
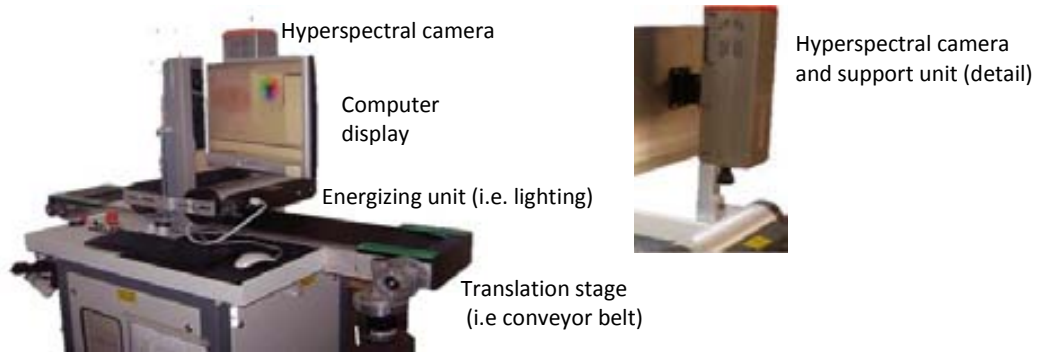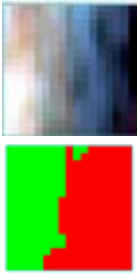
Spanish ham

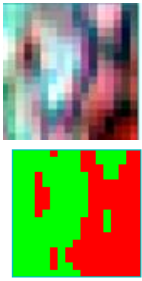A 1)   A 2)   A 3)

Spanish ham

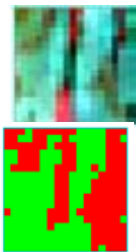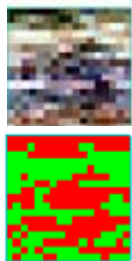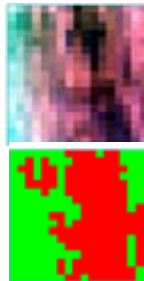A 1)   B 2)   B 3)   B 4)

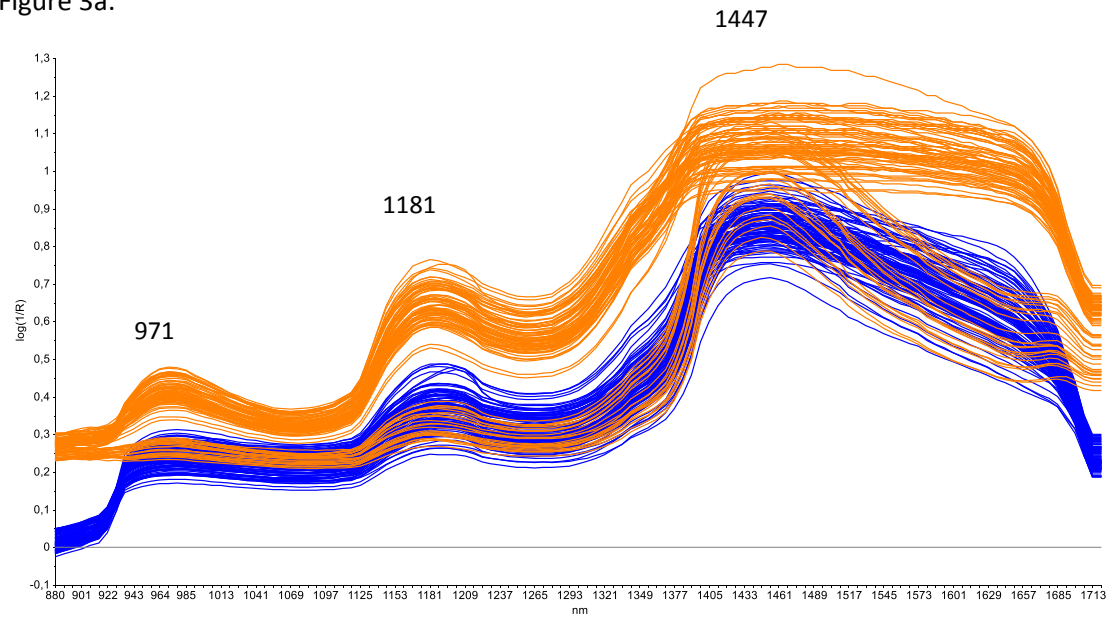ITALIAN HAM

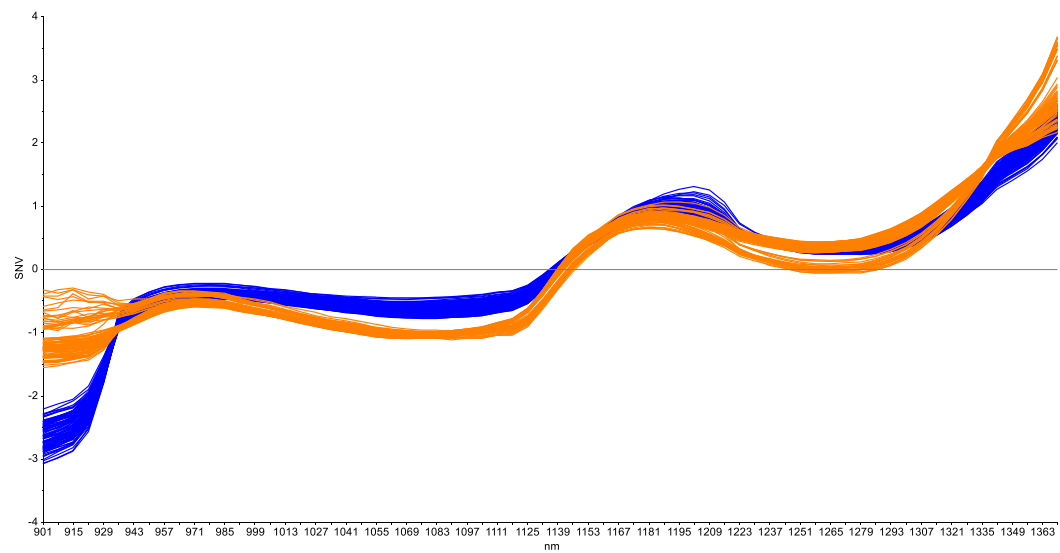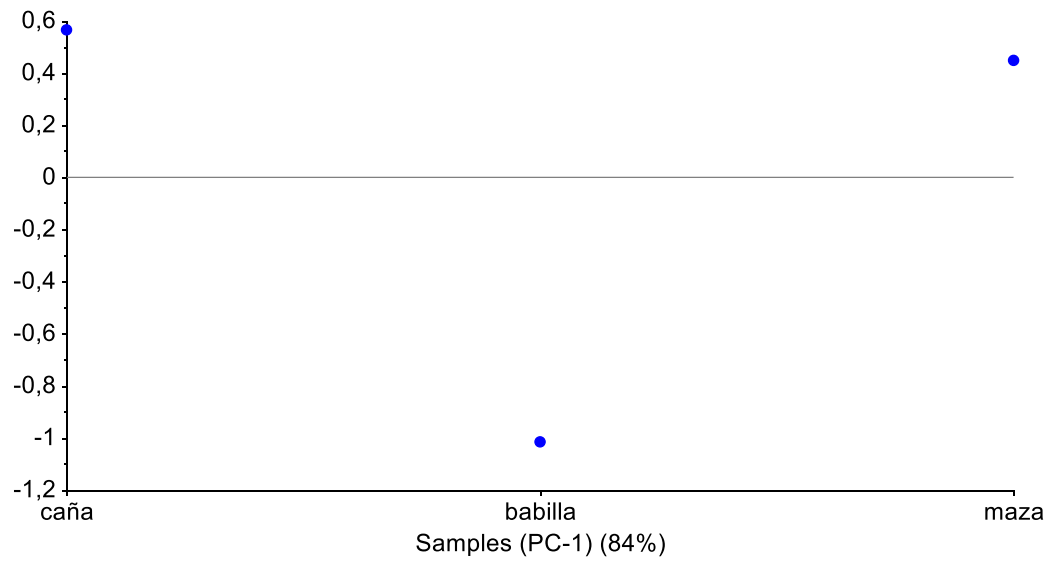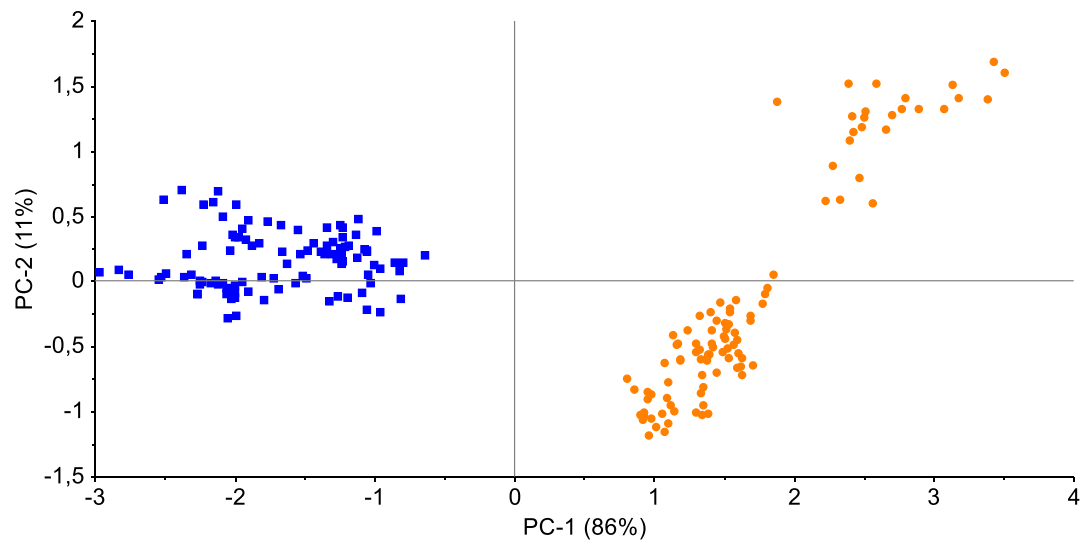C I)   C 2)   C3)   C 4)
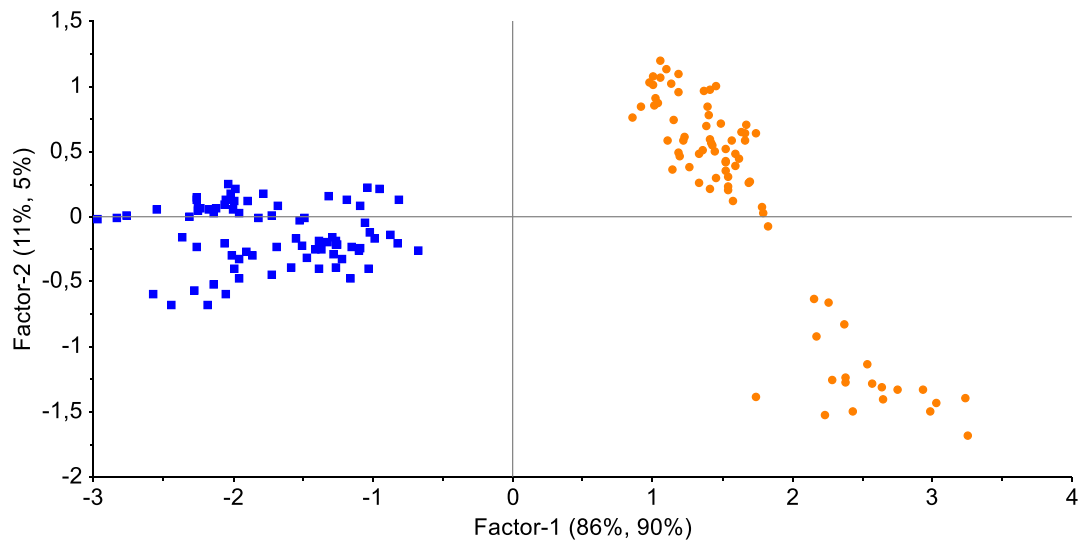
Figure 3a.

Figure 3b.

Figure 4.

Figure 5

Figure 6.

Figure 7.
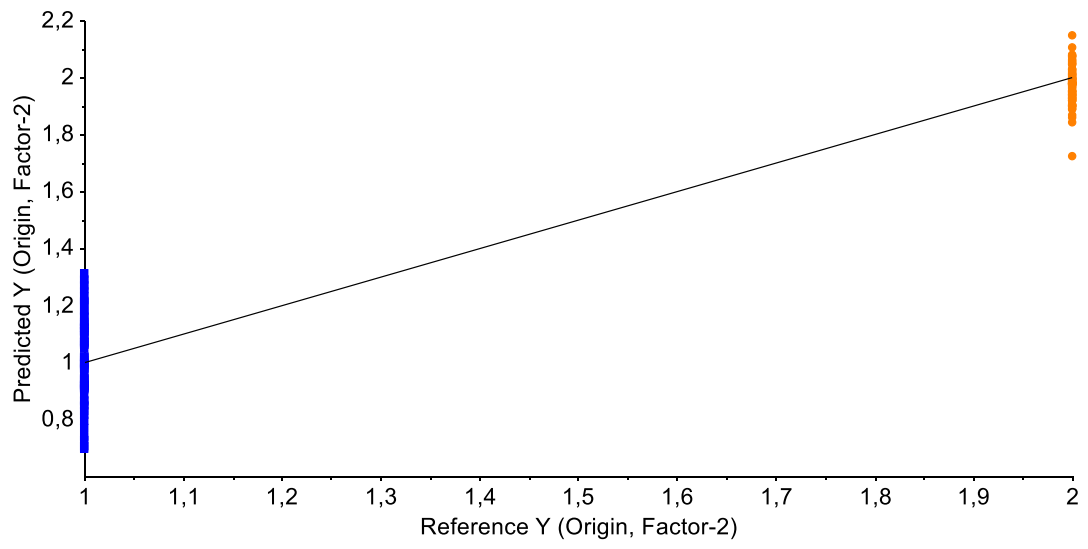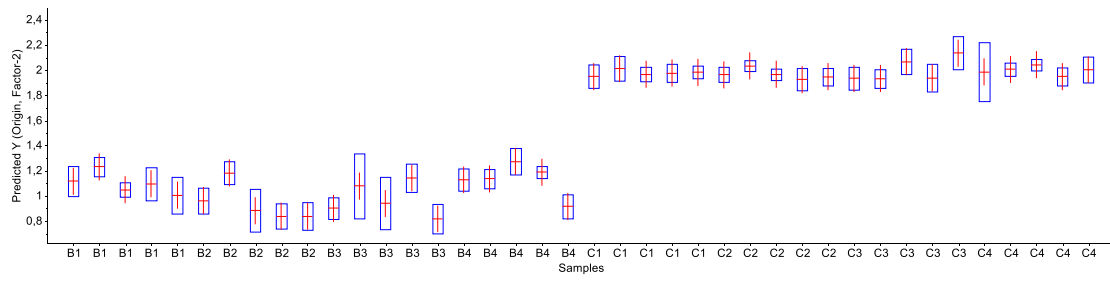
Figure 8.

ANEXO III

Speciation of Iron and Zinc in Iberian cured ham by XANES (EN PREPARACIÓN)

Speciation of Iron and Zinc in Iberian cured ham by XANES

Maribel Restituyo Silis[1], Marta Avila [2], Manuel Valiente[1]*

[1] Universitat Autònoma de Barcelona. Dept of Chemistry. Center GTS. Campus de la UAB, 08193 Bellaterra (Barcelona), Spain

[2] Alba Sincrotron, (Barcelona), Spain

Abstract

The X-ray absorption near-edge structure (XANES) was used to identify directly the metal speciation and local bonding environment of Fe and Zn in Iberian ham collected in Huelva, Spain. Special attention was paid to analysis of samples collected from different cured time. The combination of of of traditional approach to data as well as usage of multivariate techniques provided reliable information on the local Fe and Zn structure. The obtained average oxidation state of Fe species in all samples was found to be at about +3, for Zn the most species found in our samples were inorganic. The number and proportion of metals species in ham samples were calculated by a coupled Principal Component Analyzed (PCA) and Linear Combination Fitting (LCF) procedure. However, the results show that in our samples the oxidation state of Fe is a combination from Fe+2 to Fe+3 while the percentage for Fe+2 is more in the inner region of the muscle occurs the opposite in the outer region and contrariwise. In case of Zn, the percentage of inorganic compounds are always more than organic compound. For the XANES spectra of samples with different cured time and from different sampling site, we observed obvious differences, except the spectra corresponding to 40 months of curing where the spectra look similar between them.

Introduction

Process traceability is a difficult task when it concerns long time food processing. It is the case of ham curing procedure. The curing of ham is also associated with a color darkened evolving of meat during the curing process. When this process is carried out without the addition of nitrite and nitrate salts the color change is due to an ion exchange process between Fe and Zn ions. The dry-cured Iberian ham is an interesting product in this respect since it is characterized by a corresponding change of red color despite neither nitrite nor nitrate are added during the process. [1]

The red pigment extracted by acetone/water (75%/25%) emitted strong fluorescence and was identified as Zn Protoporphyrin IX (ZPP) by mass analysis. [2] ZPP, which is a Zn protoporphyrin complex, is structurally similar to him, which is an Fe-protoporphyrin complex. [3] However, the mechanism of ZPP formation is still speculative and the relationship between ZnPP and Fe-protoporphyrin formed in dry-cured ham has not been elucidated.

X-ray absorption fine structure (XAFS) is a powerful technique to investigate chemical speciation. The XAFS in which the energy region is near the absorption edge is called X-ray

absorption near edge structure (XANES). It provides information of electronic structure of absorption atoms and reflects oxidation state and chemical speciation of elements. The XANES spectroscopy can be used as a "fingerprint" to compare with those of reference material to obtain the information of speciation. The technique is a non-destructive, keeping the original speciation in the samples, thus relative information can be obtained. As different elements have different absorption edge energy, the interference among elements is small. Usually the technique is performed with synchrotron radiation source, the high intensity and other advantages of synchrotron radiation significantly improve the precision of experiments. [4]

XANES spectroscopy is an element-specific technique that can provide information on the oxidation state and the coordination environment of metal ion in the sample. K-edge XANES spectra are recorded by monitoring the absorption of X-rays, associated with the excitation of a K shell electron to a higher energy state, as a function of X-ray energy. The onset of these transitions gives rise to the K absorption edge. In this work, absorption is detected from the intensity of the Fe and Zn K transmission, emitted when an outer-shell electron falls into the K-shell vacancy created by the electronic transition. The energy and intensity of the transition are dependent upon the oxidation state, coordination symmetry, and ligand type, and thus, XANES features can provide detailed chemical information. In general terms, transitions (including the absorption edge) shift to higher energy with increasing oxidation state and gain intensity in low-symmetry environments.

As an example of the application of XANES, study carried out us on speciation of iron and zinc in their organic sample presented here. XANES spectrum reflects he local structure around the adsorbing atom and provides information about oxidation state of an excited atom and the coordination symmetry. By talking references of well-defined chemical species, analysis of XANES can be used to determine metal speciation, i.e., determination of the chemical forms along with the relative quantity of the different species in a given sample. For speciation using XANES, the commonly used methods are: principal component analysis (PCA), target transformation (TT) and linear combination fitting (LCF).

The XANES spectra obtained allow the identification of Fe and Zn species in target samples containing low concentrations of Fe that have not been altered by extraction techniques, the ability to distinguish between compounds of the same metal and between different compounds with the same oxidation state, as well as a semi-quantitative determination of oxidation states present in each sample. To our knowledge, this is one of the few studies to describe Fe oxidation states and speciation in Spanish dry-cured ham.

The aim of our work was to investigate the Fe and Zn species are involved during the ripening of Iberian hams.

Samples and methodologies

2.1 Samples collections

Four samples of muscle of Babilla o Contramasa were removed from four hams in different stages in the processing of Spanish Iberian dry-cured ham: after salt equalization (t≈3 months) and after different drying times (t≈ 14, 26 40).

The Babilla muscle samples were cut into small pieces using a ceramic knife and prepare a serial longitudinal and transverse sections (10 μm thick) were in the outer region and in the inner region of muscle reference (ma) and (mb) respectively.

2.2 Methodologies

2.2.1 Synchrotron radiation

The XANES spectra were measured at the XAFS station of MAX-LAB Synchrotron Radiation Facility. The BALDER line on the MAX IV 3 GeV ring has focused on a high flux of photons in a wide energy range, 2.4-40 KeV. The kedge absorption of the element was measured with a double crystal monochromator with in-vacuum interchangeable Si (111) and Si (311) crystals. Data collection was done in continuous scan from 7045.750000 to 7175.750000 for iron and 9595.760000 to 9725.760000 for zinc, in mode transmission with 100 step and 10 s acquisition time per point.

2.2.2 Xas experiment and data analysis

For iron, a total of 13 references spectra were considered, Iron chloride, ammonium iron (II) sulfate hexahydrate, Cytochrome C, Hemoglobin porcine, 5, 10, 15, 20-Tetrakis (pentafluorophenyl) -21H, 23H-porphyrin iron (III) chloride, Myoglobin, Hemin, Hematin, Iron oxide (II), Goethite, hematite, Magnetita, iron chloride (II). For zinc a total of 7 reference spectra was considered, including Zinc metallic foil, Zinc chloride, Zinc sulfate, Protoporphyrin IX zinc, Zinc metallothionein and 5, 10, 15, 20-Tetraphenyl-21H, 23H-porphine zinc, Zinc sulfite. The spectra for zinc metal foil, Goethite, hematite, Magnetite were donated in collaboration with other research groups. Except Zinc metallothionein, all other iron and zinc compounds were bought from Sigma Aldrich, a chemical reagent company in America. All reference spectra were collected in transmission mode using ionization chambers. Prior to XAS experiments, each iron and zinc compound was diluted with cellulose to obtain an edge jump of about one. In case of the samples, the concentration of these elements is quite low (μg/g level), in order to improve the intensity

of the signal, the fluorescence mode with great incident angle was used. During the experiments, different detectors were used based on the Fe and Zn content contained in each reference and sample. For references spectra were recorded in transmission mode using ionization chambers, for samples spectra were recorded in fluorescence mode. The sample was put on a movable shelf, thus the incident angle of the beam can be regulated, measurements were performed at room temperature. Depending on Fe and Zn concentration several scans were averaged to improve the signal-to-noise ratio of XANES spectra.

Data reduction (deducted background and normalized) was carried out using the special software Xanes Datyloscopie, developed by DR. Konantin Klementiev.

By comparing the XANES spectra of zinc-containing Iberian ham with the reference, we were performed using fitting by user-defined formula, a method where reconstructs the sample spectrum using a combination of selected model spectra.
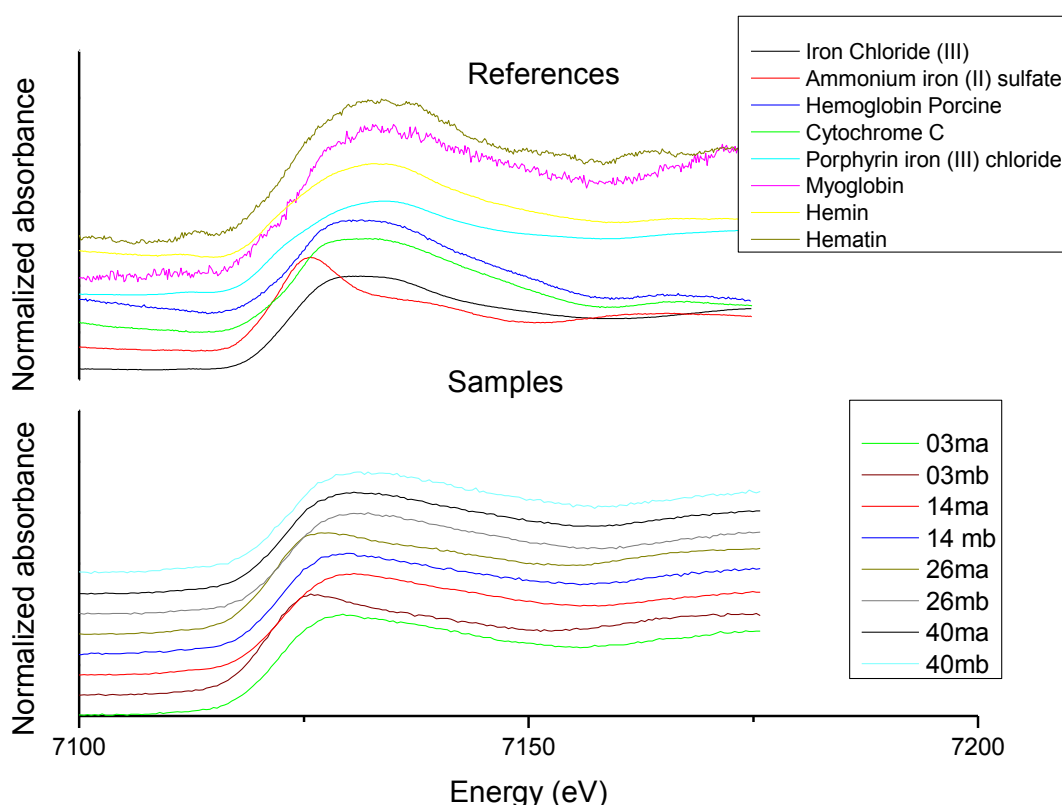

Figure1. XANES spectra at the Fe-K absorption edge for both Iron references and sample spectra. The spectra are presented after a background removal and
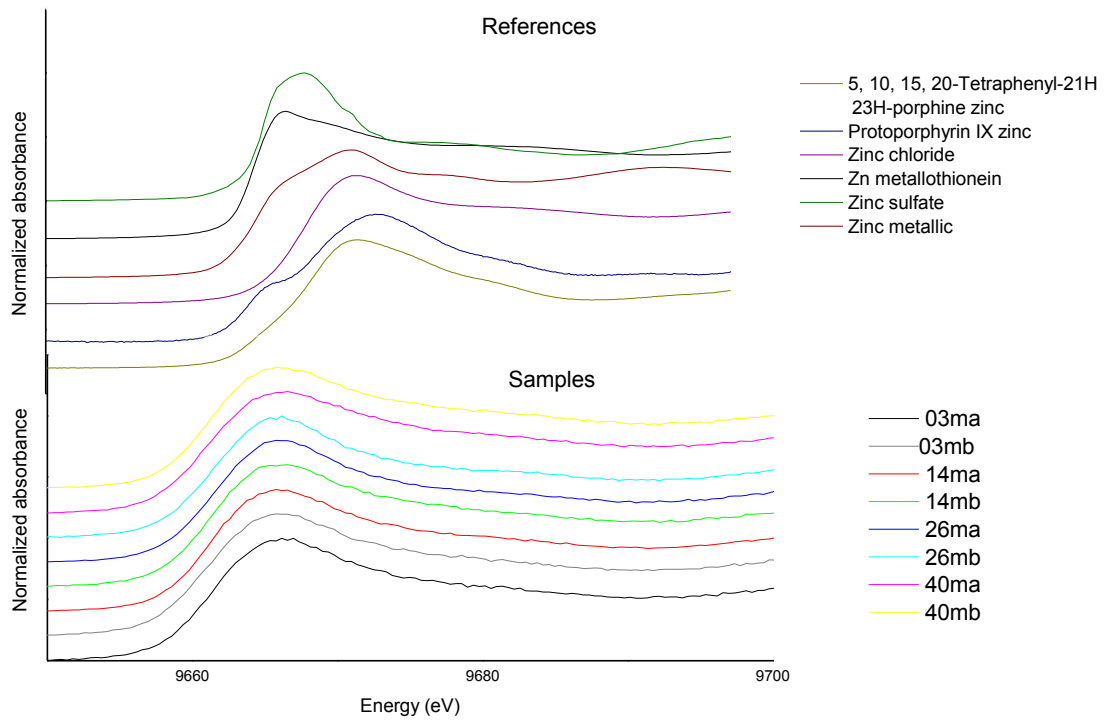
normalization was accomplished.

Figure2. XANES spectra at the Zn-K absorption edge for both Zinc references and sample spectra. The spectra are presented after a background removal and normalization was accomplished.
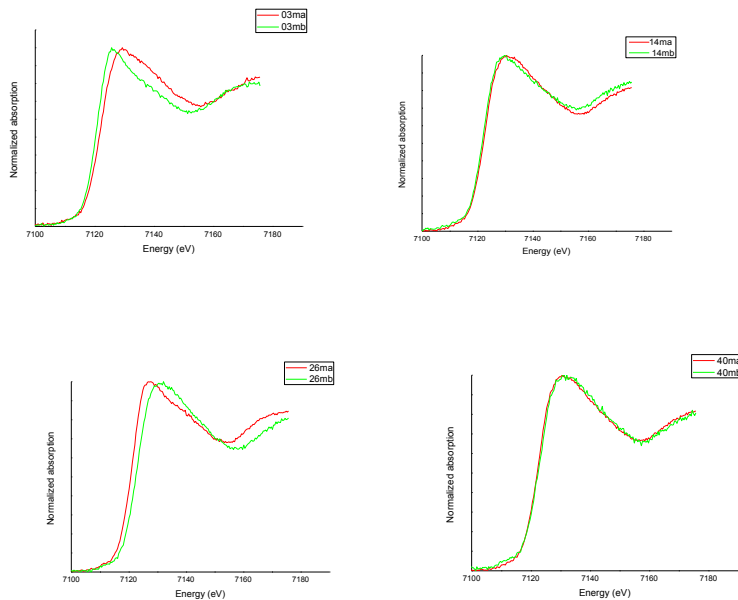

Figure 3. Fe sample spectrum. Comparison between spectra of the same curing time and different region, outer (A) and inner region (B) from Iberian ham.
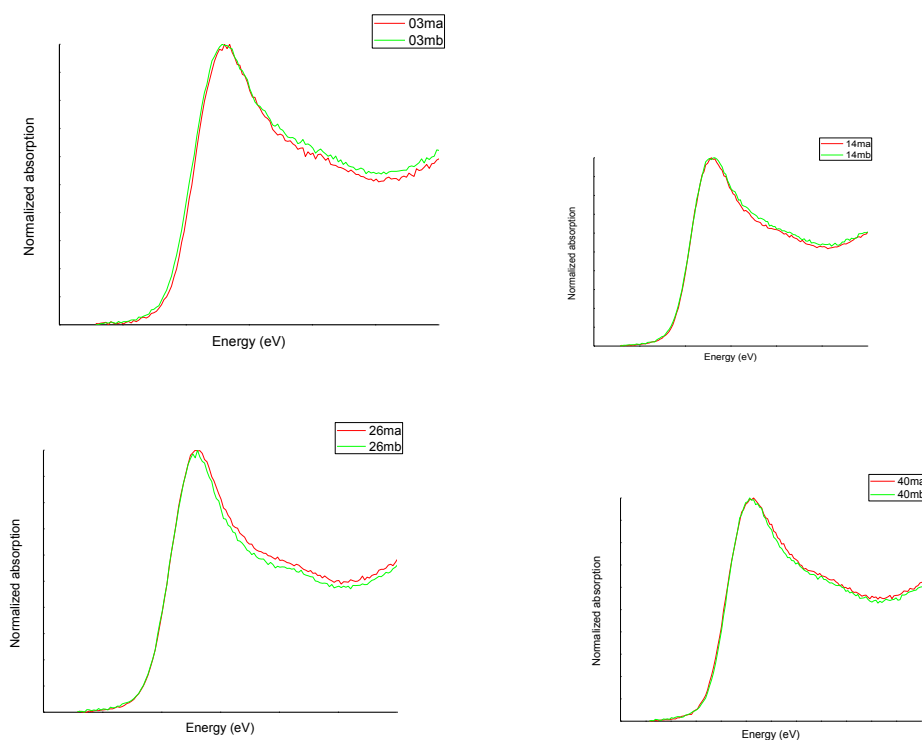
Figure 4. Zn sample spectrum. Comparison between spectra of the same curing time and different region, outer (A) and inner region (B) from Iberian ham.

Data analysis

For data interpretation, principal component analysis (PCA), target transform testing (TT), and linear combination fitting (LCF) were carried out using XANDA Dactyloscope (Konstantin Klemetiev, Maxlab Synchrotron Radiation Laboratory) for constructing the difference spectra and determining the position of the edge corresponding to the point having µx=0. 5 in the normalized spectrum.

PCA analysis was used to obtain information about the number of components (significant independent sources of variations) statistically meaningful to quantitatively reproduce the experimental data set of normalized XANES spectra. Primary components refer to those, which contain the signal and, in principle, are sufficient to reconstruct each experimental spectrum by suitable linear combination. Secondary components refer to those, which contain only the noise. A major advantage of PCA approach is that no a priori assumption is needed as of the number of references and the type of reference compounds used.

As default the number of components necessary to reconstruct the experimental spectra is limited to those components that show significant eigenvalues/ weights.

PCA analysis of the total XANES spectra, excluding the reference compounds indicated that only have tree principal compounds for Fe and Zn, thus it is possible to reduce by this method all the XANES spectra data using the three components (abstract components. All other components are below of level of experimental noise.

In the figure 5 show the visual interpretation,with the amplitude of the components.

After confirming the number and identity of components in the eight ham samples by using PCA and TT, we performed the LCF. (See figure 5 for iron and 6for zinc), as the significant components defined in the PCA have no chemical or physical meaning, TT procedure attempts to determine if a chosen reference spectrum (i.e., from a given model compound) can be considered as a legitimate "end-member" component. Mathematically, this means that it can be represented in the same mathematical space as defined by the components of the same spectra. This was done by multiplying the reference spectrum by the eigenvector column and row matrix. If this resultant spectrum matches well with the reference, then the reference spectrum is a possible species in the unknown data sets.
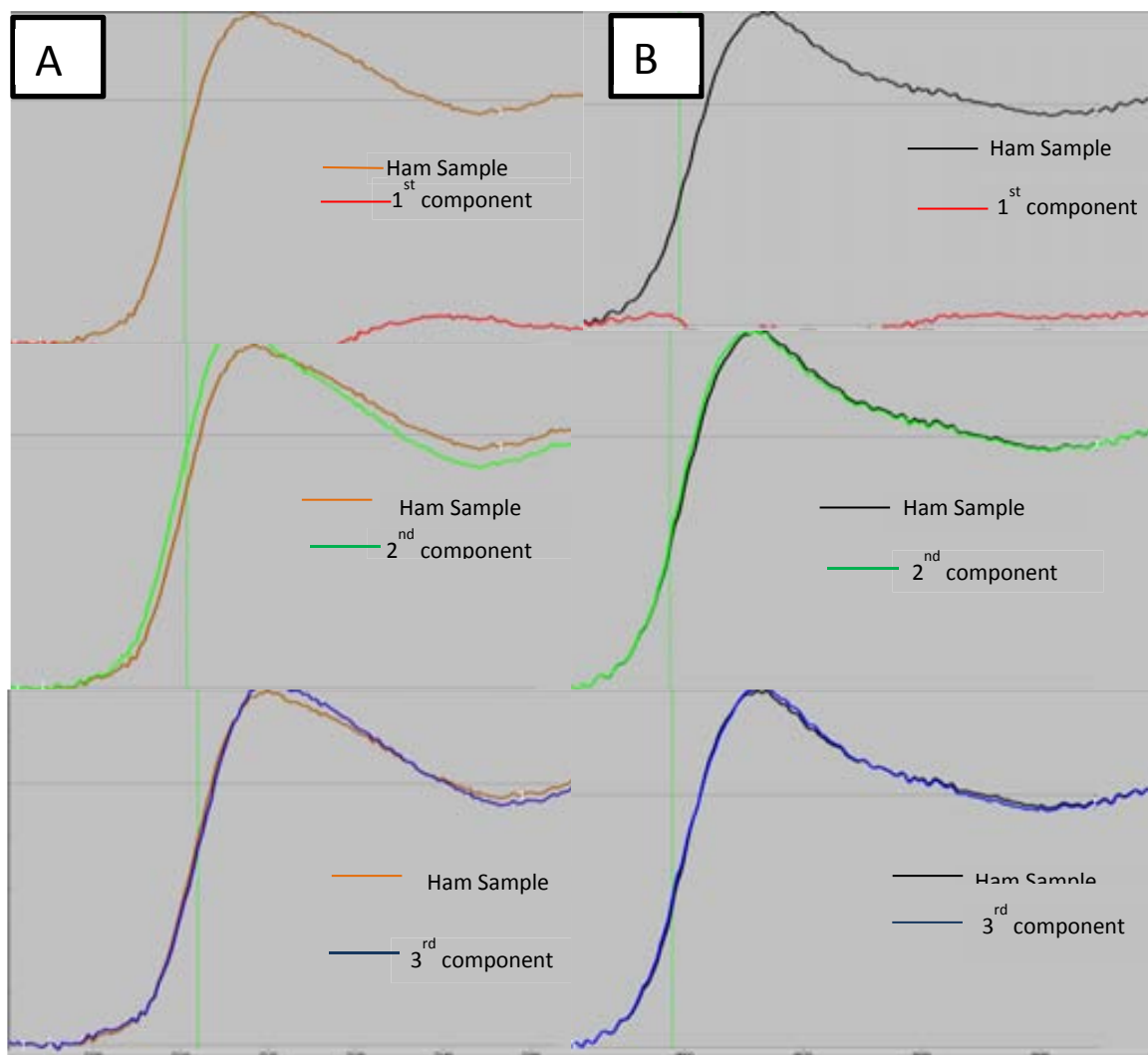
Figure 5. Abstract component obtained by PCA; A Iron and B Zinc
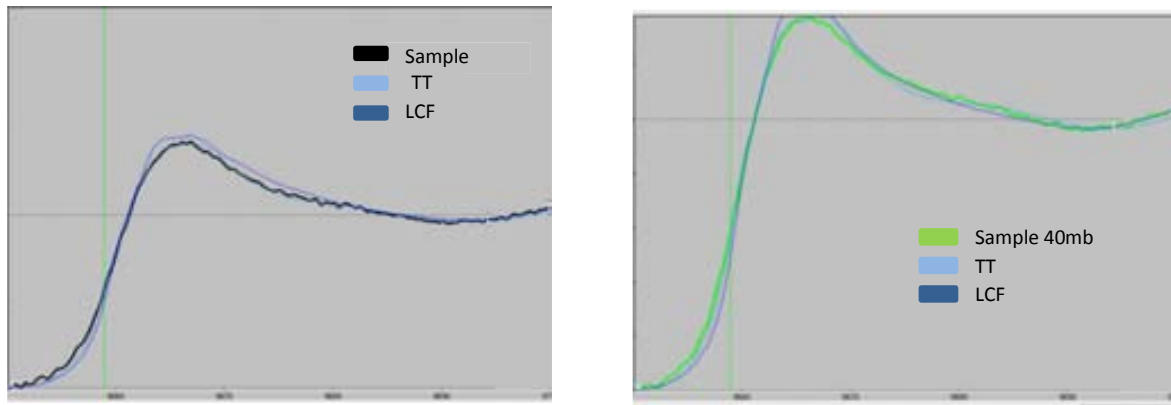
Figure 6. Zinc TT and LCF results, the corresponding XANES spectra together with their transformed spectra previously identified by TT. Fitting was optimized by minimizing the residue of the fit, for all accepted fits R was ≈6.
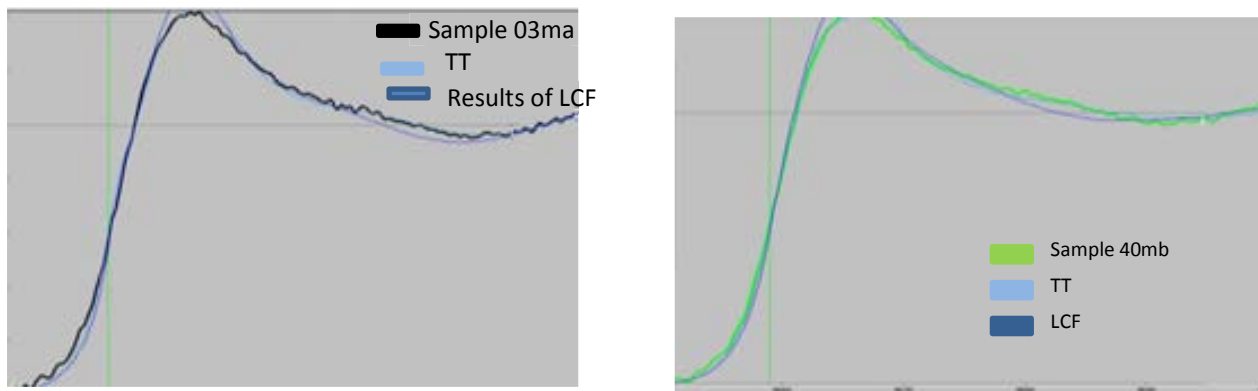
Figure 7. Zinc TT and LCF results, the corresponding XANES spectra together with their transformed spectra previously identified by TT. Fitting was optimized by minimizing the residue of the fit, for all accepted fits R was ≈6.

Visual examination was also used to check the consistency of fit. For Zinc the best fits for ham samples spectra were obtained with a combination all references spectra.

As can be observed in the ham sample that we presented (see the material support for the other ham samples) the line belonging to the TT and LCF are very similar to the sample, the points where have the most differences between them are in the EXAFS region, for the rest of the points seem very similar.

Results and discussion

In our results, in case of iron, we found a significant differences between samples, only the sample with 40 months of curing has the same contribution of the same reference compound in its composition, as we expected in the case of zinc the situation is more stable due to their Zn composition is not complicated, this conclusion could be supported in its the reconstruction of the spectra which are very similar between sample, TT and LCF.

The difference of Fe spectra obtained from ham samples (Fig.3) as can be seen a very good agreement with the experimental data was obtained that presented in the table 1.

We had thirteen references spectra in total, however, two of them (Hemoglobin and Cytochrome C) are not considered in final results because they are not presented in ham sample.

The fit of the above two elements was performed and the result of the references contribution is shown in the figure 7 and 8.
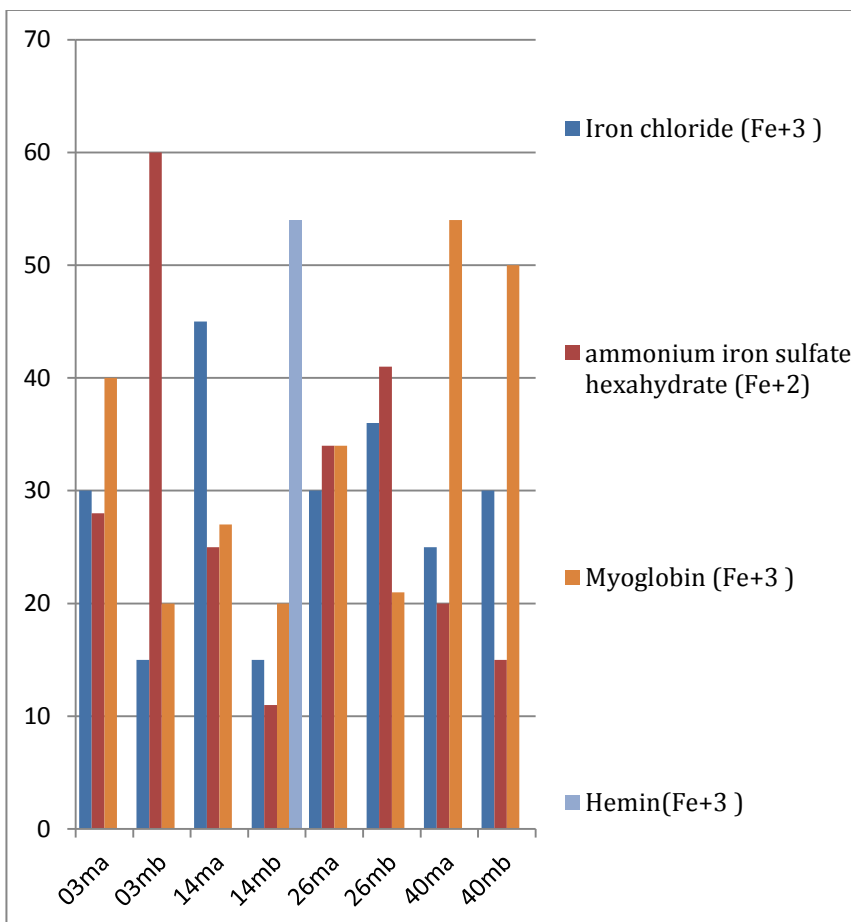
Figure 8. Percent contributions of each Fe reference spectrum to the fit obtained from the four ham samples, obtained from fitting by user formula analysis. The reference that has not a contribution in our sample, It is not considered.
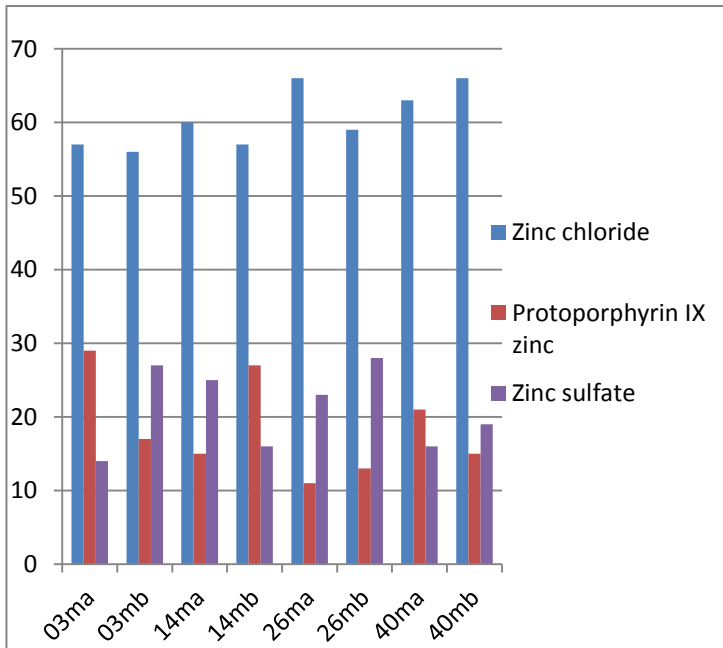
Figure 9. Percent contributions of each Zn reference spectrum to the fit obtained from the four ham samples, obtained from fitting by user formula analysis.

Despite the fact that Iberian ham is an organic material, thus a very complex system, the fit has performed satisfactorily.

We reported the best fitting result, in case of iron the R value is ≈6 and for zinc the R value is ≈ 4, the R-factor reported that:

$$\frac{Sum\ ((data\text{-}fit)\ \^{}2)}{Sum\ (data\^{}2)}$$

XANES spectra are best interpreted with reference to a series of standards in which the oxidation state and coordination environment are well understood.

Time of curing	Region		Fe^{+2} (%)	Fe^{+3} (%)
03	Outside	Org	----	40
		Inorg	28	30
	Inside	Org	----	20
		Inorg	60	15
14	Outside	Org	----	27
		Inorg	25	45
	Inside	Org	----	74
		Inorg	11	15
26	Outside	Org	----	34
		Inorg	34	30
	Inside	Org	----	21
		Inorg	41	36
40	Outside	Org	-----	54
		Inorg	20	25
	Inside	Org	-----	50
		Inorg	15	30

Table 1. The percentage of contribution for Fe^{+2} and Fe^{+3} present in the Iberian ham

Time of curing	Region	Zn organic (%)	Zn inorganic (%)
03	Outside	29	71
	Inside	17	83
14	Outside	15	85
	Inside	27	73
26	Outside	11	89
	Inside	13	87
40	Outside	21	79
	Inside	15	85

Table 2. The percentage of organic and inorganic Zinc compound present in the Iberian ham.

Reference

1. Parolari, G., Benedini, R., & Toscani, T. (2009).Color formation in nitrite-free dried hams as related to Zn–protoporphyrin IX and Zn–chelatase Activity.Journal of Food Science,74, C413–C418.

2. Wakamatsu, J., Nishimura, T., & Hattori, A. (2004a). A Zn–porphyrin complex contributes to bright red color in Parma ham. Meat Science,67, 95–100.

3. Wakamatsu, J., Odagiri, H.,Nishimura, T., & Hattori, A (2006). Observation of the distribution of Zn protoporphyrin IX (ZPP) in Parma ham by using purple LED and image analysis. Meat Science,74, 594-599.

4. Wang l., Lu X., Wei X., Jiang Z., Gu S., Quian G., and Huang Y. Quantitative Zn speciation in zinc-containing steelmaking wastes y X-ray absorption spectroscopy.J. Anal. t. Spectom., 2012, 27, 1667.

5. Martín L., Antequera T., Ventanas J., Benítez-Donoso R., Córdoba J., Free amino acids and other non-volatile compounds formed during processing of Iberian ham. Meat Science 59. 2001 363-368.

ANEXO IV

Intercomparison of Arsenic species in mollusks from coastal region SUDOE using LC-ICP-MS and Synchrotron technique. (EN PREPARACIÓN)

Intercomparison of Arsenic species in mollusks from coastal region SUDOE using LC-ICP-MS and Synchrotron technique

Maribel Restituyo[1], Riansares Muñoz[2], Carmen Camara[2] and Manuel Valiente[1]

1) Universitat Autònoma de Barcelona. Dept of Chemistry. Center GTS. Campus de la UAB, 08193 Bellaterra (Barcelona), Spain.
2) Department of Analytical Chemistry, Faculty of Chemistry, Universidad Complutense Madrid, Ciudad Universitaria, 28040 Madrid, Spain.

Abstract

The aim of this study was to evaluate the bioavailability of arsenic (As) through wild and cultured mollusks from tree coastal SUDOE region (France, Portugal and Spain). The marine species from France and Portugal were wild oyster and species from Spain were cultivated mussels, the total arsenic and chemical speciation of this element were analyzed for conventional technique ICP-MS for total As and LC-ICP-MS and HPLC-ICP-MS for As speciation.
The concentrations of As in oyster dry tissue fluctuated between 18 µg/g for mussel dry tissue 14 µg/g. Arsenic speciation indicated arsenobetaine as the major arseno-compound for Both 79-47 % respectively.
 A strong positive correlation was observed using XANES technique which revealed the presence of predominantly arsenic compounds is arsenobetaine. The best combination linear fit results for Oyster were more than 80% and for mussel more than 65 %.

Introduction

Arsenic and arsenic compounds are well known as pollutants in aquatic ecosystems, they are naturally present in marine ecosystems, and these can become contaminated from mining activities, which may be of toxicological concern to organisms that bioaccumulate the metalloid into their tissues. Humans are exposed to arsenic sources that can occur naturally and through anthropogenic inputs to the environment, and this exposure can lead to a wide variety of adverse effects on health, including skin and several internal cancers and cardiovascular and neurological effects, attributed to chronic exposure to high levels of As, primarily from drinking water and food [1, 2]. About 70 % of arsenic uses are related to production of pesticides, principally monosodium methane arsenate (MSMA), disodium methane arsenate, dimethylarsinic acid (cacodylic acid), and arsenic acid [3]. Also, arsenic has been used in medicine, veterinary drugs, and in the manufacture of glassware, metal alloys, microelectronics, and wood preservatives [3–6]. The toxic properties of arsenic are dependent on the chemical form in which it is found (e.g., toxic inorganic arsenicals species vs the organic forms of arsenic such as arsenobetaine are non-toxic) []. In the SUDOE region, including France (the Arcachon Bahia, Portugal (Sado Sea) and Spain (Mediterranean Sea, specifically in Delta del Ebro) there are important fisheries, human settlements, industrial developments, and activities such as intensive agriculture, aquaculture, and poultry. Arsenic has been investigated in biota from this region, with only some measurements

reported for the oyster [7] and mussels [8]. Both wild oyster species and cultivated mussel are widely utilized for human consumption and have important commercial value were investigated.

The aim of the present study was to provide information on As levels and the presence of arseno-compounds in this mollusk from different locations along the coast of France, Portugal and Spain. Additionally, we combine the results with the traditional techniques in order to evaluate the total As concentration and a possible correlation with our studies.

Materials and Methods

Study Area and Sampling

The European Proyect ORQUE_SUDOE The wild oysters were collected from three different coastal:

    S1- Bahia de Arcachon (France)

    S2- La Rocher (France)

    S3- Sado Sea (Portugal)

The cultivated mussel was collected from:

    S4- Delta de Ebro (Spain)

Each sample consisted of 50 Kg (oyster) and 20 Kg (mussel) with similar size (75-100 mm). No shell or soft tissue abnormalities in the collected mollusks were found. Just after sampling, live mollusks were transported to the laboratory and subsequently freeze-dried over 72 h (-49 °C) and then removed the mollusks without shell and liophilazed and pulverized into homogenized powder. This powder used for two purposes (to do the pellets for the synchrotron and for analysis of As total), the first step was the analysis of total AS, samples (0.500±0.003 g of dry tissue) were digested with 3 ml of H_2O_2 (30 %) and 5 ml of concentrated and purified HNO_3 (puriss p.a. ≥65 %) in a Digi-prep digestion system. The mixture was heated to 50 °C for 60 min and then increase the temperature to 90 °C maintained under these conditions for 3 h. The samples were diluted with MilliQ water to a final volume of 10 ml. Blank samples and standard reference material (lyophilized mussel tissue) [9] were digested with the same procedures to control for accuracy and precision. The total As Analysis was determined using ICP-MS. The total metal content is given the table 1.

Procedures for speciation analysis

Chemical speciation of As was determined for other fellow laboratories of ORQUE SUDOE project.

The second step was to perform pellets of dry-homogenized mollusks of the same size (1 cm).

The reference material used in order to compare ours samples were:

As_2O_3 (labelled as As^{III}), $C_5H_{11}AsO_2$ (AsB) and As_2O_5 (As^V).

Samples	Elements [ppm]						
	As	Se	Zn	Cr	Cu	Ni	Pb
1	18	4,82	1882	1,0	121	1,0	1,1
2	23	4,69	2174	0,9	143	0,9	1,0
3	15	5,10	112	2,7	7,5	2,7	3,1
4	15	2,96	1029	0,8	47	0,7	0,5
5	19	4,53	2222	1,2	254	0,9	1,0
6	26	3,24	2128	1,0	67,5	0,6	1,2
7	22	3,08	1524	1,6	143	1,3	1,0
8	11	2,72	3858	1,0	630	1,9	0,5
9	12	2,26	97	0,6	3,41	1,0	0,2
10	13	2,51	1273	0,6	67	1,0	0,8

Table 1. Total concentration of the elements analyzed.

Statistical Analysis

In order to estimate the reproducibility and calculated the coefficient of variation of total As content, we extrapolate our data in the multiple-comparison test with the other results from different laboratories involved in the project, the total variance was less 2 % (the results it not present).

X-ray Absorption Spectroscopy (XAS analysis)

XAS analysis was carried out at the Alba synchrotron facilities, Arsenic Kedge (11867 eV) XANES (X-ray Absorption near edge structure) spectra were Measured at CLAESS beamline.

The white radiation beam coming from the CLAESS wiggler has been monochromatised using a double crystal Si (111) monochromator. Higher harmonic contribution to the selected energy has been eliminated setting a rejection angle in the vertical focusing mirror of about 3.7 mrad. A beam size of FWHM 2000x1000 mm2 was used. Due to the low As the concentration in most of the sample (less than 20 ppm) measurements on four samples have been performed in fluorescence mode by means of an

Amptek CdTe detector. Reference spectra on As_2O_3, $C_5H_{11}AsO_2$ (AsB), and As_2O_5 were collected in transmission mode by means of ionization chamber detectors.

Results and Discussion

Arsenic concentrations are summarized as mean values for each mollusk sample in Figure 1.

The comparison between different sample spectra and reference compounds are given in figure 2.

No radiation damage has been detected within the spectral noise. Oyster spectra show very similar XANES features, characterized by a very sharp "white line". No significant edge shift is observed in the four samples, indicating that in all the samples As is found with the same oxidation state (As^{+3}). Remarkably oyster XANES spectra results are very similar to the spectrum collected on the arsenobetaine. In the following we use as a quantitative approach in the speciation of As least-squares linear combination

(LC) fitting, i.e. we refine the sample spectrum directly as a sum of the references spectra adjusting the fraction of each component in the sum. Since all the spectra have been correctly calibrated, no energy offset has been included in the fitting procedure.

Athena package has been used in the data analysis.

The LC fit of sample 1 is shown as an example in figure 3, where the weighted standard compounds and the best LC fit curve are also shown.

Results obtained on the four samples are reported in Table 2. As evident from the table, the major component identified in these samples is arsenobetaine (AsB).

The XANES technique detects the presence of the oxidation state of As and the dominant compound, a parallel analysis by the UCM using LC-ICP-MS, reported that the concentration ranges of arsenobetaine fall from 60 to 80% the total amount of arsenic.
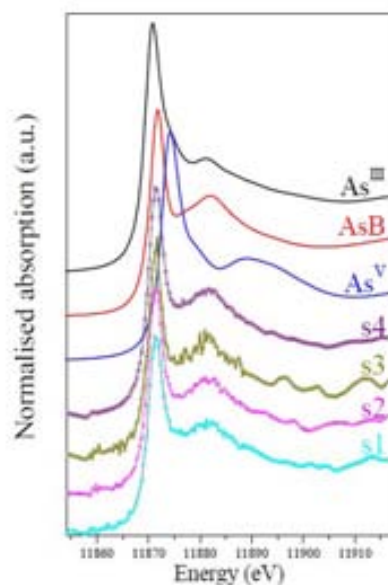
Figure 2: As K-edge spectra collected on sample 1, sample 2, sample 3, sample 4 respectively. As_2O_3 (labelled as AsIII), C5H11AsO2 (AsB) and A_2O_5 (AsV) are also shown for comparison
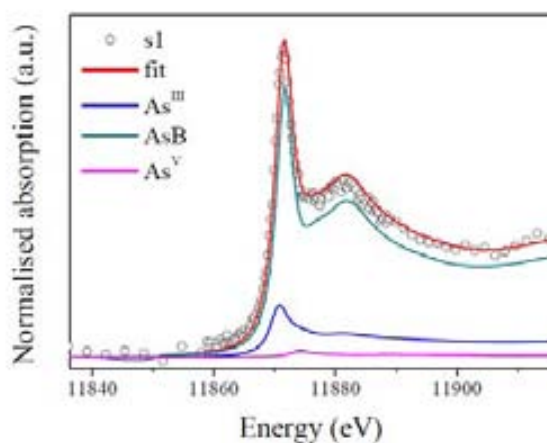
Figure 3: Linear combination fittings of binary mixtures of sample1. References weighed after the fit are also shown.

Muestra	Parámetros	AsB	As^{III}	As^{V}
S1	R=0.0208, X^2=0.15, RX^2=0.008	85±4	15±4	
S2	R=0.024, X^2=0.38, RX^2=0.010	71±6	29±12	
S3	R=0.018, X^2=0.05, RX^2=0.0081	96±7	4±1	
S4	R=0.018, X^2=0.30, RX^2=0.010	75±5	25±5	

Table 2. Summary of linear combination fittings of XANES spectra of oyster samples.

The results of the fit were performed in Athenas program, which calculate speciation of arsenic in

samples of oysters and mussels of different sampling points S1, S2, S3, S4. The same treatment used,

standardization and calibration of energy was used for all spectra before making the setting in the range of energy comprised of 11847 to 11897 eV, including 129 spectral points.

Setting a linear combination, it means that considers the spectrum of the sample directly as a sum of reference spectra trying to set the fraction of each component in the sum. Since all spectra have been calibrated correctly without displacement of energy that has been included in the adjustment procedure.

We first analyzed the total concentration of arsenic and then by speciation same absorption spectra and whose percentages in treating linear fit has been corroborated by other speciation studies by LC-ICP-MS, showing that this technique is very precise when making speciation.

Based on the results, we can say that:

- ✓ *By analyzing experimental XANES spectra in the K-As edge and overlap with references, we observed a correlation compatible with the dominant reference (ASB).*

- ✓ *In addition, adjusting linear combination gives us the exact percentage of influence that has references used in each of our samples, AsB being the major component in all of them.*

- ✓ *The samples collected from the west coast of France, open to the Atlantic sea, shows interaction with respect to the content of As^{III} with other metals, which means that for the sample S1 which has a 15% As^{III}, concentrations of Cu, Zn, Se, Cr, Ni, Pb, are smaller than S2 has the sample containing 29% of As^{III}. This trend of these samples (oysters) from France, could be the result of the impact of this species as mentioned earlier interferes with some performances and physiological stress response.*

Bibliography

1. Le XC (2002) Arsenic speciation in the environment and humans. In: Frankenberger WT (ed) Environmental chemistry of arsenic. Marcel Dekker, New York, p 95

2. Liu C, Liang C, Huang F, Hsueh Y (2006) Assessing the human health risks from exposure of inorganic arsenic through oyster (Crassostrea gigas) consumption in Taiwan. Sci Total Environ 361:57–66.

3. Kumaresan M, Riyazuddin P (2001) Overview of speciation chemistry of arsenic. Curr Sci 80:837–846

4. Mandal BK, Suzuki KT (2002) Arsenic round the world: a review. Talanta 58:201–235

5. Peshut PJ, Morrison RJ, Brooks BA (2008) Arsenic speciation in marine fish and shellfish from American Samoa. Chemosphere 71:484–492

6. Shah AQ, Kazi TG, Arain MB, Jamali MK, Afridi HI, Jalbani N, Baig JA, Kandhro GA (2009) Accumulation of arsenic in different fresh water fish species—potential contribution to high arsenic intakes. Food Chem 112:520–524.

7. Lango-Reynoso F, Landeros-Sánchez C, Castañeda-Chávez M (2010) Bioaccumulation of cadmium (Cd), lead (Pb) and arsenic (As) in Crassostrea virginica (Gmelin, 1791) from Tamiahua Lagoon System, Veracruz, Mexico. Rev Int Contam Ambien 26:201–210

8. Gutiérrez-Galindo E, Flores-Muñoz G, Villaescusa-Celaya J, Arreola-Chimal A (1994) Spatial and temporal variations of arsenic and selenium in a biomonitor (Modiolux capax) from the Gulf of California, Mexico. Mar Pollut Bull 28:330–333.

9. NIST (2008) National Institute of Standards and Technology, Certificate of Analysis. Standard Reference Material® 2977, mussel tissue.

ANEXO V

Structural study of zinc site in metallothioneins of molluscs using XANES. (EN PREPARACIÓN)

Structural study of zinc site in metallothioneins of molluscs using XANES

Maribel Restituyo Silis[1], Laura simonelli[2], Carlo Marini[2], Marta Avila[2], Ma Angels Subirana[1] and Manuel Vailente[1]

[1] Universitat Autònoma de Barcelona. Dept of Chemistry. Center GTS. Campus de la UAB, 08193 Bellaterra (Barcelona), Spain

CELLS-ALBA, BP1413, 08290 Cerdanyola del Vallès, Barcelona, Spain

Abstract

Some marine invertebrates, such as oysters and mussels, concentrate trace metals in their tissues. The occurrence of metallothionein (MT), a low molecular weight, sulfur-containing, metal-binding protein, has been correlated with elevated levels of trace metals in these organisms. It is our hypothesis that, while metallothioneins are involved in the sequestration of elevated levels of trace metals, the primarily function of these MT are to regulate the normal metal metabolism. In this paper, we describe recent laboratory experiments designed in order to synthesize the metallothionein that is emcountered in snails and mouses. In addition, a mechanism to describe the accumulation of Zinc in oysters and mussels has been proposed. The possible roles of metallothionein, as well as the distribution of metals in the tissues are emphasized.

Two types of cluster of Zn-metallothionein were synthesized and by means of Zn K-edge extended X-ray-absorption fine structure (EXAFS) its local structure has been investigated. The results on three oysters and one mussel showed a primary coordination of Zn with the sulfur atoms of the MT, presumably from cysteine residues at a distance 0.225 nm + 0.001 nm for all of them.

Introduction

The mechanism in which the animals accumulate heavy metals is important to understand the cycling of heavy metals in the environment. Studies on aquatic molluscs, particularly mussels and oysters, and on terrestrial molluscs, particularly snails, suggest that variation in metal accumulation in their soft tissues is due to the body size, age, and season [1]. Other studies showed that after giving diets supplemented with various levels of heavy metals, the growth of snails varied amongst them [2]. Owing to the snails complex metabolism, the details of a complete biochemical relationship between the metal concentration in their environment and in their tissues are not well known. Previous studies have demonstrated that heavy

metals, once accumulated in the molluscs soft tissues, may decrease when the molluss is moved to a non-contaminated environment [3].

The advantage of the use of molluscs is that the metabolic elimination of metals accumulated in their soft tissues is relatively slow compared with other organisms [4]. On the other hand, the shells are known to preserve the accumulated metals within their crystalline, calcitic or aragonitic structure, and the metals are not lost even after the death of the organism [5]. If they are firmly stored within their bodies, it is most probable that the metals exist in complexes with ligands of S, O, or N. Castané et al. [6] stated that the snails high capacity for metal accumulation and storage of metals is attributed to the induction of metal-binding proteins such as metallothioneins (MTs). In this concern MTs constitute a superfamily of cysteine-rich, low molecular weight proteins with high metal binding capacity. They are involved in a variety of biological processes, and they are supposed to be the main responsible for regulating the intracellular levels of biologically essential metal ions (Zn^{2+} and Cu^+) and for the protection of the cells from the deleterious effects of toxic metal ions (i.e., Cd^{2+}, Pb^{2+}, Hg^{2+}) [7]. Therefore, to found the specificity of metal on MTs is fundamental to understand the structure-function relationship.

Zinc is an essential element for all living organism as it stimulates the activity of about of a few hundred of enzymes with important functions in the body. Though the actual amount of zinc necessary for living organisms is small its effects are very important. However, high amounts of Zinc in the organism can be fatal.

Zn is coordinated in the MTs forming two clusters that contain few atoms of zinc bounded to sulfur atoms from the Cys domains. These clusters can have different number of Zn atoms and also the MTs can have different domains.

Elucidating how the organisms store these metals is the primary goal of this research.

In this study, Zn in the body parts of cultivated mussel and wild oysters, were investigated using X-ray Absorption Spectroscopy (XAS). An attempt has also been done to quantify the chemical species of each heavy metal by applying principal component analysis (PCA).

MATERIALS AND METHODS

Chemicals and reagents

As there are no commercial MTs, different Zn-MTs were synthesized: Zn-MTs with different variation of atoms of Zn (Zn_5- Zn_4) obtained from the snail *Helix pomatia* and Zn-MTs with different number of atoms (Zn_3) and MT domains (α MT 1 and βMT 1) from a mouse. These samples were prepared following the procedures described by Palacios et al. [8].

The analytical characterization of the synthesized Zn-MT was carried out by the Genetics Department of the University of Barcelona following the procedures described in their publications [7, 8]. Essentially, the complex named Zn–HpMT was obtained using Helix pomatia or DNA fragments coding from mouse (αMT1 and βMT1 domains) by metal displacement reactions for the recombinant metal-HpMT preparation of standard solutions of Zn metal ions to the sample at equivalent molar ratios.

The expression, purification, quantification and compositional characterization of Zn-MT were carried out at the same group in collaboration with the Department of Chemistry of the Universitat Autonoma de Barcelona, following the procedure reported by Palacios et al. [8].

The biological samples were collected on the coast from La Roche (France), Arcachon Bahia (France), Sado sea (Portugal) and Delta de Ebro (Spain). The samples from France and Portugal were wild oysters, while the sample from Spain was a cultivated mussel.

	Name	Origin	Country	Type of sample
Sample 1	OS_BA_WO	Arcachon Bahia	France	Wild oyster
Sample 2	OS_LR_WO	La Roche	France	Wild oyster
Sample 3	OS_SADO_WO	Sado Sea	Portugal	Wild oyster
Sample 4	OS_BAR_CM	Delta del Ebro	Spain	Cultivated mussel

All samples were lyophilized prior to homogenization with a mortar and a pestle before analysis by X-ray Absorption Spectroscopy.

Quantification of metal content

Quantitative multi-elemental analysis of each sample was performed using ICP-MS. (Details of the instrumentation used and sample preparation was given in a previous work [As o Descrip. again]). The results obtained are shown in table 1:

Table 1. Concentration of heavy metal in the samples.

Sample	Element concentration [ppm]								
	As	Cd	Cr	Cu	Hg	Ni	Pb	Se	Zn
1	23,29	1,34	0,89	147,58	0,21	0,90	1,22	5,02	2288,28
2	16,6	1,08	0,47	47,99	0,12	0,56	0,57	3,29	2043,58
3	15,03	6,43	0,63	1464,46	0,13	2	0,60	3,37	6288,69
4	14,36	0,43	0,51	3,54	0,11	1,29	0,22	2,72	98,54

The results obtained showed XXX

X-ray absorption spectroscopy

X-ray absorption spectroscopy allows the determination of the local structure around the absorber atom. X-ray Absorption near edge structure (XANES) spectra were measured at CLAESS beamline at ALBA synchrotron facilities at Zinc K-edge (9659 eV). The white radiation beam coming from the CLAESS wiggler has been monochromatised using a double crystal Si (111) monochromator. Higher harmonic contribution to the selected energy has been eliminated setting a rejection angle in the vertical focusing mirror of about 3.7 mrad. A beam size of FWHM 2x1 mm^2 was used for the experiment. Due to the low concentration of Zn in most of the samples (less than 20 ppm), the measurements were done in fluorescence mode using a CdTe fluorescence detector. All reference spectra from Zn-metallothionein were collected in transmission mode by means of two ionization chambers.

RESULTS AND DISCUSSION

Figure 2 shows the X-ray-absorption spectrum of Zn-MT from snail and mouse, at Zn K-edges. The data for the other samples shows in the figure 3. The fine structure following each of the absorption edge contains local structural information about the specific element, i.e. Zn. For these spectra show fine structure typical of that expected from the back-scattering from Sulphur atoms [9] the differences in terms of position of minima and maxima are due primarily to the difference in the metal-sulphur separations in the two cases.

Zn environment in the sample

References

[1] Alan Beeby & S. L. Eaves., Short-term Changes in Ca, Pb, Zn and Cd Concentrations of the Garden Snail Helix aspersa Miiller from a Central London Car Park . Environmental Pollution (Series A) 30 (1983) 233-244

[2] Rainbow P., Trace metal bioaccumulation: Models, metabolic availability and toxicity. Environment International 33 (2007) 576–582

[3] Rzymski P., Niedzielski P., Klimaszyk P., Poniedziałek B. Bioaccumulation of selected metals in bivalves (Unionidae) and Phragmites Australis inhabiting a municipal water reservoir. Environ Monit Assess (2014) 186:3199–3212

[4] Rainbow P. Biomonitoring of Heavy Metal Availability in the Marine Environment. *Marine Pollution Bulletin,* Vol. 31, Nos 4-12, pp. 183-192, 1995

[5] Bajger G., Konieczka P., Namies J. Speciation of trace element compounds in samples of biota from marine ecosystems. Chemical Speciation and Bioavailability (2011), 23(3)

[6] Castañé P., Topalián M., Cordero R., Salibián A. Influence of speciation of heavy metals in aquatic environment as a determinant of their toxicity. Rev. Toxicol. (2003) 20:13-18

[7] Artells E., Palacios O.,Capdevila M., Atrian S. Mammalian MT1 and MT2 metallothioneins differ in their metal binding abilities. *Metallomics,* 2013, 5, 1397--1410

[8] Palacios O., Pe´rez-Rafael S., Pagani A., Dallinger R., Atrian S., Capdevila M. Cognate and noncognate metal ion coordination in metal-specific metallothioneins: the Helix pomatia system as a model. J Biol Inorg Chem (2014) 19:923–935

[9] Hasnain S., Wardell E., Garner C., Schlosser M., Beyersmann D. (1985) Biochem. J. 230, 625-633

ANEXO VI

Figuras y tablas

Figura A. representación de las partes del jamón curado

Figura B. equipo de Digestion Digi-PREP MS, IPREM, Pau, Francia.

	Muestra	Liofilización			Digestión acida				Diluciones			
		Peso antes	Peso seco	Contenido de agua	HNO$_3$	H$_2$O$_2$	Milli-Q	Volumen Final	1er	Acidez	MT	MM
		g	g	%	ml	ml	ml	ml		%	125	2000
España	**1**	4,56502	3,53347	22,60	4	2	19,00	25	50	16	125	2000
	2	4,47766	3,70114	17,34	4	2	19,00	25	50	16	125	2000
	3	4,50487	4,19835	6,80	4	2	19,00	25	50	16	125	2000
	4	4,17578	4,03519	3,37	4	2	19,00	25	50	16	125	2000
	5	5,1053	2,5678	49,70	4	2	19,00	25	50	16	125	2000
	6	5,1053	2,5678	49,70	4	2	19,00	25	50	16	125	2000
	7	5,1053	2,5678	49,70	4	2	19,00	25	58	16	125	2000
	8	5,0198	2,5161	49,88	4	2	19,00	25	50	16	125	2000
Portugal	9	5,0198	2,5161	49,88	4	2	19,00	25	50	16	125	2000
Francia	10	5,0198	2,5161	49,88	4	2	19,00	25	47	16	125	2000
	11	5,0619	3,1309	38,15	4	2	19,00	25	49	16	125	2000
	12	5,0619	3,1309	38,15	4	2	19,00	25	50	16	125	2000
Italia	13	5,0619	3,1309	38,15	4	2	19,00	25	49	16	125	2000
	14	5,1073	2,7644	45,87	4	2	19,00	25	50	16	125	2000
	MR	0,5011			4	2	19,00	25	50	16	125	2000
	B				4	2	19,00	25	0	16	125	2000

Tabla A. Diluciones realizadas para metales ppb (MT) y para ppm (MM). MR es el materia de referencia, y B es el Blanco.

COMPOSICION ELEMENTAL MATERIAL DE REFERENCIA RM8414			
ELEMENTOS	FRACCION EN MASA		Desviación estándar
Na	weigh %	0,21	0,008
K	weigh %	1,517	0,037
Mg	mg/kg	690	95
Ca	mg/kg	145	20
Mn	mg/kg	0,37	0,09
Fe	mg/kg	71,2	9,2
Co	mg/kg	0,007	0,003
Cu	mg/kg	2,84	0,45
Zn	mg/kg	142	14
As	mg/kg	0,009	0,003
Sr	mg/kg	0,052	0,015
Cd	mg/kg	0,013	0,011
Pb	mg/kg	0,38	0,24
Al	mg/kg	1,7	1,4
Rb	mg/kg	28,7	3,5
Cr	mg/kg	0,071	0,038
Ni	mg/kg	0,05	0,04

abla B. Composicion elemental del material de referencia RM 8414

FiguraC. ICP-MS utilizado, IPREM, PAU, Francia.

Figura D. Sistemas de columnas de separación específicas para los isotopos de $^{87/86}$ Sr.
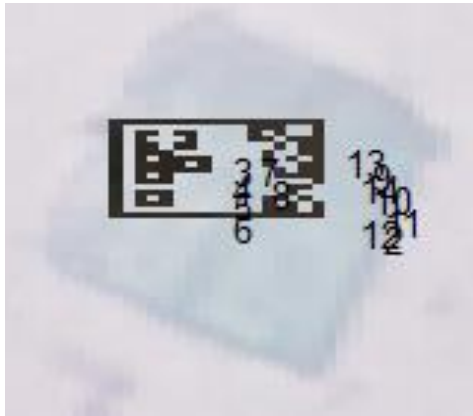
Figura E. Selección de la ROI en una muestra de jamón.
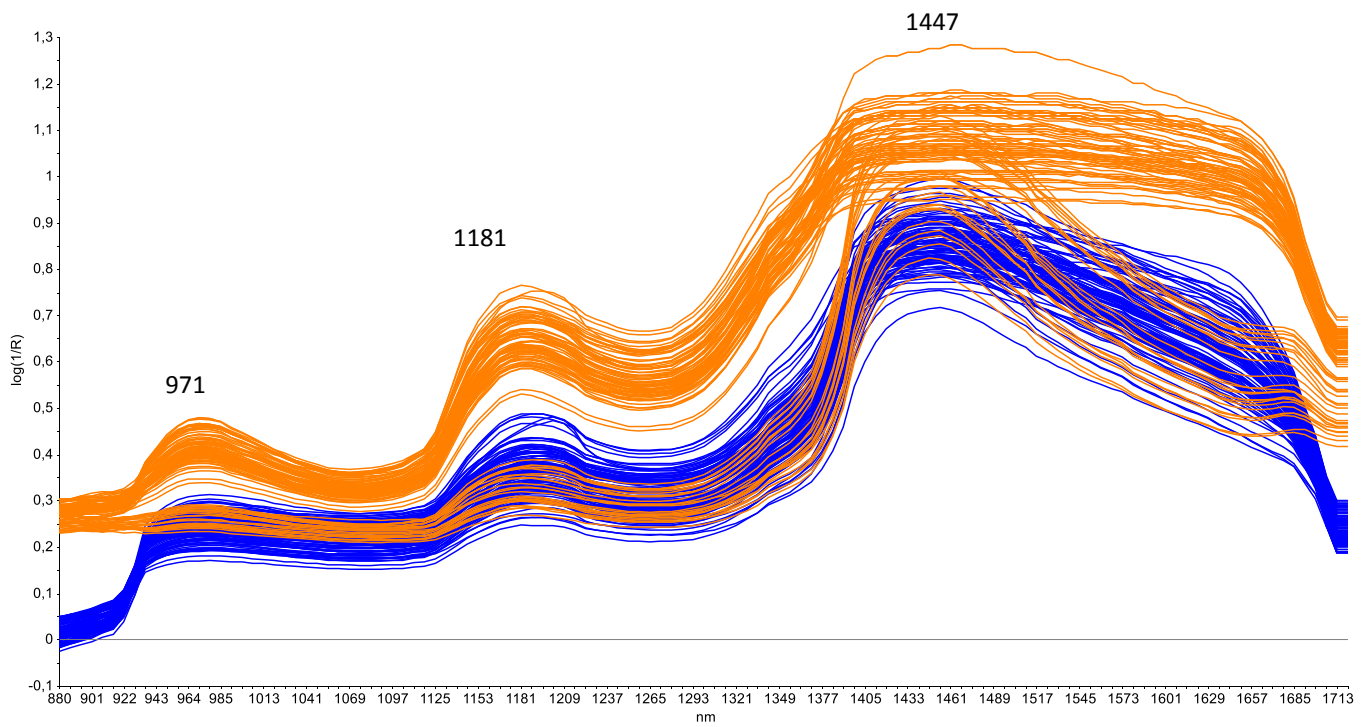
Figura F. Longitudes de onda usadas en la construcción de la imagen RGB, 971, 1181 y 1447 como azul, verde y rojo.

Spanish ham

A 1)   A 2)   A 3)
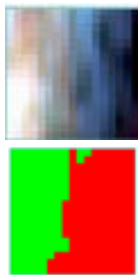
Spanish ham

A 1)   B 2)   B 3)   B 4)

ITALIAN HAM

C I)   C 2)   C3)   C 4)

FiguraG Muestras del Jamon tratadas con el software ENVI, las de arriba es el resultado del RGB y las de abajo es el resultado de la clasificación IsoData.

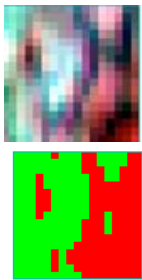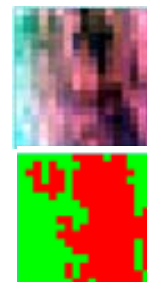| E/S		Española										Portugal	Francia			Italia	
		1	2	3	4	5	6	7	8	9	10	11	12	13	14	15	16
		ppm															
B		1633	5,2	2,8	2,4	3,0	14	1,7	≤	3	≤	2	≤	≤	≤	0,9	0,5
Mn		0,5	0,8	0,3	0,6	0,3	0.4	0,2	0.3	0,4	0,2	0,2	0,9	0,4	0,6	0,3	0,3
Fe		51	67	46	52	32	34	23	47	31	19	23	33	25	23	29	28
Cu		3	5	4	4	3	2	2	3	3	2	2	3	2	2	2	2
Zn		44	60	44	48	34	26	16	48	21	16	16	36	36	30	21	27
Rb		12	14	11	18	14	10	10	8	13	7	9	14	22	14	17	18
Sr		3	2	0,7	0,9	0,8	≤	0,6	≤	1	0,5	1	4	4	3	4	1
		ppb															
Li		48,7	22	23	21	18	23	11	12	17	14	13	98	148	48	27	14
V		7,5	6	8	≤	≤	8	4	6	8	6	6	5	≤	5	7,5	5,6
Cr		73	66	87	85	52	82	58	72	67	94	60	59	58	63	75	87
Co		18	7	4	8	5	5	4	5	5	10	4	≤	≤	≤	10	5
Ni		62	118	49	48	20	160	48	39	55	376	30	11	11	8	1996	631
Cd		54	43	15	7	28	20	8	9	7	22	15	≤	≤	≤D	62	39
Cs		41	145	104	521	203	31	332	16	241	23	106	94	115	89	419	82
Ti		≤	1,4	≤	2	≤	≤	1,6	≤	≤	1,3	1	3,4	3	4	1,2	2
Pb		72	79	132	85	22	43	18	23	69	39	13	7	≤	5	61	72

Tabla C. Resultado del contenido de metales de las muestras de jamón curado, separados por orígenes y por contenido mayoritario y metales traza.
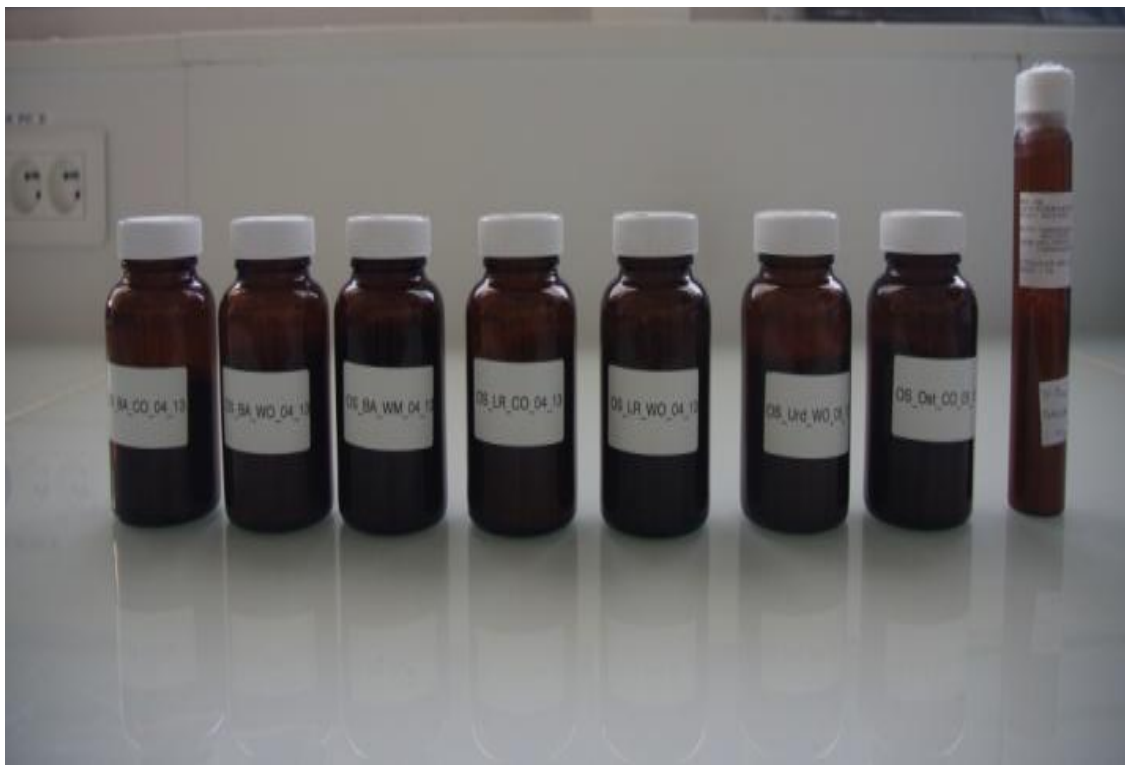
Figura H. Conservación de las muestras liofilizadas de moluscos, lista para su distribución.
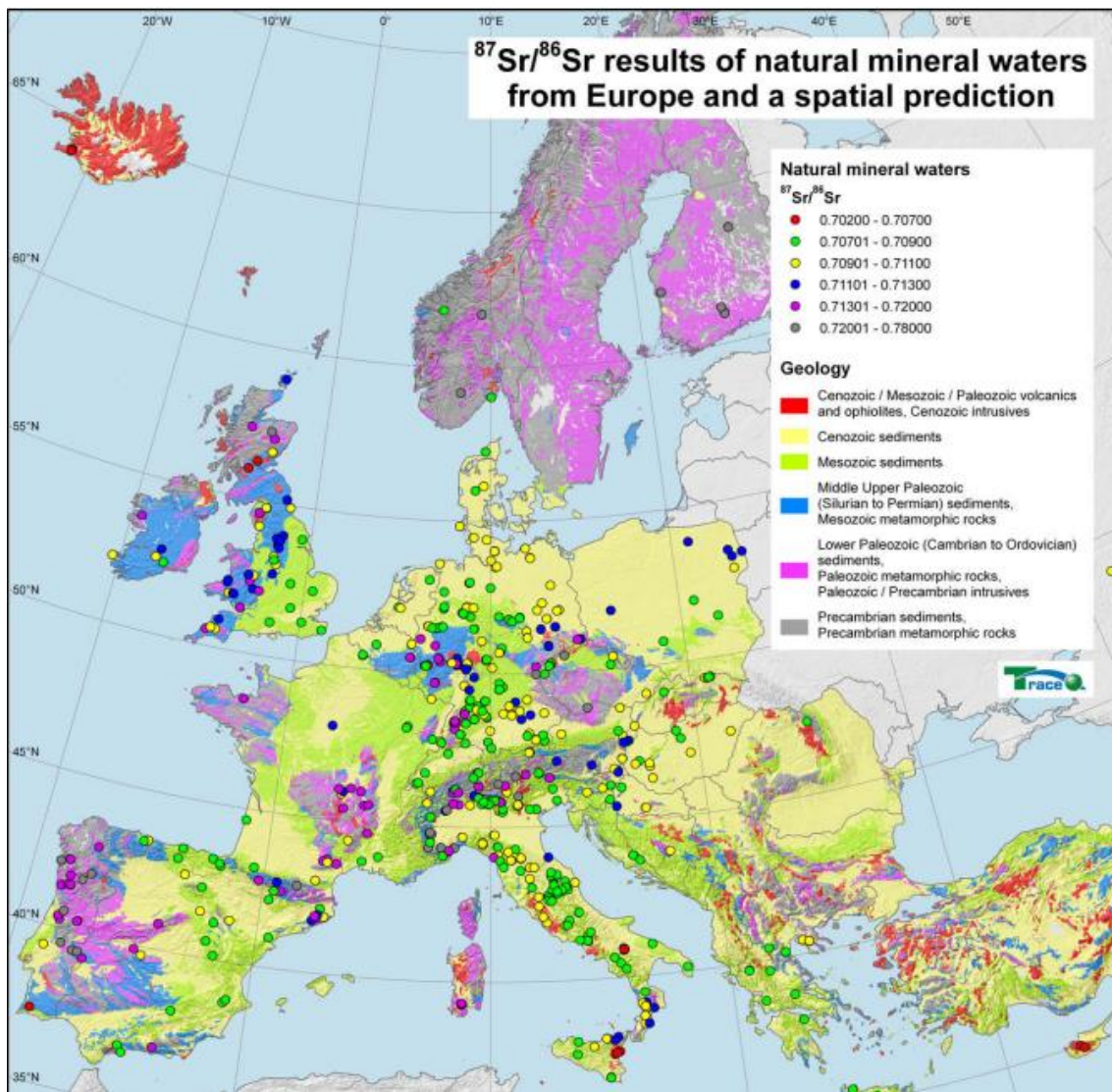
Figura I. Distribución geográfica de los isotopos de Sr [2].

Sample		$^{87/86}$ Sr Ratio
España	1	0,709259 ±0,00012
	2	0,709274±0,00012
	3	0,709473±0,00012
	4	0,709467±0,00012
	5	0,709270±0,00012
	6	0,708981 ±0,00012
	7	0,709281±0,00012
	8	0,709002±0,00012
	9	0,709505±0,00012
	10	0,709032±0,00012
Portuga	11	0,709558±0,00012
Francia	12	0,708545±0,00012
	13	0,708538±0,00012
	14	0,708578±0,00012
Italia	15	0,709227±0,00012
	16	0,709245±0,00012

Tabla D. Valores de la relación de $^{87/86}$ Sr y su desviación estándar en las muestras de jamón curado, separado por orígenes.

Valores para el Fe					
		REFERENCIAS			
Muestras	FIT Parametros	Cloruro de hierro	Sulfato de hierro amoniacal	Mioglobina	Hemin5
03_A_MERGE	R=0.0038, X^2=0.143, RX^2=0.00115	30±1	28±4	40±9	
03_B_MERGE	R=0.0256, X^2=0.887, RX^2=0.00716	15±2	60±10	20±7	
14_A_MERGE	R=0.0038, X^2=0.131, RX^2=0.00107	45±1	25±5	27±5	
14_B_MERGE	+R=0.0030, X^2=0.110, RX^2=0.00090	15±1	11±4	20±5	54±9
26_A_MERGE	R=0.01108, X^2=0.429, RX^2=0.0034	30±2	34±8	34±7	
26_B_MERGE	R=0.0016, X^2=0.053, RX^2=0.00043	36±1	41±6	21±4	
40_A_MERGE	R=0.0024, X^2=0.0809, RX^2=0.00043	25±10	20±8	54±10	
40_B_MERGE	R=0.00307, X^2=0.0852, RX^2=0.00068	30±9	15±5	50±12	

VALORES PARA EL ZINC				
		REFERENCIAS		
Muestras	FIT Parametros	Cloruro de zinc	Protoporfirina de zinc IX	Sulfato de zinc
03_A_MERGE	R=0.0015269 X^2=0.04454 RX^2=0.0004790	57±4	29±2	14±1
03_B_MERGE	R=0.0025914 X^2=0.07052 RX^2=0.0006716	56±2	17±1	27±2
14_A_MERGE	R=0.0075027 X^2=0.19374 RX^2=0.0018451	60±8	15±1	25±3
14_B_MERGE	R=0.0017613 X^2=0.05093 RX^2=0.0004850	57±1	27±1	16±1
26_A_MERGE	R=0.0027178 X^2=0.08521 RX^2=0.0009262	66±5	11±1	23±2
26_B_MERGE	R=0.0059513 X^2=0.19870 RX^2=0.0019106	59±2	13±4	28±2
40_A_MERGE	R=0.0022972 X^2=0.06559 RX^2=0.0006247	63±2	21±2	16±1
40_B_MERGE	R=0.0024441 X^2=0.07407 RX^2=0.0007964	66±2	15±1	19±2

Tabla E. Parámetros de la combinación lineal de los espectros de Fe y Zn.

ANEXO VII

Procedimiento de liofilización

Liofilización de mejillones

alícia

Índice

Objetivo

Liofilización de 15 kg de mejillón para la Facultad de Ciencias Químicas, entrada norte, edificio de Ciencias el despacho C7/239.

Procedimiento

Recepción de muestras

- Se recibieron 10 kg de mejillón refrigerado con la siguiente referencia:

- Se colocaron en bandejas de HDPE
- Se taparon con film, sin que este tocase al producto, para evitar contaminaciones cruzadas dentro del congelador

Congelación del mejillón entero para la extracción de él

1. Congelación del molusco

- Se pusieron a congelar las bandejas que contenían los mejillones, 24 horas a -18 ºC en un congelador (KOMA) libre de otros alimentos. Durante este periodo no se abrió el congelador, lo que aisló de la luz al producto.

2. Extracción del molusco

- Se dejaron las bandejas a temperatura ambiente 6 horas para que los mejillones se abriesen y se pudiese sacar el molusco crudo del interior.
- Se extrajeron manualmente los moluscos, utilizando guantes de nitrilo no flockados y material de PP, para evitar cualquier tipo de contaminación.

- Se filtraron las muestras con un colador (supervac de plástico) para eliminar el exceso de agua.
- Se colocaron en vasos de PP de un solo uso para poder ser congelados y posteriormente liofilizados.

Congelación del molusco para liofilizar

- Se distribuyeron los vasos que contenían los moluscos en bandejas de HDPE y se taparon con film sin que este tocase el producto.
- La cantidad de vasos fueron: 1º Liofilización: 2 bandejas con 7 vasos en cada una y 1 bandeja con 4 vasos y 2º Liofilización: 2 bandejas con 7 vasos en cada una y una bandeja con 2 vasos. Si cada vaso está alrededor de 55-60 gramos esto significa que la obtención de 15 kg de mejillones en solo mejillón sin casi nada de agua está alrededor de 1kg-2kg.
- Se congelaron a - 60 ºC (optic ivymen system), libre de otros alimentos y no se abrió el congelador hasta colocar-los en la máquina de liofilización pero por culpa de una incidencia en la máquina liofilizadora (ver anexo) estuvieron en el congelador 4 días.

Liofilización

- Se realizaron dos procesos de liofilización debido a la capacidad del aparato, datos aproximados;
  1º obtención de mejillones: dos bolsas una de 200 gramos y otra de155 gramos

Liofilizadora: Telstar Lyoquest -80ºC

Programa:

1. Cool + Vaccum 25'
2. Vaccum 0,01, 0 ºC, 2h
3. Vaccum 0,01, 0ºC, 24h
4. Vaccum 0,01, 20ºC, 53h

- La sala donde se encuentra la liofilizadora tiene control de humedad, temperatura y se mantiene la luz cerrada excepto cuando se trabaja en ella. Es una habitación almacén donde no se interviene si no es para trabajar con la máquina de liofilización.

Envasado

- Se envasaron al 100% de vacío sin la inyección de gas conservante.

- Se taparon con papel de aluminio para evitar, lo máximo, que les diese la luz.
- Y se mantienen conservándose en un armario a humedad 1% donde se conservan los productos liofilizados.

Anexo reparación de la máquina liofilizadora

La entrega de muestras se demoró debido a que durante la puesta a punto de la liofilizadora se detectó que no quedaba suficiente gas para la ultracongelación y se tuvo que llamar al servicio técnico. Aquí les presentamos la factura de Alícia correspondiente a la reparación.

ANEXO VIII

Ficha de los datos de control de mejillones

FICHA TECNICA DE ESPECIES		Nº DE FICHA	
		FECHA	17/10/2013

DATOS DE LA COMPAÑIA					
NOMBRE	FEDERACIÓN DE PRODUCTORES DE MOLUSCOS DELTA DE L'EBRE				
NIF / CIF	G43929975				
DIRECCIÓN	Avd. Goles de l'Ebre, 208				
CIUDAD	DELTEBRE	PROVINCIA	TARRAGONA	CP	43580
TELÉFONO	977480466	FAX	977480466		
CORREO ELECTRONICO	Gerardo@fepromodel.com				

ESPECIFICACIONES DE LA MUESTRA	OBSERVACIONES
NOMBRE CIENTIFICO: mitylus galloprovincialys	
NOMBRE COMERCIAL:mejillón de roca del Mediterraneo	
VARIEDAD, CLASE Y/O ESPECIE:molusco bivalvo	
TAMAÑO PROMEDIO: 50 piezas kilo(6-8 cms longitud)	
FECHA DE CULTIVO: todo el año	
FECHA DE RECOLECCION:de Mayo a Septiembre	
TEMPERATURA Y CONDICIONES ATMOSFERICAS: bahías delta del Ebro	
ALIMENTACION:natural fitoplancton	
NUTRIENTES SUMINISTRADOS: ninguno	

ESPECIFICACIONES DEL LUGAR DE CULTIVO	OBSERVACIONES
AREA O SUPERFICE DEL CULTIVO: bateas de 1500 a 3000 m2	
METODO DE CULTIVO: bateas fijas en cuerdas suspendidas	
TEMPERATURA: de 14ªC- A 31º©	

DENSIDAD DEL CULTIVO:
    Nº BATEAS 160
    LONGITUD DE 150 A 250 aproximadamente
    Nº CUERDAS 1 Cuerda x m2
    SEPARACION ENTRE LAS CUERDAS: Variable	

TRATAMIENTO POSTERIOR A LA RECOLECCION:desgranaje de la cuerdas, limpieza, clasificación, depuración obligatoria por ser zona B y posterior calibraje, limpieza y selección.	

ANEXO IX

Referencia BCR 710

BCR 710

Towards a new Certified Reference Material for butyltins, methylmercury and arsenobetaine in oyster tissue

R. Morabito, P. Massanisso, C. Cámara, T. Larsson, W. Frech, K.J.M. Kramer, M. Bianchi, H. Muntau, O.F.X. Donard, R. Lobinski, S. McSheehy, F. Pannier, M. Potin-Gautier, B.M. Gawlik, S. Bøwadt, Ph. Quevauviller

Increasing awareness of the determination of chemical species in the environment evolves jointly with the need to control the validity of analytical measurements in a wide variety of matrices. There are few Certified Reference Materials (CRMs) available for various chemical species, and they are certified for species of one single element (e.g., species of tin and mercury). Three years of collaboration within the framework of European Commission research programmes involving more than 20 laboratories have made it possible to produce an oyster reference material for species of tin, mercury and arsenic (BCR-710) and to perform the necessary experimental work for its certification. This article summarises the feasibility study and describes the various steps in the preparation, production and characterisation of this material for its content of arsenobetaine, methylmercury, tributyltin and dibutyltin. These steps included stability and homogeneity testing as well as value assignment based on a collaborative approach involving a group of European laboratories. Further work is going on to certify total contents for a range of trace metals.
© 2004 Elsevier Ltd. All rights reserved.

R. Morabito, P. Massanisso
ENEA – PROT, Via Anguillarese 301, I-00060 Rome, Italy

C. Cámara
Departamento de Quimica Analitica, Universidad Complutense, E-28040 Madrid, Spain

T. Larsson, W. Frech
Department of Chemistry, Analytical Chemistry, Umea University, S-90187 Umea, Sweden

K.J.M. Kramer
Mermayde, NL Bergen, The Netherlands

M. Bianchi
Ecoconsult, Via Marconi 15, I-21026 Gavirate, Italy

H. Muntau
Università di Sassari, Via E. De Nicola 1, I-07100 Sassari, Italy

O.F.X. Donard, R. Lobinski, S. McSheehy, F.Pannier, M. Potin-Gautier
Université de Pau, LCABIE, 2 avenue Pierre Angot, F-64000 Pau, France

B.M. Gawlik
European Commission DG JRC, Institute for Environment and Sustainability, Via E. Fermi, I-21020 Ispra (Va), Italy

S. Bøwadt, Ph. Quevauviller*
European Commission, rue de la Loi 200, B-1049 Brussels, Belgium

*Corresponding author.
E-mail: philippe.quevauviller@cec.eu.int

1. Introduction

In its task of improving the analytical quality of laboratories in European Union (EU) Member States, the Institute for Reference Materials and Measurements (IRMM) of the European Commission (EC) makes available certified reference materials (CRMs) that are known as Bureau Communautaire de Reference (BCR) reference materials [1]. One of its missions is to produce CRMs for contaminants in important environmental matrices and food, the use of which is considered of importance to the environmental policy of the EU.

The toxicity of metals, their environmental mobility and their tendency to accumulate in living systems are closely correlated with their chemical forms. Hence, knowledge of the total element contents provides only limited information about the potential risks (e.g., from human consumption). Indeed, in most cases, the toxicities of different chemical species of the same element are completely

different (e.g., organic forms in comparison to inorganic ones), and that stresses the need to determine individual chemical species instead of total element concentrations [2–5]. While the analyses of chemical forms of elements is still not widespread in routine environmental work, some compounds are increasingly often determined in support to regulations (e.g., organotin compounds (in particular butyltins) and methylmercury) or in environmental risk assessment studies (e.g., arsenic, chromium and selenium species).

Analytical methods used for determining these species normally involve various analytical steps, such as extraction, derivatisation, separation and final detection, which increase the risk of analytical errors [3,6–8]. For this reason, series of interlaboratory studies have been organised in the past 10 years to evaluate systematically and improve the performance of current methods used in speciation analysis, with the final aim of producing various CRMs [9,10].

The range of CRMs available for the quality control (QC) of speciation analysis is steadily increasing. However, these materials are generally certified for chemical species of a single element (e.g., organotins, trimethyl lead and methylmercury) [3,11], which makes it difficult for quality to be controlled in multi-species determination, in particular for the analysis of sensitive biological organisms, such as molluscs. In principle, indeed, proper QC would require that CRMs certified for each category of chemical forms of elements should be available and analysed, which is time-consuming and often hardly feasible.

One possible approach to this problem is the certification of reference materials containing a range of chemical species of several elements.

The 'oyster-tissue' matrix is of interest to the human food sector. In addition, oysters are often used for environmental monitoring of marine waters [12]. The BCR (now IRMM) has already produced CRMs for other biological matrices, including methylmercury in tuna fish (BCR-463, 464) [13], organotin species in mussel tissue (BCR-477) [14], and organic arsenic species in tuna fish (BCR-627) [15], as well as sediment CRMs for methylmercury (BCR-580) [16]. More recently, new sediment CRMs were also made available for organotin species (BCR-462R and 646) [17].

A feasibility study was organised to check whether the laboratories involved could analyse a oyster-tissue matrix for organic species of the elements arsenic, mercury, selenium and tin with sufficient agreement in the concentrations found. After two rounds of intercomparison in this feasibility study, good agreement was obtained for most of the investigated species with the exception of organic species of Se, for which the analytical methods had to be further developed. It was therefore decided to prepare a new oyster material and to

continue with the certification exercise for the organic species of As, Hg and Sn.

2. Feasibility study

The first part of the project comprised two interlaboratory comparison studies that aimed to test the feasibility of preparing an oyster-matrix reference material and to detect and to remove eventual pitfalls.

2.1. Design of the interlaboratory study

A group of 18 European laboratories from 11 European countries was formed and a first meeting was held, when the selection of reference materials and instructions for participating in the interlaboratory study were discussed. For the first intercomparison study, a batch of oyster tissue had been collected at an oyster farm in Chioggia, near Venice, Italy. Some 530 kg of raw material (62 kg of fresh tissue) was prepared in a similar way to the CRM (see Section on Preparation of the candidate CRM). Two samples were prepared: a high-level spiked sample (T36); and, a natural sample mixed with T36 material, resulting in a low-level spiked sample (T37). Assuming similar behaviour of both samples, the homogeneity and stability were verified for the T36 material only. Each laboratory received two bottles and was requested to report results of six independent replicate determinations along with a detailed description of the method(s) used. The results and methods were discussed at a technical meeting with all participants that reported the results in time (12 laboratories).

For a second interlaboratory comparison study, a new batch of oyster tissue was collected and prepared again at the oyster farm in Chioggia, following similar procedures to those for the first material. This resulted in a non-spiked oyster-tissue sample (T38). Assuming similar behaviour to the previous samples, homogeneity and stability were not verified. Each laboratory received two bottles and was requested to report results of six independent replicate determinations. The results and methods were discussed via e-mail conferencing.

2.2. Homogeneity and stability checks

The between-bottle homogeneity of the test materials was verified for the spiked sample T36 on the basis of 10 independent analyses from 10 different bottles, while the within-bottle homogeneity was verified by five independent analyses of the content of one bottle. The coefficients of variation were obtained for the between- and within-bottle homogeneity tests (CV_B and CV_W, respectively), together with their respective uncertainties U_{CV} (defined as $U_{CV} \approx CV/\sqrt{2n}$, where $n = $ number of replicates).

The arsenic species (AsIII, AsV, AsBet, DMA) were separated by high-performance liquid chromatography (HPLC), followed by inductively coupled plasma mass spectrometry (ICP-MS) as method of final detection.

The method applied for the determination of methylmercury (MeHg) was TMAH extraction, butylation with Grignard reagent, capillary gas chromatography (GC) separation, microwave induced plasma (MIP) excitation with atomic emission spectrometry (AES) for detection. Limitations and sources of systematic errors during butylation and GC separation have been described [18].

No analytical method concerning sample treatment for Se speciation in animal tissue had been published at the time of the feasibility studies, so several approaches to sample treatment and chromatographic separation to determine the Se species were included in the project (Se-methionine, Se-cystine and inorganic Se) by HPLC-ICP-MS.

The tin species (MBT, DBT, TBT, MPhT, DPhT, TPhT) were separated by GC followed by MS as method of final detection.

The results of the homogeneity tests are given in Table 1, illustrating the variability of results obtained from the various species.

The between- and within-bottle CVs were reasonably similar for a number of species, notably AsBet, AsV, DMA, MeHg and the butyltins (Table 1). CVs were particularly high for the Se species, and for between-bottle homogeneity of the phenyltins. This was attributed to analytical artefacts rather than to inhomogeneity of the samples. Consequently, no inhomogeneity was suspected.

Stability was verified on samples stored at +40 °C (extreme transport conditions), +20 °C, +4 °C and −20 °C (expected 'safe' conditions) at $t = 1$ week, $t = 1$ month and $t = 3$ months. Arsenic species were not tested at +4 °C. Since the interlaboratory comparison study

was to be completed in about $t = 3$ months, no longer stability study was deemed necessary. As the homogeneity study revealed that the analysis of Se species would require further development, these species were not tested for stability.

The results showed that elevated temperatures (+40 °C) shall be avoided, but, except for the phenyltins, most species may survive short (1-week) elevated temperature conditions. Storage at +4 °C or below is much preferred. When stored at +4 °C for MeHg and the butyltins no instability could be detected over the period of the study. The arsenic species AsIII, AsBet and DMA were stable at +20 °C, at least for one month.

2.3. Results of the interlaboratory trials

The purpose of the technical discussion of the results of interlaboratory studies was threefold. It served not only to discuss the (agreement between) analytical results of the intercomparison studies, but also to discuss openly the techniques applied, the pitfalls or difficulties observed – why data sets showed large discrepancies, why there were large (or very small) standard deviations and systematic errors (caused by e.g., calibration errors and interferences), high blank values and recoveries that were low or too high – and the best way to evaluate recovery, and to provide advice to the meeting to solve problems. These technical discussions are considered an important aspect of improving the analytical performance for the analytes/matrices considered. Finally, the technical meeting was to advise on whether the results were of sufficient quality to continue the exercise and go for certification of identified species in oyster tissue.

The results submitted in the interlaboratory comparison study 1 (T36, T37) were discussed amongst all participants in a technical meeting; they were pre-

Table 1. Homogeneity tests for the 'oyster tissue' (feasibility study 1)

Species	CV_W	U_W	CV_B	U_B
AsIII	7.3	2.3	16.0	3.6
AsBet	7.1	2.2	13.9	3.1
AsV	8.5	2.7	13.1	2.9
DMA	13.6	4.3	10.5	2.4
MeHg	1.7	0.6	2.2	0.6
SeCys2	39.8	12.6	44.1	13.9
SeMet	17.0	6.0	63.7	20.1
MBT	4.4	1.4	8.0	2.0
DBT	3.5	1.1	6.9	1.7
TBT	4.0	1.3	5.8	1.5
MPhT	5.9	1.9	13.7	3.4
DPhT	7.2	2.3	14.2	3.5
TPhT	5.2	1.6	18.6	4.7

The between- and within-bottle coefficients of variation (CV_B, CV_W) and respective uncertainties U_{CV} (defined as $U_{CV} \approx CV/\sqrt{2n}$, where n = number of replicates) are presented in %.

Table 2. Summary of the results of the interlaboratory study 1 (T37, spiked sample) and the interlaboratory study 2 (T38, natural (Venice) oyster tissue)

Species	Intercomparison 1 (T37, spiked)			Intercomparison 2 (T38, natural)		
	Mean (mg/kg)	SD (mg/kg)	n	Mean (mg/kg)	SD (mg/kg)	n
AsIII	5.17	2.78	4	0.036	0.025	2
AsBet	8.11	4.04	4	9.53	1.59	8
AsV	6.70	3.37	4	0.145	0.084	3
DMA	79.9	32.8	5	0.665	0.156	7
MMA	3.20	0.06	1	–	–	
MeHg	4.95	1.70	9	0.057	0.007	9
SeCys2	60.7	1.7	1	0.38	0.06	1
SeMet	–	–		1.150	0.450	2
SeIV	33.9	3.4	1	0.194	0.011	1
MBT	4.74	3.29	8	0.146	0.082	6
DBT	2.03	0.60	10	0.152	0.061	10
TBT	2.37	0.50	10	0.430	0.102	10
MPhT	7.89	8.00	6	0.0074	0.0006	1
DPhT	0.180	0.106	7	0.123	0.176	3
TPhT	0.750	0.340	9	0.016	0.009	2

sented in the form of bar-graphs showing the laboratory codes and the methods used, the individual means and standard deviations and the mean of laboratory means with its standard deviation. Many laboratories had problems with the analysis of the sample T36 because of the too high concentration of species in this (high-level) spiked matrix. A summary of the results for T37 (low-level spiked) as mean values and standard deviations for all accepted data are presented in Table 2.

The overall agreement obtained by the participating laboratories for the interlaboratory comparison 1 (low-level spiked sample) was not sufficient to envisage certification. Often the CV was much higher than anticipated from earlier intercomparison studies. It was remarked by the participants that the oyster-tissue matrix proved to be more difficult than mussel tissue (BCR-477). Another reason was that the species added to the sample in the spiking process were apparently not as equally distributed in the matrix as the naturally present species. Several laboratories had problems with a low recovery. Also, the number of laboratories was not considered sufficient in all cases.

As a consequence, and after a discussion of the technical problems, a second interlaboratory comparison study was launched using a new batch of non-spiked oyster matrix (T38). A detailed guideline was provided to the participants. The results and the discussion indicated that the lower (natural) concentration offered additional problems to several participating laboratories. Notably, the phenyltins and some arsenic species (AsIII, AsV) were below the detection limits in many cases and could be analysed by only a few laboratories. This resulted in a situation where a combination of both sufficient agreement between results and a sufficiently large number of

laboratories was potentially met for only the following species: AsBet, DMA, MeHg, MBT, DBT and TBT.

In the technical meeting, it was decided to continue the certification exercise for these species, but to encourage participants to report on other species as well. To ensure that a sufficient number of participants could report data, additional laboratories were invited to participate in the certification exercise. To verify their analytical potential for this exercise, these additional laboratories were requested to analyse the sample T38. Only when their results matched the feasibility 2 interlaboratory comparison results were they invited to participate in the certification exercise.

3. Preparation of the candidate CRM

A batch of oysters (*Crassostrea gigas*) was collected in Arcachon Bay, France, because of

(a) its important oyster farming activity;
(b) its history of pollution (mainly trapped in the sediments); and,
(c) the proof from a preliminary study that all species concerned would be present in about the desired natural concentrations, so that it would be possible to avoid spiking the matrix.

The material was obtained from a commercial supplier. To ensure minimum sedimentary particulate matter in the oyster tissue, the oysters had been stored suspended in the water column for about 3 months. A total of 1300 kg of raw material was collected in March 2000. Shelling was performed manually immediately after collection. After opening, the wet tissue was

collected. The mantle water was allowed to drip off, thereby minimising the final salt content, and reducing problems in the further processing (crushing the frozen material without thawing). The wet tissue was packed into 2 kg batches, and contained in clean plastic bags. The bags were placed in an ice-box filled with ice. Every hour, the ice-box was transported to a commercial fish-processing plant where batches were stored deep frozen at −20 °C until completion of shelling operation. A total of 70 kg of fresh oyster tissue was thus obtained. The entire operation took two days. Care was taken to avoid contamination during all steps of the collection and the handling of the material.

After completion of the preparations, the frozen material was placed in polystyrene containers and dry ice was added to keep the material deep frozen. It was transported by van to the JRC-Institute for Environment and Sustainability (formerly Environment Institute), Ispra, Italy, where it was stored at −20 °C until further processing.

Following thawing at ambient temperature, the tissue was first minced using a commercial meat-mincing apparatus. This minced material was further treated using an Ultra Turrax device. No spiking of analytes was applied to the candidate CRM. The bulk material thus obtained was homogenised by slowly stirring for 8 h in a cold room (+6 °C). Under continued stirring, the bulk was subdivided into 2 kg batches, which were immediately frozen at −15 °C.

This material was transported deep frozen to a commercial freeze-drying company at Polesine Parmense, Parma Province, Italy, and freeze-dried. In this way, 13 kg of dry material was obtained.

After return to the laboratory, the freeze-dried material was ground using a Retsch ZM1 mill, equipped with tungsten-carbide blades. The ground powder was sieved over a 125-μm sieve. The fraction >125 μm was discarded. The fraction <125 μm (11.5 kg) was homogenised in a PVC-homogenisation drum for 1 month.

Samples were taken for bulk-homogeneity testing, based on the determination of total mercury by solid-sampling Zeeman AAS (SS-ZAAS). After confirming bulk homogeneity (<1%, referred to the precision of the testing method), manual bottling was performed using glass bottles. In this way, 800 bottles were produced, each containing 13 g dry powder.

The mean moisture content (as calculated from 28 sets of data) found in this certification campaign was $(4.55 \pm 0.64)\%$.

4. Homogeneity study

4.1. Methods used: MeHg

Approximately 300 mg of oyster-tissue sample was accurately weighted into 10-ml glass centrifuge tubes.

The samples were digested with 4 ml of 20% tetra-methylammonium hydroxide (TMAH, Sigma, Steinheim, Germany) in an ultrasonic bath for 1 h at room temperature. 2 ml of a pH 9 borate buffer (Riedel-de Haën) was added to the digested solution. HCl (4 mol/l, prepared from concentrated sub-boiling distilled HCl originally from Merck) was added dropwise to the solution for neutralisation, followed by 1.0 ml of 1.0 mol/l sodium diethyldithio-carbamate (DDTC, Aldrich, Steinheim, Germany) and 1.0 ml of saturated NaCl (Merck, Darmstadt, Germany). The samples were shaken for 5 min on an automatic shaker (IKA-VIBRAX-VXR, Labasco, Partille, Sweden) and 1.0 ml of toluene (Burdick and Jackson, Muskegon, USA) was added. Next, the sample was shaken for 5 min and centrifuged for 15 min at 5400 rpm (Wifug centrifuge, Bradford, UK), after which the toluene phase was transferred into another centrifuge tube standing in an ice water bath. Another 1 ml of toluene was added to the sample and the above procedure was repeated. To the combined toluene, 0.3 ml of 2.0 mol/l of n-butylmagnesium chloride in tetrahydrofuran (Aldrich, Steinheim, Germany) was added and the tubes were shaken occasionally. The reaction was completed within 5 min and the excess of Grignard reagent was quenched with 0.5 ml of 0.6 mol/l HCl. Subsequently, the samples were centrifuged for 3 min at 5400 rpm and the organic phase was transferred to 2 ml screw capped glass vial for GC-MIP-AES analysis.

Determinations were performed using a Varian 3030 (Palo Alto, CA, USA) GC, connected to an Agilent 7500 ICP-MS. The GC was fitted with a SPB-1 column (30 m × 0.53 mm i.d., 3 μm stationary phase, J&W Scientific, Rancho Cordova, CA, USA). Helium was used as carrier gas at 15 psi. 2 μL of sample were injected on an on-column injector.

4.2. Methods used: As-species

4.2.1. Sample preparation. Bottles were allowed to come to ambient temperature during 1 h. The bottles were then shaken manually for 5 min and allowed to stand for 10 min before sampling. Between 250 and 255 mg of sample was weighed into clean dry extraction/centrifugation tubes. To each tube, 50% MeOH (15 mL) was added and the tubes were sonified for 1 h in an ultrasonic bath. The tubes were centrifuged and the extract was decanted into a round-bottomed flask. To each tube, 90% MeOH (15 mL) was added and the residue was re-extracted for 1 h in an ultrasonic bath. Centrifugation/decantation was repeated and the extracts combined. Finally, the residue was washed with 90% MeOH (10 mL) and was re-extracted for 20 min in the ultrasonic bath. The combined extract was reduced to near dryness by using a rotary evaporator. The extract was redissolved in 10 mL H_2O and ultracentrifuged to remove any solid particles before

analysis. The extracts were stored in glass vials in a refridgerator.

4.2.2. Instrumental.

A Supelco SAX anion-exchange column was selected as giving the optimum baseline separation. The elution was carried out using a gradient of 2–25 mmol/l phosphate buffer at pH 6. Detection of eluting arsenic was carried out with an ELAN 6000 ICP-MS. The samples were injected diluted by 10 with a 100-µL sample loop. According to the intensity of the resulting AsBet peak, standard additions on two levels were made. The chromatograms were converted and integrated using Turbochrom software. MS-Excel was used to plot the standard addition curves and only best fit lines with R^2 greater than 0.99 were accepted. The concentration in dry weight was calculated from the sample volume and mass.

4.2.3. Quality assurance.

For verification of the method, BCR-627 tuna fish was extracted and quantified each time a batch of homogeneity or stability analyses was carried out.

4.3. Methods used: Sn species

4.3.1. Sample preparation.

To approximately 500 mg sample was added 25 µL of a solution of tripropyltin-chloride (internal standard) 2 mg/L as tin in hexane, and ultrasonically extracted (5 min at 35 °C) by a mixture of 15 mL of 0.03% (w/v) tropolone in methanolic solution and 1 mL of concentrated hydrochloric acid. The extraction was repeated twice. The supernatant was transferred to a separation funnel and 100 mL of a 5% (w/v) NaCl water solution (to avoid the formation of an emulsion) and 15 mL of dichloromethane were added to the collected extracts.

After separation, the organic phase was passed through sodium sulphate to eliminate traces of water. The extraction into 15 mL of dichloromethane was repeated. The organic phases were combined, and then evaporated at 25 °C by Rotavapor down to a final volume of 2 mL. This volume was reduced almost to dryness under a gentle stream of nitrogen, after addition of isooctane (as keeper). 2 mL of a 2 mol/l ethereal solution of pentylmagnesium bromide were added and the mixture was shaken for 5 min. The excess of Grignard reagent was destroyed by first carefully adding few drops of water and shaking gently and then 5 mL of a 1 mol/l sulphuric acid solution.

The derivatised compounds were extracted twice into 1 mL of hexane and the extract was concentrated to a volume of about 1 mL under a gentle stream of nitrogen. A clean-up step was carried out on a Florisil column (3 · g) eluting the retained derivatised compounds with 10 mL of hexane/toluene (1:1). The

organic solution was vented with a nitrogen flow down to a volume of 0.5 mL. 1 µL of the final extract was injected into the GC-MS system.

4.3.2. Instrumental.

GC/MS analyses were performed on a Hewlett-Packard HP 5890 GC/HP 5970B MSD system (HP-5MS capillary column (30 m × 0.25 mm × 0.25 µm), methyl-5% phenylsilicone) by SIM (selected ion monitoring) operation. Peak identification was based on the matching of retention times (±0.5%) and isotopic mass ratios (±20%) for the diagnostic ions.

4.3.3. Calibration and quality assurance.

External calibration with IVM pentylated standards, using pentyltri-propyltin as internal standard, was used for the determination of the organotin concentrations.

For quality assurance, the BCR-477 was extracted and quantified each time a batch of homogeneity or stability analyses was carried out.

4.4. Between- and within-unit homogeneity

The between-bottle homogeneity was verified on the basis of 20 independent analyses from 20 different bottles while the within-bottle homogeneity was verified by 10 independent analyses of the contents of one bottle. The species tested were MeHg, AsBet, MBT, DBT and TBT. The coefficients of variation were obtained for the between- and within-bottle homogeneity tests (CV_B and CV_W, respectively), together with their respective uncertainties, U_{CV}, defined as:

$$U_{CV} \approx CV/\sqrt{2n},$$

where n is the number of replicates.

The results for the homogeneity study indicated that the analyses were well under control. The CVs were all at or below 9.5%; for MBT, higher CVs were obtained. The homogeneity study revealed that, for the species MeHg, AsBet and TBT, the overlap in CVs was within their uncertainty, U_{CV}. Differences between the within-bottle and the between-bottle CVs observed for DBT and for MBT were considered to be an analytical artefact rather than an indication of inhomogeneity. The sample intake of the certification analyses was sometimes lower (down to 100 mg for MeHg, down to 200 mg for arsenic and tin species) than those used for the homogeneity study (As species, 250 mg; Hg species, 300 mg; and, Sn species, 500 mg). As all participants were requested to report on triplicate analyses from two independent bottles, the between-bottle homogeneity was tested using a nested analysis of variance approach (nested ANOVA). No significant difference could be detected. Consequently, no inhomogeneity was suspected. The CV data of the homogeneity study are available in the Certification Report of the BCR-710 material [19].

Estimates for the contribution resulting from the homogeneity to the overall uncertainty of the certified values are discussed below.

5. Stability study

The stability test was based on a series of analyses for samples stored at +4 °C, +20 °C and at −20 °C, performed in triplicate at $t = 1$, $t = 3$, $t = 6$, $t = 12$ and $t = 18$ months (AsBet up to $t = 12$ months). In addition, to mimic adverse transport conditions, analyses were carried out on samples stored at +40 °C, at $t = 1$ month. The methods of analysis were the same as for the homogeneity study. The studies were carried out by comparing the contents of different analytes in samples stored at different temperatures with those stored at a low temperature at the various occasions of the analysis. The samples stored at −20 °C were used as reference for the samples stored at +4, +20 and +40 °C. Comparisons were made using the ratio's (R_T) of the mean values (X_T) of three measurements made at +4, +20 and +40 °C, respectively, and the mean value ($X_{−20 °C}$) from three determinations made at the same occasion of analysis on samples stored at a temperature of −20 °C: $R_T = X_T/X_{−20 °C}$.

The uncertainty, U_T, was obtained from the coefficient of variation (CV) of three measurements obtained at each temperature:

$$U_T = (CV_T^2 + CV_{−20 °C}^2)^{1/2} \times R_T.$$

With ideal stability, the ratios R_T should be equal to 1.00. In practice, however, there are some random variations because of uncertainty in the measurement.

For MeHg, storage at any tested temperature seemed possible. In most cases, the value 1 was between $R_T − U_T$ and $R_T + U_T$. The lower ratios at $t = 6$ and 12 months (just not overlapping with 1) were considered to be analytical artefacts rather than indications of instability. After 18 months storage no instability could be detected at either +4 or +20 °C.

For AsBet, storage at any temperature was also shown to be possible. Only after 12 months storage at +20 °C, the value 1 was just not between $R_T − U_T$ and $R_T + U_T$. Applying storage conditions at +4 °C, no instability was observed for the period tested (12 months).

For the butyltins, storage at +40 °C clearly demonstrated instability (degradation of DBT and TBT) and as a result the formation of MBT. At +20 °C, there was enrichment of MBT, and possibly of DBT (but not at $t = 18$ months); for TBT, there was a clear trend showing degradation at this temperature. Only at +4 °C was the value 1 between $R_T − U_T$ and $R_T + U_T$ in most cases (true for all three species after 18 months' storage). The lower ratios at $t = 3$ and 6 months (MBT, DBT) and $t = 1$

and 3 months (TBT) were considered to be analytical artefacts rather than indications of instability.

In conclusion, provided samples are stored at +4 °C or below, no instability was suspected. Appropriate estimates for the uncertainty calculation of the certified values are discussed below. All data supporting the above discussion are available in the Certification Report [19].

6. Analytical methods

Each laboratory that took part in the certification exercise was requested to make a minimum of six independent replicate determinations of each element on at least two different bottles of the CRM on different days. In the meeting of the laboratories participating in the certification, the sources of error and the measures taken to eliminate them were discussed. The laboratories participating in the certification exercise performed the determinations only when the method was under control (i.e. the standard deviations observed in the laboratory were in accordance with the normal practice of the laboratories). The results of different methods (see Table 3) as applied in different laboratories were compared to detect sources of method error. The calculations of the certified values were based on the technically accepted results that are made available in the Certification Report [19].

7. Technical and statistical discussion

All the results accepted for certification by the participating laboratories are given in the Certification Report [19]. All the results were discussed at a technical evaluation meeting to confirm the accuracy of the methods of analysis.

7.1. Technical discussion

For most species, the discussion could be rather brief because of the agreement in the results. In a number of cases, data were withdrawn by the laboratory for good reasons (e.g., interferences observed, poor separation of signals, and calibration problems).

7.1.1. Mercury species. For MeHg, one laboratory explained its use of three different methods. Method (a) included H_2SO_4 in the destruction step, which apparently resulted in the inclusion of inorganic Hg in the MeHg analysis: about twice the value obtained by method (b), based on HCl. As both methods (a) and (b) were based on the hypothesis that all organic Hg was present in the form of MeHg, without further identification/confirmation, these results could not be accepted.

Total Hg (seven data sets) was included in the Certification Report [19] to allow for budget studies. No

Table 3. Summary of techniques used in the certification

Lab. code	Sample pre-treatment, separation, calibration	Final determination
Arsenobetaine		
08	Trypsin extraction, HPLC separation	ICP-MS
09	Extraction with hot water, HPLC separation (cation exchange), UV irradiation	HG-AFS
11	Water extraction, clean-up with hexane, HPLC separation	ICP-MS
14	Methanol/water extraction, HPLC separation (anion exchange)	ICP-MS
15	Water extraction, HPLC separation (anion exchange)	ICP-MS
20	Microwave methanol/water extraction, LC separation (anion exchange), UV irradiation	HG-AFS
24	Methanol/water extraction, HPLC separation	ICP-MS
26	Methanol/water extraction, HPLC separation	ICP-MS
29	Methanol/water extraction, filtration at 0.45 μm, HPLC separation	ICP-MS
32	Methanol/water extraction, HPLC separation (anion exchange), UV irradiation	HG-AFS
Methylmercury		
01	Microwave digestion with TMAH, *in situ* derivatisation with $NaBEt_4$, CGC separation	ICP-MS
03	HCl/toluene extraction, addition of L-cysteine, packed GC separation	ECD
06a	Microwave digestion with TMAH, *in situ* derivatisation with $NaBEt_4$, CGC separation	ICP-MS
06b	Spiking with ^{201}Hg isotope labelled MeHg, methanol extraction, *in situ* derivatisation with $NaBEt^4$, CGC separation	ID-ICP-MS
08	TMAH extraction, acidification with HCl, addition of KBr, $CuSO_4$, dichloromethane	CV-AFS
10a	TMAH extraction, addition of HCl, DDTC complexation, derivatisation with BuMgCl, CGC separation	MIP-AES
10b	Spiking with ^{201}Hg isotope labelled MeHg, TMAH extraction, filtration at 0.45 m, HPLC separation	ID-ICP-MS
13	H_2SO_4/KBr extraction, addition of $CuSO_4$, dichloromethane, derivatisation with $NaBEt_4$, packed GC separation	CV-AFS
14	TMAH extraction, addition of HCl, derivatisation with $NaBPr_4$, CGC separation	AED
17	Acetone/toluene/HCl extraction, addition of cysteine, derivatisation with $NaBPh_4$, CGC separation	MS
23c	HCl/toluene extraction, addition of thiosulphate solution, purge and trap with packed GC	CVAAS
25	Extraction with KOH/methanol, derivatisation with $NaBEt_4$, CGC separation	CV-AFS
32	TMAH/dichloromethane extraction, derivatisation with $NaBEt_4$, packed GC separation	AFS
Di- and tributyltin		
02	Methanol, ethylation (using $NaBEt_4$), capillary GC separation	FPD
03	Tropolone/methanol/HCl, derivatisation with pentylmagnesium bromide, clean-up of Florisil column, capillary GC separation	MS
10	Addition of water/NaCl, tropolone/diethylether extraction, derivatisation with pentylmagnesium bromide, capillary GC separation	ICP-MS
12	Spiking with ^{117}Sn enriched TBTCl, sodium acetate/acetic acid/methanol extraction, HPLC separation	ID-ICP-MS
14	TMAH/HCl extraction, ethylation (using $NaBEt_4$), capillary GC separation	AED
17a	Methanol/tropolone/HCl extraction, derivatisation with pentylmagnesium bromide, capillary GC separation	MS
17b	Methanol/tropolone/HCl extraction, derivatisation with pentylmagnesium bromide, capillary GC separation	FPD
21	Diethylether/tropolone extraction, Grignard derivatisation (pentylation), capillary GC separation	ITD-MS
24	NaOH/methanol extraction, addition of $NaBH_4$, capillary GC separation	FPD
25	TMAH/acetic acid extraction, derivatisation with $NaBEt_4$, clean-up on SPE cartridges, capillary GC separation	FPD

AED: atomic emission detection; AFS: atomic fluorescence spectrometry; CVAAS: cold vapour atomic absorption spectrometry; CVAFS: cold vapour atomic fluorescence spectrometry; ECD: electron capture detection; FPD: flame photometric detection; HG: hydride generation; HPLC: high-performance liquid chromatography; ID: isotope dilution; ICP-MS: inductively coupled plasma mass spectrometry; MIP-AES: microwave-induced plasma atomic emission spectrometry; MS: mass spectrometry.

statistical outliers were found and the result is reported as an indicative value.

7.1.2. Arsenic species.
For AsBet, the results of one laboratory, corresponding to a sub-set of a larger number of independent analytical results, were about twice the mean values of the other laboratories, and hence a statistical outlier. No reason could be given. Because the reported data were a selection of all results, and they were a statistical outlier, the data set was withdrawn. The laboratory tried to confirm the results and after reanalysis the new data set on AsBet (47.04 ± 0.97, $n = 6$) is closer to the results used for certification, still without overlap, though.

Another laboratory discovered that the reported values were too low as a result of an incomplete photo-oxidation step. The results were withdrawn.

One participant used an HPLC-ICP-MS technique where the separation of the peaks was much improved (see Fig. 1). It was demonstrated that, when using more traditional separation techniques, the peak of AsBet could include a small contribution of other

Figure 1. Separation of inorganic and organic arsenic species in oyster-tissue extract by means of HPLC-ICP-MS. Peak identification: 1: AsIII; 3: MMA; 4: DMA; 6: As-sugar 1b; 7: AsV; 14: AsBet; 15: TMAO; 16: AsCho; 17: TMAs; 2, 8–13: unknown species. (Courtesy U. Kohlmeyer and J. Kuballa, GALAB Laboratories, Germany).
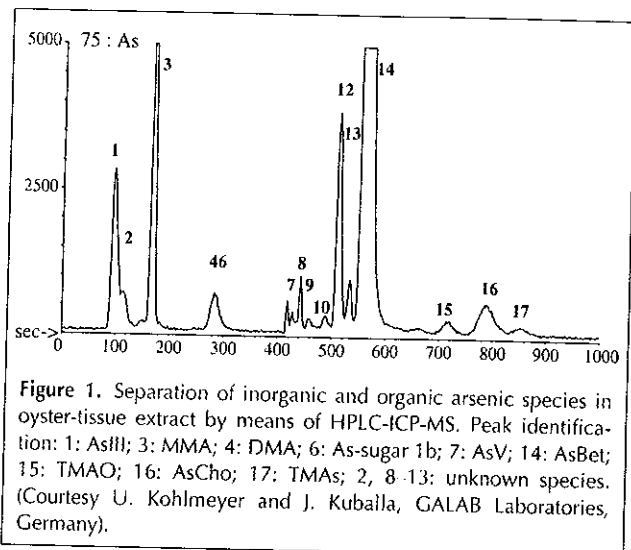
As-compounds. It was concluded that, according to the state of the art at the moment of the certification exercise, it could not be excluded that a small interference of other arsenic compounds is included in the AsBet results; this interference is, however, below the confidence limit reported for this CRM.

For DMA, the results of one laboratory showed a large SD, and – in comparison to the other results – a shift towards higher concentrations. The DMA peak showed on the edge of the much larger AsBet peak, which made quantification difficult, and justified withdrawal of the results.

The meeting agreed that the set of results was apparently state of the art, but that it was not sufficient to become a certified value. It therefore concluded that the result should be reported as an indicative value.

For MMA, few results were reported. As the results did not agree, even an indicative value was not considered as being helpful to the future user.

Other arsenic species were reported by few laboratories. The following remarks were made:

- AsIII: no agreement between results; AsIII readily oxidises in solution, the reason why the species will remain difficult to analyse;
- AsV: no agreement between results; the concentration is near the detection limit of the methods used;
- AsCho: only one data set reported;
- AsSugars: no agreement between results; two distinct species have been identified, and, for future work, they will be reported as identifiable entities; and,
- AsResidual: no agreement; as this 'rest' fraction cannot be properly identified (e.g., in mol/kg), certification is not foreseen.

Total As (nine data sets) was included in the Certification Report [19] to allow for budget studies. Results compared reasonably well, but two distinct clusters were observed (not linked to analytical techniques). Considering the rather low concentration level the results were nevertheless considered useful, and the meeting agreed to accept the data set for inclusion in the certification report as indicative value.

7.1.3. Tin species. For TBT, an outlying laboratory checked its methods and discovered problems with the calibrants; new results with new calibrants (mean = 0.1197 mg/kg) resulted in data that agree well with the other data sets (the results were withdrawn). Ten data sets were retained. Although the CV = 19.1% may seem high, the concentration level is rather low; the CV compares well with that of e.g. BCR-477, giving reason to accept these results for certification.

For DBT, similar calibration problems to those for TBT were encountered by one laboratory and the results were therefore withdrawn. Another laboratory had a large SD resulting from a large difference between three results on day one, and three results on day two. This was clear evidence that the method was not under control, so the data set was withdrawn. The relative standard deviation (CV = 21.5%) is, considering the concentration level, considered not too large (also in comparison to the value for BCR-477). As a result, the eight remaining data sets were considered acceptable for certification.

For MBT, same calibration problems were experienced by the above-mentioned laboratory. Other laboratories experienced difficulties with derivatisation. The remaining 6 data sets showed insufficient agreement to allow for certification. The results are, however, included as an indicative value.

Because of their low concentrations, TPhT, DPhT and MPhT could not be quantified. For this reason, the material is proposed to be used as a 'blank' oyster matrix for these compounds.

7.2. General statistical evaluation of the results

For each set of technically accepted results, the mean value and the standard deviation were calculated. The sets of results found acceptable on technical and statistical grounds are represented in the form of "bar-charts" in Figs. 2–4, in which the length of a bar corresponds to the 95% confidence interval of the mean of laboratory means.

The certified values were calculated as the arithmetic means of laboratory means (taking into account the number of sets accepted for certification after both technical and statistical scrutiny); they are featured as vertical dotted lines on the bar-graphs; the uncertainty is given by the half width of the 95% confidence interval of the mean of laboratory means.

```
         BAR-GRAPHS FOR LABORATORY MEANS AND 95% CI

                .070              .090              .110              .130
                +.........+.........+.........+.........+.........+.........+

         01                                           |        <---*---->

         03                             <------*----->|

         06a                                          |   <------*------>

         06b                                          |        <--*-->

         08                          <----------*--------->

         10a                                          | <----*---->

         10b                                          |      <------*------->

         13                                           |     <---*--->

         14                       <------------*------------->

         17              <------------*----------->    |

         23c                    <-----*----->          |

         25                                      <------*----->

         32                        <--------*------->  |
                                                       |
                                                       |
         |MEANS|                              <--------M------->
                                                       | error bar is not symmetric
```

Figure 2. MeHg in BCR-710 (in mg/kg).

```
         BAR-GRAPHS FOR LABORATORY MEANS AND 95% CI

                20.0              30.0              40.0
                +.............+.............+.............+.............+.............+
                                                 |
         09                              <----*------>
                                                 |
         14                                  <--*-->
                                                 |
         15                           <----*--->  |
                                                 |
         20                                      |          <------*----->
                                                 |
         24                            <--*->    |
                                                 |
         26                                      |     <------*------>
                                                 |
         29                  <------------*----------->|
                                                 |
         32                         <-----*------>|
                                                 |
         |MEANS|                    <----------M---------->
                                                 |
```

Figure 3. AsBet in BCR-710 (in mg/kg).
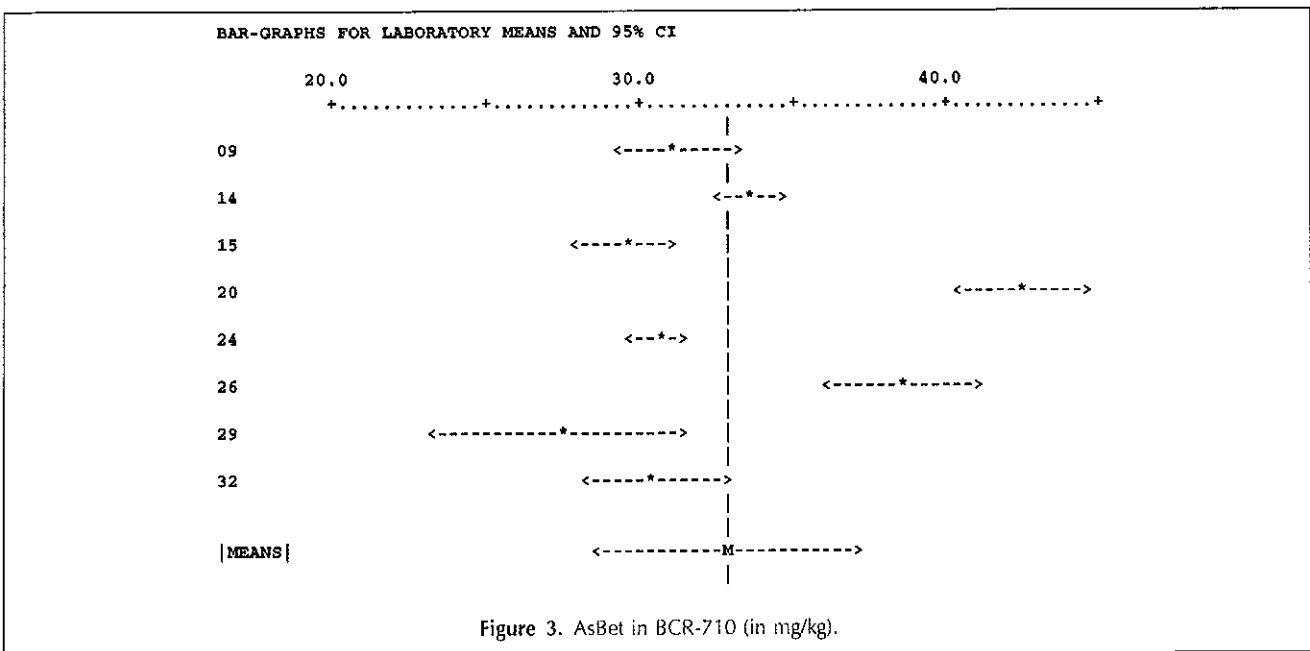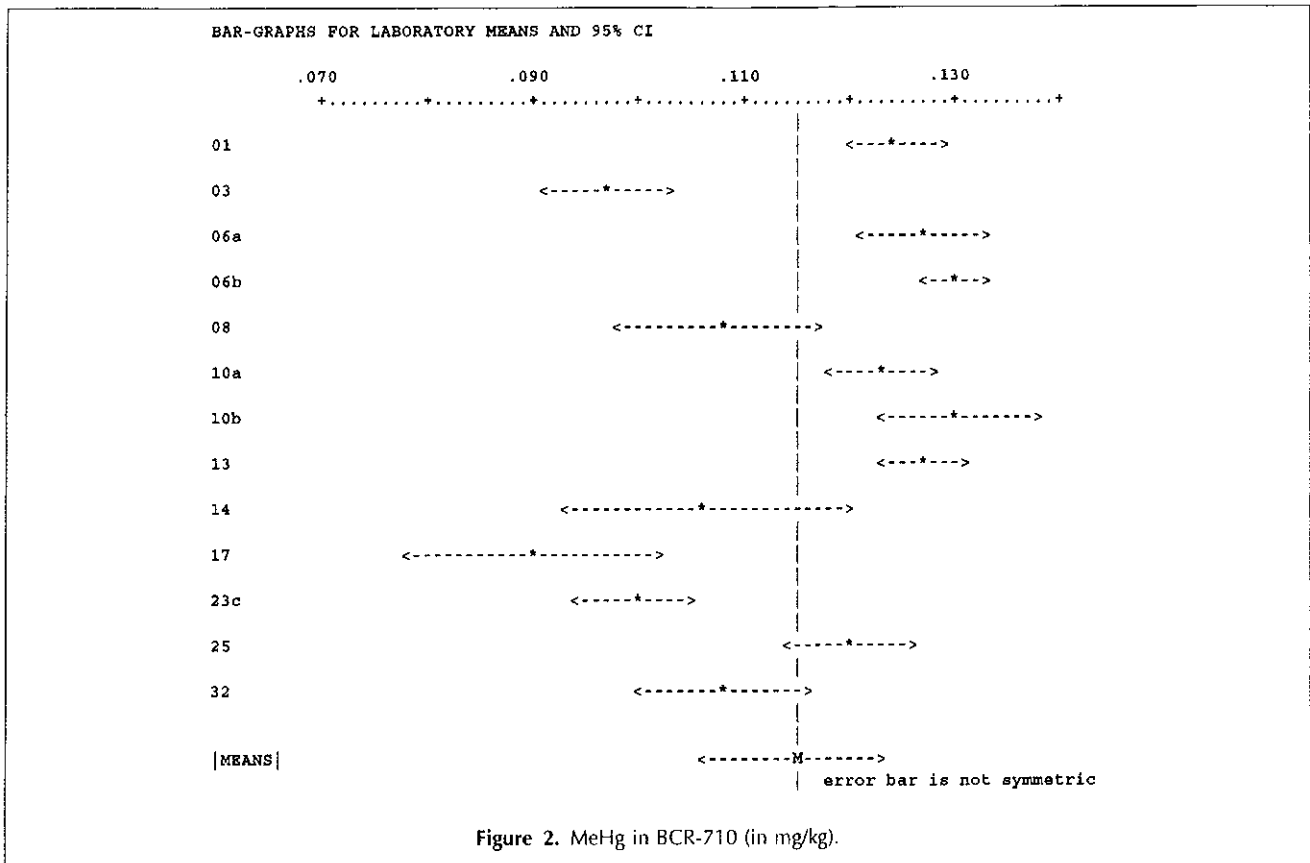
The sets of results have been submitted to a series of statistical tests that are described in the Certification Report, along with a detailed discussion of the statistical data [19]. The tests enabled verification that the population of results accepted for certification had a normal distribution before the 95% confidence interval of the mean of means was calculated (Kolmogorov–Smirnov–Lilliefors tests). In addition, it was checked that

```
          BAR-GRAPHS FOR LABORATORY MEANS AND 95% CI

           .080        .100        .120        .140        .160        .180
          +.....+......+.....+....+.....+......+.....+......+.....+....+......+.....+

   02                                        <--------*-------->

   03                                                          <------*------->

   10                  <---------------*-------------->

   12                                      <-*>

   14                  <--*--->

   17a                                    <-------*------->

   17b                                  <---------*-------->

   21               <---*-->

   24                                             <------------*----------->

   25                                    <-----*---->

   |MEANS|                               <----------M---------->
```

Figure 4. TBT in BCR-710 (in mg/kg).
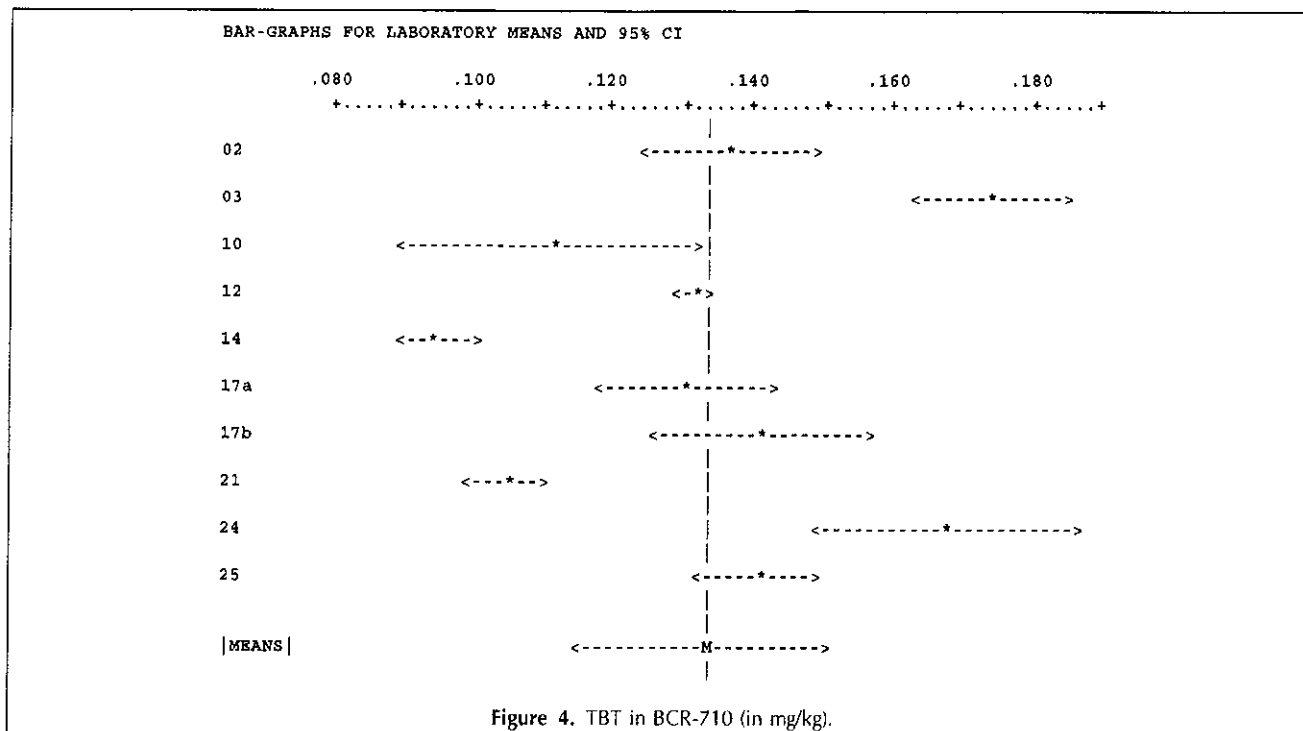
Table 4. Uncertainty budget for the certified values of BCR-710

	Mean	n	u_{char} (%)	s_{bb} (%)	u_{bb}^* (%)	u_{lts}	U_{CRM} (%)	U_{CRM}
MeHg	0.11473	13	3.32	3.7	3.5	5.9	15.43015	0.017703
AsBe	32.97698	8	5.45		6.52	4.46	19.19422	6.329673
TBT	0.13327	10	6.03		1.92	1.85	13.18633	0.017573
DBT	0.08203	8	7.6	6.97	3.57	3.92	22.06421	0.018099

The estimate for stability, u_{lts}, will be used to calculate a shelf-life of the material. The expanded uncertainties are calculated with a coverage factor of $k = 2$.

there were no outlying mean values (Nalimov test). The set of variances was often not homogeneous because different methods are used each having a different repeatability and reproducibility. If one single method was used, then a homogeneous set of laboratory variances would have been required.

8. Certified values and their uncertainties

The evaluation of uncertainties in the context of certification exercises has evolved over the past decade. Nowadays, certified values should be accompanied by uncertainty statements in compliance with the requirements made by Guide for the Expression of Uncertainties in Measurement (GUM) [20]. While the design of new certification projects consider the needs for proper estimation of the various uncertainty sources, such as stability and homogeneity, older campaigns aimed only at qualitative statements (yes/no decisions) as to

whether a material was stable and homogeneous. The evaluation described next is based on a concept described by Pauwels et al. [21] and uses available data discussed in the previous sections of this article.

Based on the findings obtained in the stability and the homogeneity studies as well as the scattering of results in the batch characterisation, estimates for u_{bb} (homogeneity), u_{lts} (long-term-stability) and u_{char} (batch charac-

Table 5. Certified contents of methylmercury, arsenobetaine, tributyltin, dibutyltin and their uncertainties in BCR-710

Certified compounds	Certified values (mg/kg as cations)	Uncertainty (µg/kg as cations)
MeHg	0.115	0.018
AsBet	33	7
TBT	0.133	0.018
DBT	0.082	0.018

Table 6. Indicative values of the contents (mass fractions) of the species DMA and MBT, and of the (total) elements As and Hg

Species, element	Mean (mass fraction)	SD	Unit	p	Techniques used
DMA	0.82	0.18	mg/kg	6	HPLC-(UV)-HG-AFS HPLC-ICP-MS
MBT	0.050	0.014	mg/kg	6	GC-AED GC-FPD GC-ITD-MS GC-MS
As (total)	25.7	2.7	mg/kg	9	AsAFS ICP-MS ICP-OES γ-Spectrometry
Hg (total)	0.26	0.05	mg/kg	7	CVAAS CVAFS DMA

NB. These values cannot be used for any checks of accuracy.
SD: standard deviation; p: number of data sets.

terisation) were obtained and combined according the following equation:

$$U_{CRM} = 2 \cdot \sqrt{u_{bb}^2 + u_{lts}^2 + u_{char}^2}.$$

Because of the transport conditions selected for dispatch, the uncertainty constituent for short-term stability (u_{sts}) is negligible and consequently not included in the overall uncertainty. The estimation of the other uncertainty sources is described below.

From the homogeneity data, an estimation of u_{bb} was derived. According to this approach, s_{bb} (being the standard deviation between units) or u_{bb}^* (being the upper limit of inhomogeneity that can be hidden by the method repeatability) are used as estimates of u_{bb}. Values for s_{bb} and u_{bb}^* were calculated accordingly. Whereas estimates for s_{bb} were derived from differences in the observed CVs, values for u_{bb}^* were calculated as:

$$u_{bb}^* = s_{meas} \cdot 4\sqrt{\frac{2}{\nu_{Smeas}}},$$

where s_{meas} is obtained directly from the 10-fold repeated analysis on one randomly selected unit and ν_{Smeas} the degrees of freedom of s_{meas}.

If the value of s_{bb} is below the minimum value as determined by the repeatability of the method and the number of replicates performed, u_{bb}^* is used to estimate u_{bb}. The results of these calculations are shown in Table 4.

Similarly, a quantitative estimate of the uncertainty related to stability, u_{lts}, was obtained. The uncertainty was estimated for a shelf-life of 12 months only, as the data was insufficient to allow a further projection without seriously compromising the usefulness of the certified values. Thus, the estimated uncertainty contribution,

u_{lts}, can be used to establish expiry dates once appropriate stability testing data are available (e.g., after having performed an isochronous experiment).

Finally, an estimate for u_{char} ("batch characterisation") was derived from the standard error obtained on the mean of laboratories means, and an uncertainty budget has been calculated (Table 4).

The certified values were calculated as the arithmetic means of laboratory means (taking into account the numbers of sets accepted for certification after both statistical and technical scrutiny). The certified values and their associated uncertainties are given in Table 5.

9. Indicative values

After evaluation of the results and the discussion in the technical meeting, it was agreed that the species DMA and MBT, and the total element content of Hg and As were to be reported, not as certified but as indicative values (mass fractions, based on dry weight), with their standard deviations and the analytical techniques used for the respective species/element. All are presented in Table 6.

10. Conclusions

Besides the certification work described in this paper, further analyses are on-going to certify the total contents of a range of trace metals. As soon as this certification is completed, the BCR-710 reference material will be made available from IRMM. More information is available on the IRMM website (http://www.irmm.jrc.be).

Acknowledgements

References

[1] IRMM Catalogue. Available from: <http://www.irmm.jrc.be/>.

[2] S. Caroli (Editors), Element Speciation in Bio-inorganic Chemistry, Wiley, NY, USA, 1996.

[3] Ph. Quevauviller, Method Performance Studies for Speciation Analysis, The Royal Society of Chemistry, Cambridge, UK, 1998.

[4] A. Kot, J. Namiesnik, Trends Anal. Chem. 19 (2000) 69.

[5] L. Ebdon, L. Pitts, H. Crews, O.F.X. Donard, Ph. Quevauviller (Editors), Trace Element Speciation for Environment, Food and Health, The Royal Society of Chemistry, Cambridge, UK, 2001.

[6] Ph. Quevauviller, R. Morabito, Trends Anal. Chem. 19 (2000) 86.

[7] R. Morabito, P. Massanisso, Ph. Quevauviller, Trends Anal. Chem. 19 (2000) 97.

[8] C. Pellegrino, P. Massanisso, R. Morabito, Trends Anal. Chem. 19 (2000) 107.

[9] Ph. Quevauviller, Spectrochim. Acta, Part B 53 (1998) 1261.

[10] Ph. Quevauviller, E.A. Maier, Interlaboratory Studies and Certified Reference Materials for Environmental Analysis – The BCR Approach, Elsevier, Amsterdam, The Netherlands, 1999.

[11] R. Cornelis, H. Crews, O.F.X. Donard, L. Ebdon, Ph. Quevauviller, Fresenius J. Anal. Chem. 370 (2001) 120.

[12] K.J.M. Kramer (Editors), Biomonitoring of Coastal Waters and Estuaries, CRC Press, Boca Raton, FL, USA, 1994.

[13] Ph. Quevauviller, I. Drabaek, M. Bianchi, H. Muntau, B. Griepink, Trends Anal. Chem. 15 (1996) 390.

[14] R. Morabito, H. Muntau, W. Cofino, Ph. Quevauviller, J. Environ. Monitor. 1 (1999) 75.

[15] F. Lagarde, Z. Asfari, M.J.F. Leroy, C. Demesmay, M. Ollé, A. Lamotte, P. Leperchec, E.A. Maier, Fresenius J. Anal. Chem. 363 (1999) 12.

[16] Ph. Quevauviller, G. Fortunati, M. Filippelli, A. Bortoli, H. Muntau, Appl. Organometal. Chem. 12 (1998) 531.

[17] Ph. Quevauviller, F. Ariese, Trends Anal. Chem. 20 (2001) 207.

[18] H. Emteborg, J. Snell, J. Qian, W. Frech, Chemosphere 39 (1999) 1137.

[19] Certification report of BCR-710, IRMM publication, Geel, Belgium, http://www.irmm.jrc.be, 2004.

[20] ISO-IEC-BIPM-IFCC-IUPAC, IUPAP, OIML, Guide to the expression of uncertainties in measurements (GUM), Geneva, Switzerland (ISBN 92-67-10188-9), 1995, 101pp.

[21] J. Pauwels, A. Lamberty, Fresen. J. Anal. Chem. 370 (2001) 111.

Complementary Results for BCR 710 – Indicative values for total As, Hg and Sn

Concentrations expressed in mg.kg^{-1} dry mass

Unit	Humidity (%)	[As]	[Hg]	[Sn]	[AsB]	[Me-Hg]	[TBT]	[DBT]	[MBT]
Date of sample preparation	22/02/06	22/02/06	22/02/06	22/02/06	06/03/06	28/11/05	16/12/05	16/12/05	16/12/05
Date of analysis	28/02/06	28/02/06	28/02/06	08/03/06	06/03/06	28/11/05	16/12/05	16/12/05	16/12/05
235	4.58 ± 0.05	25.96	0.314	1.214	29.3	0.109	0.083	0.067	0.069
235	4.58 ± 0.05	25.17	0.280	1.215	34.9	0.115	0.119	0.077	0.059
289	4.7 ± 0.1	26.29	0.294	1.270	29.6	0.118	0.130	0.079	0.054
289	4.7 ± 0.1	26.02	0.279	1.262	28.3	0.127	0.128	0.078	0.056
343	3.93 ± 0.05	24.66	0.272	1.208	29.8	0.098	0.140	0.064	0.049
343	3.93 ± 0.05	25.23	0.286	1.249	33.2	0.100	0.133	0.069	0.057
353	4.36 ± 0.07	24.81	0.287	1.243	26.4	0.125	0.131	0.070	0.051
353	4.36 ± 0.07	25.53	0.267	1.425	27.4	0.119	0.161	0.074	0.061
639	4.8 ± 0.1	24.43	0.267	1.507	32.3	0.122	0.112	0.070	0.059
639	4.8 ± 0.1	24.08	0.279	1.351	30.8	0.094	0.116	0.071	0.061
739	4.9 ± 0.3	24.36	0.265	1.324	30.2	0.101	0.120	0.069	0.052
739	4.9 ± 0.3	25.53	0.279	1.174	31.0	0.121	0.145	0.065	0.045

ANEXO X
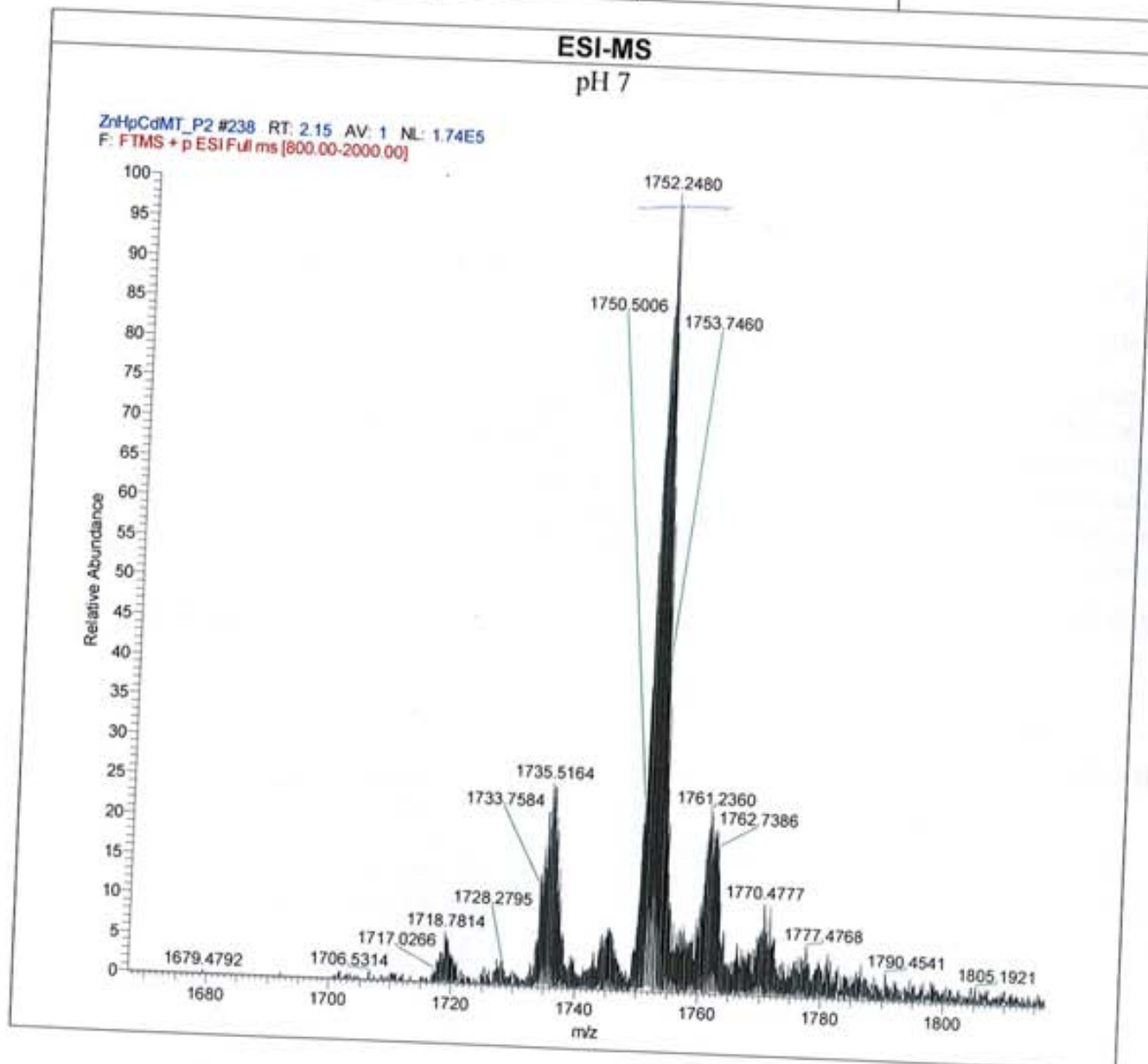
Certificados de análisis de la producción de las metalotioneinas.

MASSES

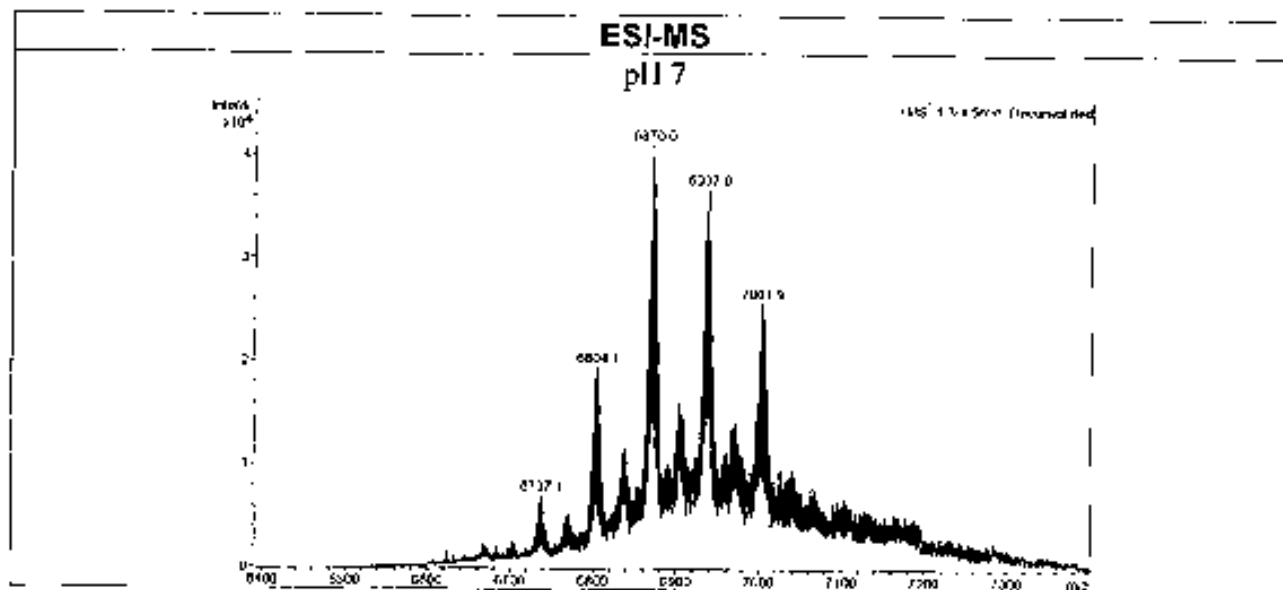| data	responsable	pH	Espècie (abundància %)	massa exp.	massa calc.
20/01/15	Òscar P.	7	Zn6 (100)	7005 (1752)	7005.7
	UB-orbitrap		Zn5 (25)	6940 (1735)	6942.3

ESI-MS

pH 7

ZnHpCdMT_P2 #238 RT: 2.15 AV: 1 NL: 1.74E5
F: FTMS + p ESI Full ms [800.00-2000.00]

Relative Abundance

1752.2480
1750.5006
1753.7460
1735.5164
1733.7584
1761.2360
1762.7386
1728.2795
1718.7814
1770.4777
1717.0266
1777.4768
1679.4792
1706.5314
1790.4541
1805.1921

m/z

Injecció 1 (grocs)

MASSES

data	responsable	pH	Espècie (abundància %)	massa exp.	massa calc.
15/07/2014	Selene Gil	7	Zn_4 (100)	6870,0	6879,10
			Zn_5 (90)	6937,0	6942,49
			Zn_6 (70)	7001,9	7005,88
			Zn_3 (50)	6804,1	6817,71
			Zn_2 (10)	6737,1	6752,32

ESI-MS
pH 7

Injecció 2 (blaus)

MASSES

data	responsable	pH	Espècie (abundància %)	massa exp.	massa calc.
15/07/2014	Selene Gil	7	Zn_4 (100)	6871,0	6879,10
			Zn_5 (100)	6937,0	6942,49
			Zn_6 (50)	7001,9	7005,88
			Zn_3 (40)	6803,1	6817,71
			Zn_2 (10)	6735,2	6752,32
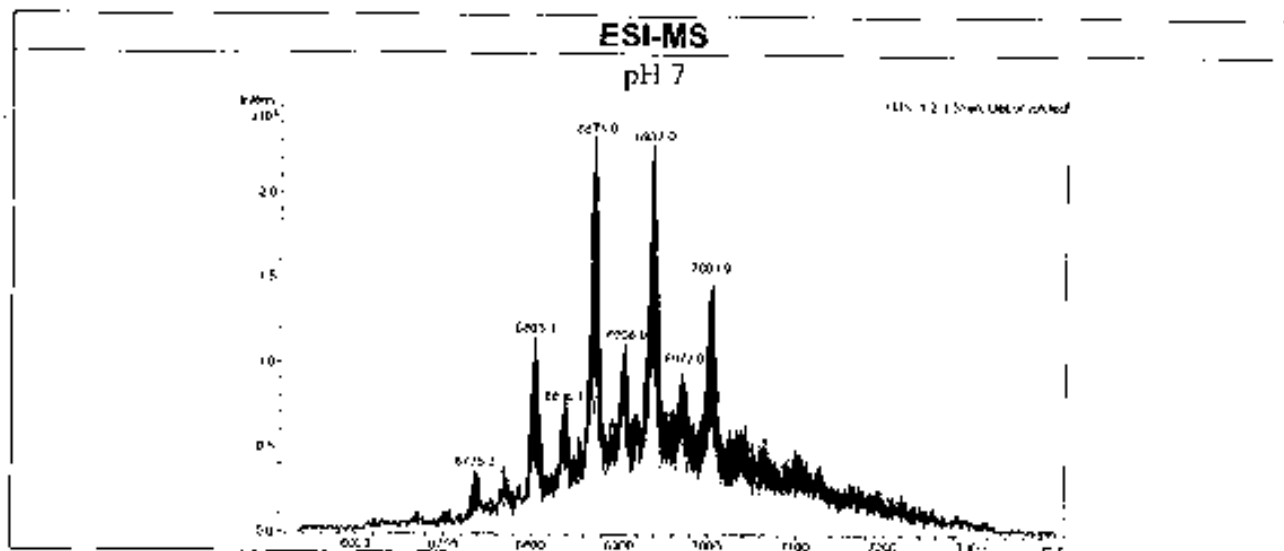
ESI-MS
pH 7

Injecció 1 (grocs)

100 x6 + 4 x50
6

MASSES

data	responsable	pH	Espècie (abundància %)	massa exp.	massa calc.
15/07/2014	Selene Gil	7	Zn_6 (100)	7004,9	7005,88
			Zn_4 (50)	6871,0	6879,10
			Zn_5 (50)	6938,0	6942,49
			Zn_3 (20)	6805,1	6817,71
			Zn_2 (10) ·	6737,2	6752,32
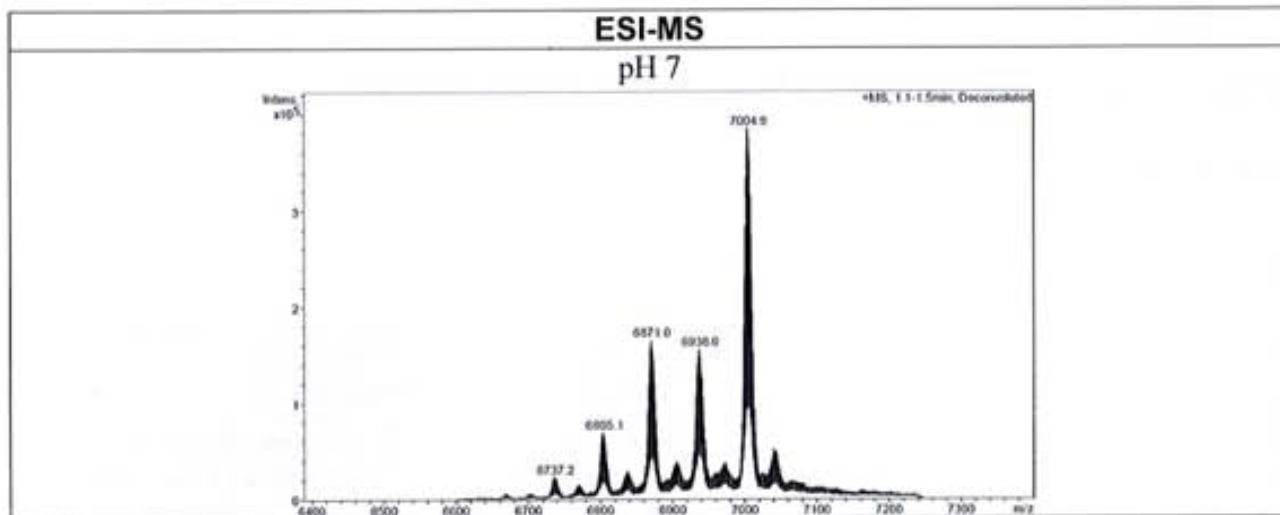
ESI-MS
pH 7

Injecció 2 (blaus)

MASSES

data	responsable	pH	Espècie (abundància %)	massa exp.	massa calc.
15/07/2014	Selene Gil	7	Zn_6 (100)	7005,9	7005,88
			Zn_4 (50)	6871,1	6879,10
			Zn_5 (50)	6937,0	6942,49
			Zn_3 (20)	6804,1	6817,71
			Zn_2 (10)	6738,1	6752,32
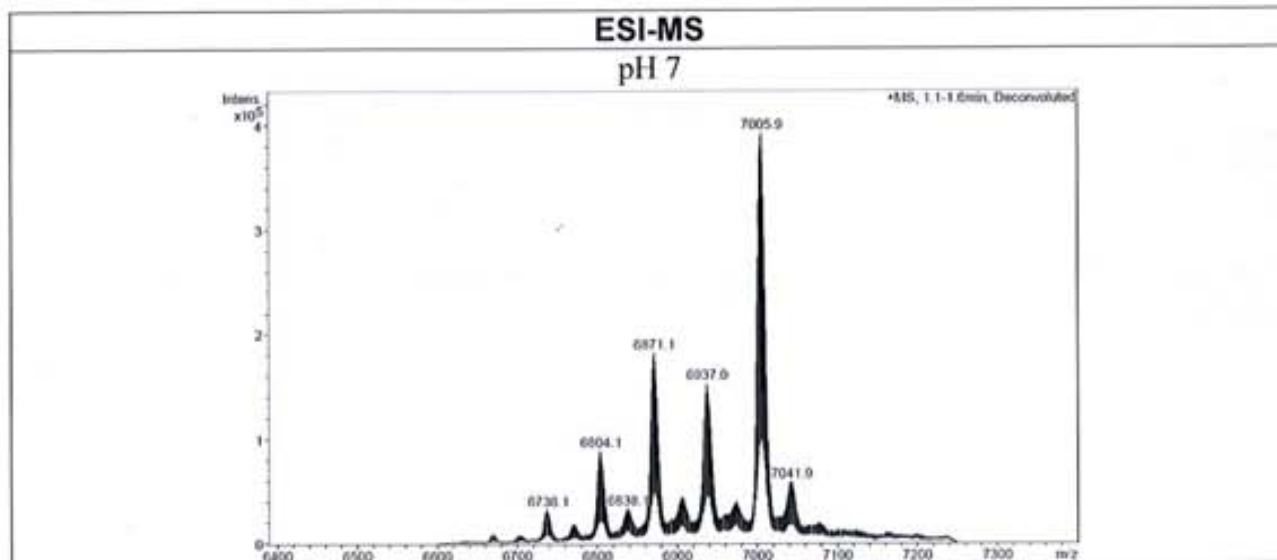
ESI-MS
pH 7

Nueva Producción

MASSES

data	responsable	pH	Espècie (abundància %)	massa exp.	massa calc.
20/01/15	Òscar P.	7	Zn6 (100)	7005 (1752)	7005.7
	UB-orbitrap		Zn5 (40)	6940 (1735)	6942.3

ESI-MS

pH 7

ZnHpCdMT_P1 #274-286 RT: 2.48-2.58 AV: 13 NL: 2.29E3
F: FTMS + p ESI Full ms [800.00-2000.00]

Relative Abundance / m/z

1752.2502
1751.2496
1753.5005
1749.9992
1735.2669
1734.2635
1736.2568
1760.2411
1761.7508
1744.7642
1762.9803
1767.4810
1726.7624
1776.9915
1790.7612
1718.5276
1783.4565
1716.7386
1701.3810